



Design and Control of Parawood Chips Combustion Boiler Process Using  
Aspen Dynamics

Jirateep Premsuksatian

A Thesis Submitted in Partial Fulfillment of the Requirements for the  
Degree of Master of Engineering in Chemical Engineering (International Program)

Prince of Songkla University

2019

Copyright of Prince of Songkla University



Design and Control of Parawood Chips Combustion Boiler Process Using  
Aspen Dynamics

Jirateep Premsuksatian

A Thesis Submitted in Partial Fulfillment of the Requirements for the  
Degree of Master of Engineering in Chemical Engineering (International Program)

Prince of Songkla University

2019

Copyright of Prince of Songkla University

**Thesis Title**            Design and control of parawood chips combustion boiler  
 process using Aspen Dynamics

**Author**                    Mr. Jirateep Premsuksatian

**Major Program**        Chemical Engineering (International Program)

---

**Major Advisor**

.....  
 (Asst. Prof. Dr. Pornsiri Kaewpradit)

**Examining Committee:**

.....Chairperson

(Asst. Prof. Dr. Veerayut Lersbamrungsuk)

.....Committee

(Asst. Prof. Dr. Pornsiri Kaewpradit)

.....Committee

(Assoc. Prof. Dr. Kulchanat Prasertsit)

.....Committee

(Assoc. Prof. Dr. Lupong Kaewsichan)

The Graduate School, Prince of Songkla University, has approved this  
 thesis as partial fulfillment of the requirements for the Master of Engineering Degree  
 in Chemical Engineering (International Program)

.....

(Prof. Dr. Damrongsak Faroongsarng)

Dean of Graduate School

This is to certify that the work here submitted is the result of the candidate's own investigations. Due acknowledgement has been made of any assistance received.

..... Signature  
(Asst. Prof. Dr. Pornsiri Kaewpradit)  
Major Advisor

..... Signature  
(Mr. Jirateep Premsuksatian)  
Candidate

I hereby certify that this work has not been accepted in substance for any degree,  
and is not being currently submitted in candidature for any degree.

..... Signature

(Mr. Jirateep Premsuksatian)

Candidate

ชื่อวิทยานิพนธ์	การออกแบบและการควบคุมกระบวนการผลิตไอน้ำจากการเผาไหม้ ยางพาราด้วยโปรแกรม Aspen Dynamics
ผู้เขียน	นาย จิรทีปต์ เปรมศักดิ์เสถียร
สาขาวิชา	วิศวกรรมเคมี (หลักสูตรนานาชาติ)
ปีการศึกษา	2562

## บทคัดย่อ

ปัญหาทั่วไปที่พบในกระบวนการผลิตไอน้ำขนาดเล็ก คือ การควบคุมอัตราส่วนของอากาศที่ใช้ในการเผาไหม้และเชื้อเพลิงที่ป้อนเข้าสู่เตาเผาอย่างไม่มีประสิทธิภาพ ซึ่งส่งผลให้สูญเสียพลังงานความร้อนโดยไม่จำเป็นและก่อให้เกิดมลภาวะทางอากาศ วัตถุประสงค์หลักของการศึกษาและงานวิจัยนี้คือ การหาสภาวะที่เหมาะสมในการดำเนินงานของระบบผลิตไอน้ำ เพื่อลดการสูญเสียพลังงานความร้อน กู้คืนพลังงานความร้อน และ ควบคุมการปลดปล่อยแก๊สคาร์บอนมอนอกไซด์ (CO) แก๊สไนโตรเจนออกไซด์ (NO<sub>x</sub>) และแก๊สซัลเฟอร์ออกไซด์ (SO<sub>x</sub>) โดยการจำลองและออกแบบระบบควบคุมด้วยโปรแกรม Aspen Plus และ Aspen Dynamics. กระบวนการหมุนเวียนแก๊สที่ได้จากการเผาไหม้กลับเข้าสู่เตาเผา (flue gas recirculation) ได้ถูกนำมาประยุกต์ใช้เพื่อลดการเกิดของแก๊สไนโตรเจนออกไซด์ รวมทั้งจำลองและออกแบบเครื่องอุ่นอากาศ (air preheater) ซึ่งมีวัตถุประสงค์เพื่อกู้คืนพลังงานความร้อน โดยนำความร้อนจากแก๊สร้อนที่ได้จากการเผาไหม้ (flue gas) นำมาอุ่นอากาศก่อนป้อนเข้าเตาเผาให้มีอุณหภูมิสูงขึ้น. ในงานนี้ได้นำเสนอวิธีการจำลองแบบพลวัต (Dynamic simulation) ของกระบวนการที่มีของแข็งอยู่ในระบบ ซึ่งเป็นข้อจำกัดของโปรแกรม Aspen Dynamics รวมทั้งออกแบบระบบควบคุมแบบอัตราส่วนของอากาศที่ใช้ในการเผาไหม้และเชื้อเพลิงที่ป้อนเข้าสู่เตาเผา (air to fuel ratio) เพื่อควบคุมปริมาณการปลดปล่อยแก๊สมลพิษดังกล่าว ระบบควบคุมระดับน้ำและความดันของหม้อไอน้ำเพื่อความปลอดภัย และระบบควบคุมความต้องการในการผลิตไอน้ำให้ได้ตามปริมาณที่ต้องการ

ผลการจำลองระบบแสดงให้เห็นว่า ผลลัพธ์จากการจำลองมีความสอดคล้องกับค่าที่วัดจริงจากโรงงานไม้แปรรูปที่จังหวัดสุราษฎร์ธานี โดยใช้ข้อมูลจากโรงงานทั้ง 27 ชุดในการเปรียบเทียบสภาวะการดำเนินงานปกติของระบบผลิตไอน้ำคือ ป้อนไม้ความชื้น 40.5% โดยน้ำหนัก ปริมาณ 1,500 กิโลกรัมต่อชั่วโมง และจากการจำลอง สภาวะที่เหมาะสมในการดำเนินงานของระบบคือ ป้อนอากาศที่อากาศส่วนเกิน 5% และหมุนเวียนแก๊สที่ได้จากการเผาไหม้กลับเข้าสู่เตาเผาในอัตราส่วน

25% รวมทั้งติดตั้งเครื่องอุ่นอากาศ ส่งผลให้สามารถกู้คืนพลังงานความร้อนได้มากถึง 29% และสามารถผลิตไอน้ำได้มากกว่าเดิมถึง 35.4%. ในส่วนของระบบควบคุมสามารถควบคุมปริมาณการปลดปล่อยแก๊สคาร์บอนมอนอกไซด์ (CO) แก๊สไนโตรเจนออกไซด์ (NO<sub>x</sub>) และแก๊สซัลเฟอร์ออกไซด์ (SO<sub>x</sub>) และจัดการกับการเปลี่ยนแปลงของตัวแปรรบกวน (disturbance variables) ได้เป็นอย่างดี

<b>Thesis Title</b>	Design and control of parawood chips combustion boiler process using Aspen Dynamics
<b>Author</b>	Mr. Jirateep Premsuksatian
<b>Major Program</b>	Chemical Engineering (International Program)
<b>Academic Year</b>	2019

## ABSTRACT

In the small scale of boiler process, a typical problem is an improperly controlled of air to fuel ratio during the combustion process. Such poor control causes heat loss and undesired emission production. In this study, the main aim was to make the process green in the sense of energy recovery and regulating the CO, NO<sub>x</sub>, and SO<sub>x</sub> emission by optimization of the operating conditions and design the control system to regulate the optimal conditions using Aspen Plus and Aspen Dynamics. The external flue gas recirculation technique was applied with the process to reduce thermal NO<sub>x</sub>. Air preheater was also designed and applied to preheat the feed air combustion temperature for energy recovery purpose. Dynamic simulation scheme was proposed to overcome a limitation of Aspen Dynamics for solid process, and the air to fuel ratio control was then designed to regulate CO, NO<sub>x</sub>, and SO<sub>x</sub> emission. Boiler level and boiler pressure controllers were designed for safety purpose. And the steam production controller was also designed for achieving the required steam. Rejection of uncertain moisture content of wood chip was considered. The results show that simulation results are consistent with 27 scenarios of the measured data collected by wood manufacturing company in the south of Thailand. The optimal operating condition of the process is 5% excess air and 25% flue gas recirculation with 40.5%wt. moisture content of wood chip and 1,500 kg/hr of wood chip flow rate. The optimal condition with the designed air preheater provided 29% heat recovery in this case and provided 35.4% of steam production higher than original process. The proposed control scheme can regulate the CO, NO<sub>x</sub>, and SO<sub>x</sub> emission under their limitations and can handle disturbance changes very well.



## ACKNOWLEDGEMENT

Firstly, I would like to express my deepest thanks to my advisor, Asst. Prof. Dr. Pornsiri Kaewpradit, who have guided, taught, given valuable information and knowledge in the compilation of this dissertation during the master degree till completed.

Moreover, I am also grateful and thankful to Asst. Prof. Dr. Veerayut Lersbamrungsuk as the chairperson, Assoc. Prof. Dr. Kulchanat Prasertsit, and Assoc. Prof. Dr. Lupong Kaewsichan as the members of thesis committees.

My gratitude goes to 5-Year Bachelor's-Master's Degree Program Scholarship 2018 of Department of Chemical Engineering, Prince of Songkla University for providing financial support.

JIRATEEP PREMSUKSATIAN

## TABLE OF CONTENTS

บทคัดย่อ	V
ABSTRACT	VII
ACKNOWLEDGEMENT	VIII
TABLE OF CONTENTS	IX
LIST OF TABLES	XIII
LIST OF FIGURES	XV
CHAPTER 1 INTRODUCTION	1
1.1 Introduction	1
1.2 Research objectives	3
1.3 Scopes of research	3
1.4 Expected benefits	4
CHAPTER 2 THEORY AND LITERATURE REVIEW	5
2.1. Boiler process	5
2.2. Basics of combustion	6
2.2.1. The effect of excess air on CO, CO <sub>2</sub> , and combustion efficiency	7
2.3. PID controller	10
2.3.1. Proportional Term	10
2.3.2. Integral Term	11
2.3.3. Derivative Term	12
2.3.4. Tuning Method	14
2.3.4.1. Open Loop Method	14
2.4. Air preheater	16
2.4.1. Introduction of an Air preheater	16
2.4.2. Design guidelines	17

2.4.2.1. Tube diameter	17
2.4.2.2. Tube number and length	17
2.4.2.3. Tube Layout, Pitch, and Clearance	18
2.4.2.4. Tube passes	18
2.4.2.5. Shell Diameter	19
2.4.2.6. Baffles	19
2.4.2.7. Fouling Considerations	20
2.4.2.8. Selection of fluids for tube and the shell side	21
2.4.3 Detailed design of Air preheater	21
2.5 Requirement tools	22
2.5.1 Aspen Plus	22
2.5.2 Aspen Dynamics	22
2.6. Literature review	23
2.6.1. Simulation of combustion process and gasification process using Aspen Plus	23
2.6.2. Dynamic simulation of combustion process and gasification process using Aspen Dynamics	24
2.6.3 Air preheater design	25
<b>CHAPTER 3 METHODOLOGY, RESULT AND DISCUSSION</b>	<b>26</b>
3.1. Original parawood chips combustion boiler process of wood manufacturing company	26
3.2. Simulation of parawood chips combustion boiler process	28
3.2.1. Effect of excess air on the pollution emissions, heat loss, and steam production.	32
3.2.1.1. CO, CO <sub>2</sub> , NO <sub>x</sub> , and SO <sub>x</sub> VS excess air	33
3.2.1.2. Stack temperature, heat loss, and steam production VS excess air	38

3.3. Simulation of parawood chips combustion boiler process with flue gas recirculation (FGR)	40
3.3.1. Effect of flue gas recirculation and excess air on the pollution emissions, heat loss, and steam production.	43
3.3.1.1. CO, NO <sub>x</sub> , and SO <sub>x</sub> emissions	43
3.3.1.2. Stack heat loss and Steam production	47
3.4. The Optimum operating condition	49
3.5. Simulation of the parawood chips combustion boiler process with air preheater	52
3.5.1. Theoretical design of air preheater	52
3.5.2. Process simulation combined with air preheater by Aspen Plus	55
3.5.3. Cost estimating of air preheater and controller and payback period calculation	58
3.6. Conventional controller design by Aspen Dynamics	60
3.6.1. Switch the steady state model in Aspen Plus to dynamic model in Aspen Dynamics	60
3.6.2. Result comparison of the approximated model and original model	64
3.6.3. Control loop description	66
3.6.4. Controller tuning parameters	70
3.6.4.1 Boiler level control	71
3.6.4.2 Boiler pressure and Steam production control	74
3.6.5. Robustness test	76
<b>CHAPTER 4 CONCLUSION</b>	<b>81</b>
<b>REFERENCES</b>	<b>84</b>
<b>APPENDIX</b>	<b>89</b>
<b>APPENDIX A OPERATING DATA OF WOOD FACTORY</b>	<b>90</b>
<b>APPENDIX B COEFFICIENT VALUE FOR AIR PREHEATER DESIGN</b>	<b>92</b>

APPENDIX C DETAILED CALCULATION OF AIR PREHEATER DESIGN	96
VITAE	109

## LIST OF TABLES

Table 2.1: Effect of increasing $K_p$ , $K_i$ , and $K_d$ independently [15].	13
Table 2.2. Choosing a Tuning Method [15].	14
Table 2.3. Open-loop Calculation of ( $K_p$ , $T_i$ , $T_d$ ) [15].	16
Table 2.4. Guidelines for positioning the fluids [18].	21
Table 3.1. Composition analysis of parawood chips (as received basis).	27
Table 3.2. Normal operating data of parawood manufacturing company.	30
Table 3.3. Optimum distribution of decomposed product yield (R-YIELD).	31
Table 3.4. The effect of excess air on the amount of CO, NO <sub>x</sub> , and SO <sub>x</sub> ppm (at 1500 kg/hr wood chips flow rate and 40.48% moisture content).	37
Table 3.5. The effect of excess air on the flue gas heat loss at stack and steam production (no flue gas recirculation).	40
Table 3.6. The effect of % excess air and % flue gas recirculation on the amount of CO, NO <sub>x</sub> , SO <sub>x</sub> ppm, and flame temperature (at 1500 kg/hr wood chip flow rate).	46
Table 3.7. The effect of % excess air and % flue gas recirculation on the flue gas heat loss at stack and steam production.	48
Table 3.8. Optimal mass flow rates of air, wood chips, and flue gas recirculation.	50
Table 3.9. Result comparison of the original process and optimal process with and without flue gas recirculation.	50
Table 3.10. Operating and properties data for air preheater design	53
Table 3.11. Designed air preheater specification.	54
Table 3.12. Result comparison of the original process and optimal process with and without air preheater.	56
Table 3.13. Simple payback period calculation.	59

Table 3.14. Comparison between Q-DECOMP value from simulation and from approximate model.	63
Table 3.15. Result comparison of the approximated model and original model.	64
Table 3.16. The result of optimal A/F ratio at different moisture content of wood chips.	68
Table A. Operating data of wood factory.	90
Table B1. Typical values of fouling coefficients and resistances [18].	92
Table B2. Safe working fiber stress (N/mm <sup>2</sup> or MPa) [17].	93
Table B3. The value of U <sub>service</sub> for shell and tube heat exchanger [17].	94
Table B4. TEMA standard tube dimensional data [17].	95
Table C1. Nomenclature.	96
Table C2. Operating and properties data for air preheater design.	99

## LIST OF FIGURES

Figure 2.1. Block flow diagram of the boiler process.	5
Figure 2.2. Combustion Diagram.	7
Figure 2.3. Excess air supplied causes excess O <sub>2</sub> appears in flue gas.	8
Figure 2.4. Too little air causes CO emission.	8
Figure 2.5. The relationship between %theoretical air and O <sub>2</sub> , CO <sub>2</sub> and CO [14].	9
Figure 2.6. The effect of increasing excess air on combustion efficiency (fuel oil) [14].	10
Figure 2.7. The effect of add K <sub>p</sub> (K <sub>i</sub> , and K <sub>d</sub> ) held constant [15].	11
Figure 2.8. The effect of add K <sub>i</sub> (K <sub>p</sub> , and K <sub>d</sub> ) held constant [15].	12
Figure 2.9. The effect of add K <sub>d</sub> (K <sub>p</sub> , and K <sub>i</sub> ) held constant [15].	13
Figure 2.10. Responding of Underdamped system.	13
Figure 2.11. Open Loop of First order system plus dead Time (s-shaped curve) [15].	16
Figure 2.12. Heat exchanger tube layouts. [18].	18
Figure 2.13. A single shell pass and a single tube pass [19].	19
Figure 2.14. 1-2 heat exchanger [19].	19
Figure 2.15. Different type of heat exchanger baffles [18].	20
Figure 3.1. Block flow diagram of the original boiler process of wood manufacturing company in the south of Thailand.	26
Figure 3.2. Process flow diagram of the parawood chips combustion boiler process under normal operating conditions.	29
Figure 3.3. Optimum boiler heat exchanger area by graphical method.	32
Figure 3.4. The comparison between simulated and measured flue gas temperature.	32



Figure 3.5. Effect of excess air on CO and CO <sub>2</sub> mass flow rate.	36
Figure 3.6. Effect of excess air on CO, NO <sub>x</sub> , and SO <sub>x</sub> ppm.	36
Figure 3.8. Effects of excess air on stack temperature and stack heat loss.	39
Figure 3.9. Effects of excess air on steam production.	39
Figure 3.10. (a) Internal flue gas recirculation, (b) External flue gas recirculation.	41
Figure 3.11. Process flow diagram of the parawood chips combustion boiler process with external flue gas recirculation technique	42
Figure 3.12. Effect of excess air and flue gas recirculation on (a) CO, (b) NO <sub>x</sub> , (c) SO <sub>x</sub> , (d) Flame temperature.	45
Figure 3.13. Effects of excess air and flue gas recirculation on (a) stack heat loss, and (b) steam production.	47
Figure 3.14. Process flow diagram of the parawood chips combustion boiler process under optimal conditions.	51
Figure 3.15. Proposed process flow diagram combined with air preheater.	57
Figure 3.16. Approximate model of wood chips decomposition.	61
Figure 3.17. Relationship between (a) heating value Q-DECOMP and wood chips flow rate at different moisture content; (b) specific enthalpy and mass fraction of moisture in wood chips.	62
Figure 3.18. Process flow diagram of approximated model.	65
Figure 3.19. Process simulation with controllers by Aspen Dynamics.	67
Figure 3.20. Relationship between A/F ratio and moisture content of wood chips.	68
Figure 3.21. Structure of “AF_calc” block.	69
Figure 3.22. The effect of proportional gain of “BOILER_LC” controller on (a) Process variable (boiler level), and (b) Controller output (BFW flow rate) at $T_i = 106$ min and $T_d = 0$ min.	72
Figure 3.23. The effect of integral time of “BOILER_LC” controller on (a) Process variable (boiler level), and (b) Controller output (BFW flow rate) at $K_p = 46$ and $T_d = 0$ min.	73

Figure 3.24. Open loop step test for “BOILER_PC” controller.	75
Figure 3.25. Open loop step test for “Steam_flowrate” controller.	75
Figure 3.26. Robustness test in case of wood chips flow rate change (from 1,500 kg/hr to 1,400 kg/hr).	78
Figure 3.27. Robustness test in case of wood chips moisture content change (from 40.5% to 45%).	79
Figure 3.28. Robustness test in case of BFW inlet temperature change (from 100 to 80 °C).	80

## CHAPTER 1

### INTRODUCTION

#### 1.1. Introduction

Combustion is a chemical reaction between the fuels (such as coal, biomass etc.) and oxygen [1]. Chemical energy, which is stored in the fuel, is transformed into the useful heat energy using in the other processes such a boiler process [2]. The boiler is an equipment for producing steam which provides a means for heat of combustion to be transferred to boiler feed water until boiling point [3]. Many factory processes require steam for utilizing in various fields such as food production, power generation etc. For a small scale of the boiler process, a typical problem is improper control of air to fuel ratio during the combustion process [4]. Such the poor control system leads to inefficient combustion process and further causes significant heat losses as well as undesired pollution emission. Then, the green process with a good control structure is then required which aimed at regulating the environmental burden especially for CO, NO<sub>x</sub>, and SO<sub>x</sub> emission and recovering energy for reducing raw material consumption.

The conventional combustion method provides high flame temperature in the furnace although, it operates in optimal air to fuel ratio. Hence, the formation of NO<sub>x</sub> is more released at the high combustion temperature. Flue gas recirculation is an effective technique for reducing NO<sub>x</sub> emission from burner. There are two ways to reduce NO<sub>x</sub>. First, the recirculated flue gases absorb heat from the burner and lower peak flame temperatures resulting in lower the formation of thermal NO<sub>x</sub>. Second, the recirculated flue gases lower the O<sub>2</sub> concentration in burner coming from combustion air, as a result the forming of NO<sub>x</sub> reaction is starved [5].

It is well known that a process simulation is an effective tool to describe behavior of the process as well as the influence of process operating variables on process performances [6]. Aspen Plus is one of the engineering modeling software which is widely used in a process/plant design under a steady-state condition. This is because it has massive benefits in solving the engineering problem such as creating a design of equipment or process, finding an optimal condition of the process, and achieving a process sensitivity analysis. However, Aspen Dynamics is required for the control structure design. Since a limitation of solid dynamic simulation via the Aspen Dynamics, many researchers have studied in this field to overcome the limitation.

Robinson and Luyben (2008) [7] performed the simulation of steady-state coal gasification in the Aspen Plus, and further developed the dynamic modeling of the coal gasification in Aspen Dynamics. High molecular weight hydrocarbon, which has the same hydrogen to carbon ratio founding in coal, is used for representing the coal in the Aspen Dynamics. PI control system was then designed for controlling the performance of the process. Jin et al. (2014) [8] also performed the dynamic modeling of oxy combustion of the coal by using Aspen Dynamics, pseudo coal was proposed. Lan et al. (2018) [9], Gaglianoa et al. (2017) [10], Pei et al. (2013) [11] and Doherty et al. (2013) [12] performed the steady-state simulation of biomass gasification. RYIELDS was used for decomposition of the biomass to the conventional elements, and RGIBBS was used as the fluidized gasifier. The simulation results showed that higher temperature of fluidized bed and higher feed air temperature give higher amount of CO and NO<sub>x</sub> but lower amount of CO<sub>2</sub>. Nevertheless, higher excess air ratio in the combustion process and higher biomass moisture provide lower CO amount. Gamrat et al. (2016) [13] and Shi et al. (2018) [5] performed the effect of flue gas recirculation on NO<sub>x</sub> emissions. In a coke oven heating system referred to [13] the 20% recirculated flue gas resulted in 50% of the NO<sub>x</sub> reduction. In the oxy-fuel natural gas combustion referred to [5], the 40% recirculated flue gas resulted in 85% of the NO<sub>x</sub> reduction.

In this study, main aim was to make the process green by design and simulation control system for recovering heat energy and regulating CO, NO<sub>x</sub>, and SO<sub>x</sub>

emissions of parawood boiler process according to the emission standard regulated by Industrial Estate Authority of Thailand or IEAT. Steady-state process simulation results were initially verified by comparing to the sets of measured data collected by wood manufacturing company in the south of Thailand. For emissions point of view, the optimization of air to fuel ratio was defined by sensitivity analysis. Moreover, the external flue gas recirculation technique was applied with the process to reduce the thermal  $\text{NO}_x$ . For heat recovery point of view, air preheater unit was designed and applied here to preheat the feed air temperature. Dynamic simulation scheme was proposed to overcome a limitation of Aspen Dynamics for solid process. Air to fuel (A/F) ratio control was then designed at the optimal condition to regulate the emissions. Boiler level and boiler pressure controllers were designed for safety purpose. And the steam production controller was also designed for achieving the required steam. Rejection of uncertain moisture content of wood chips was considered. Control robustness test was also investigated to specify the control limits.

## **1.2. Research objectives**

1.2.1. To simulate the process model for a parawood chips combustion boiler process of wood company at Surat Thani province.

1.2.1. To find the optimal operating conditions for a parawood chips combustion boiler process.

1.2.2. To design control system for recovering heat energy and regulating CO emission.

## **1.3. Scopes of research**

1.3.1. Using the 27 scenarios of measured operating data collected by wood manufacturing company from April to July 2018.

1.3.2. Steady state simulation of parawood chips combustion boiler process by using Aspen Plus v.9.

1.3.3. Dynamic simulation and control system design of parawood chips combustion boiler process by using Aspen Dynamics v.9.

1.3.4. Flue gas recirculation technique is applied to reduce  $\text{NO}_x$ .

1.3.4. Air preheater was designed and combined with the simulated process in order to recover the heat energy from flue gas.

1.3.5. Preheated air temperature requirement is above 70 °C.

1.3.6. The optimal operating conditions are defined as optimal air to fuel ratio (optimal excess air) and optimal ratio of flue gas recirculation.

1.3.7. Limitation of the  $\text{CO}$ ,  $\text{NO}_x$ , and  $\text{SO}_x$  emission, which is regulated by the Industrial Estate Authority of Thailand or IEAT, is lower than 690, 200, and 60 ppm respectively.

#### **1.4. Expected benefits**

1.4.1. The simulated process is consistent with the real process.

1.4.2. The optimal operating conditions consist of air to fuel ratio and ratio of flue gas recirculation can provide high energy recovery, higher steam production, and the  $\text{CO}$ ,  $\text{NO}_x$ , and  $\text{SO}_x$  emissions lower than their limitations.

1.4.3. The control system can regulate the set point value and can handle the disturbance changes.

## CHAPTER 2

### THEORY AND LITERATURE REVIEW

#### 2.1. Boiler process

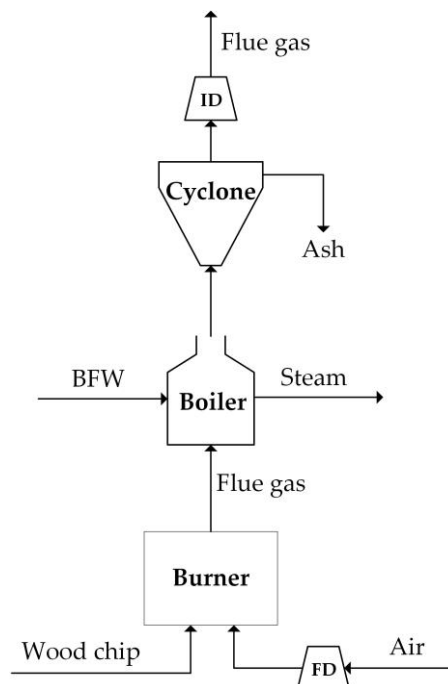


Figure 2.1. Block flow diagram of the boiler process.

The boiler is an enclosed vessel used to produce steam by applying heat energy from combustion to water until acquiring its specified temperature and pressure. Many factory processes require steam for utilizing in various fields such as food production, power generation etc [3]. Figure 2.1 shows the block flow diagram of the boiler process with the wood chips as the raw material.

The boiler system consists of a fuel system, feed water system, and steam system. The fuel system includes equipment used to supply fuel to the burner mix with the air to make the combustion and generate the necessary heat. The generated heat energy is transferred to the boiler feed water (BFW) at the boiler. The

feed water system supplies boiler feed water (BFW) to the boiler and regulates it to obtain the steam demand. The steam system stores and regulates the steam produced in the boiler. Steam is directed flow through a piping system to the required process. Throughout the system, steam pressure is controlled using valves and steam pressure gauges [3].

## 2.2. Basics of combustion

Combustion occurs when fuels such as solid fuel, liquid fuel, or gas fuel react with oxygen in the air to produce heat energy. The heat energy from burning fuels is used for the industrial processes such as producing steam, steam turbine etc. When the complete combustion occurs, carbon dioxide (CO<sub>2</sub>) and water (H<sub>2</sub>O) are produced, formed from the carbon and hydrogen in the raw material and oxygen (O<sub>2</sub>) in the air. On the other hand, the undesired pollution emission such as carbon monoxide (CO), nitrogen oxide (NO<sub>x</sub>) and the heat loss are produced when the incomplete combustion occurs.

The simple example of the combustion reaction is the combustion of methane (CH<sub>4</sub>), the most component of natural gas, with O<sub>2</sub> in the air. When this reaction is balanced, each molecule of CH<sub>4</sub> reacts with two molecules of O<sub>2</sub> forming one molecule of CO<sub>2</sub> and two molecules of H<sub>2</sub>O and then energy is released as heat energy. The reaction as shown in equation (2.1) [14].



In the real combustion process, other products are produced. A typical example of the real combustion process is shown in figure 2.2. Fuel is reacted with O<sub>2</sub> in the air to produce the products shown on the right side. The mixing of O<sub>2</sub> in the air and carbon (C) in the fuel to form CO<sub>2</sub> and generate heat is a complex process, requiring the appropriate mixing turbulence, enough activation temperature and sufficient time for the reactants to come into contact and react. Unless combustion is



appropriately controlled, high amounts of undesired products can form such as CO and soot, result from poor air to fuel ratio or too little air. Other undesired products, such as nitrogen oxides (NO, NO<sub>2</sub>), form in high amounts when the flame temperature is too high. For solid fuels such as coal and wood, ash provides from incombustible elements in the fuel [15].

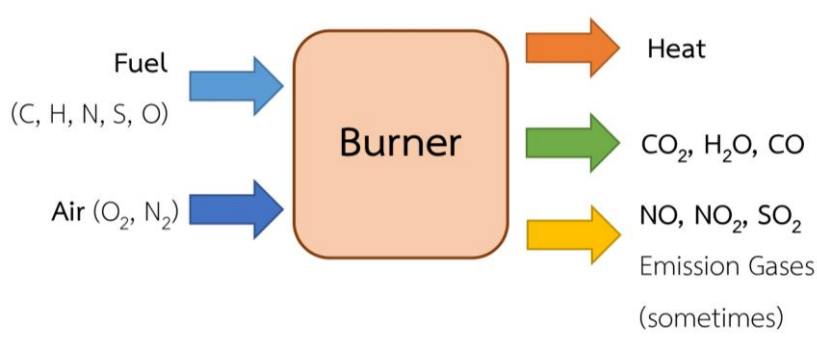


Figure 2.2. Combustion Diagram.

Carbon monoxide, nitrogen oxides, sulfur dioxide, and particles are undesired emissions. These chemical compounds are toxic, contribute to smog and acid rain and can cause respiratory problems. The proper operating conditions in the combustion such as optimal excess air, optimal flame temperature provide less undesired emissions.

### 2.2.1. The effect of excess air on CO, CO<sub>2</sub>, and combustion efficiency

To assure there is sufficient O<sub>2</sub> to completely react with the fuel, extra combustion air feed is supplied. This extra supplied air, called “Excess Air,” is represented as the percent amount of air above the amount of theoretical air for complete combustion. An appropriate estimate of excess air can be calculated using the equation (2.2) [14]. This calculation uses the concentration of O<sub>2</sub> and CO (% by mole) measured in the flue gas at stack.

$$\% \text{ Excess air} = \frac{\% \text{O}_2 - \frac{\% \text{CO}}{2}}{20.9 - \left( \% \text{O}_2 - \frac{\% \text{CO}}{2} \right)} \times 100 \quad (2.2)$$

When  $\text{O}_2$  appears in the flue gas at stack, it means that air was supplied more than the needed point of complete combustion. It is called the excess air condition. Figure 2.3 shows the diagram of excess air condition. When too little air is fed to the burner, the  $\text{O}_2$  is not enough to completely form  $\text{CO}_2$  with all the carbon in the fuel. Instead, some  $\text{O}_2$  reacts with carbon to form carbon monoxide (CO). CO is an extremely toxic gas occurred from incomplete combustion and efforts must be operated to minimize CO formation. Figure 2.4 shows the diagram of too little air condition.

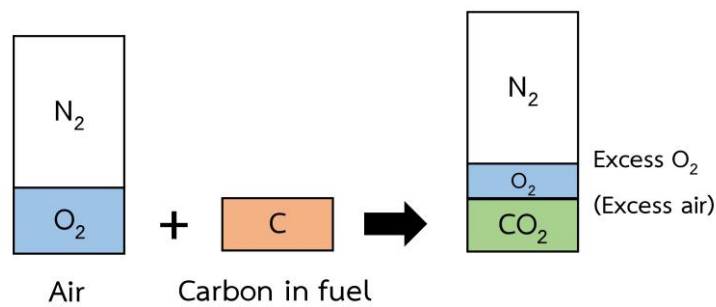


Figure 2.3. Excess air supplied causes excess  $\text{O}_2$  appears in flue gas.

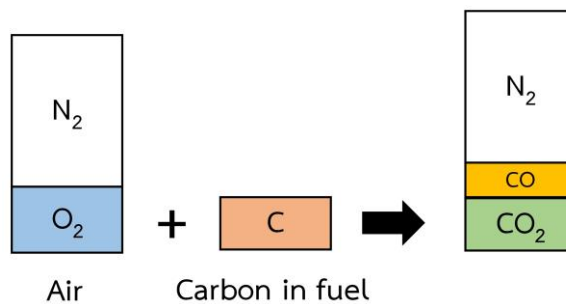


Figure 2.4. Too little air causes CO emission.

Theoretically, the most efficient and cost-effective use of fuels occurs when the  $\text{CO}_2$  concentration in the flue gas at stack is maximized. Theoretically, this occurs when there is enough  $\text{O}_2$  in the supplied air (0% excess air). The theoretical air required for the complete combustion relies on fuel composition and the flow rate of fuel. In real combustion, the actual supplied air must be more than the theoretical air.

The typical relationship between the  $O_2$  fed and the concentration of  $CO_2$  and  $CO$  in the flue gas at stack is shown in figure 2.5 [14]. As the amount of air is increased and approaches 100% of the theoretical air (0% excess air), the amount of  $CO$  decreases rapidly and the amount of  $CO_2$  increases. After the maximum of  $CO_2$  is reached, more combustion air begins to dilute the flue gas, causing the amount of  $CO_2$  to drop. The maximum value of  $CO_2$  relies on the type of fuel used.

Higher excess air causes lower combustion efficiency because it wastes fuel. More supplied air cools the combustion process by absorbing heat energy and transporting heat out the flue gas at stack. For this reason, optimization of supplied excess air can achieve significant fuel savings. Figure 2.6 [14] shows the effect of increasing excess air reduces combustion efficiency.

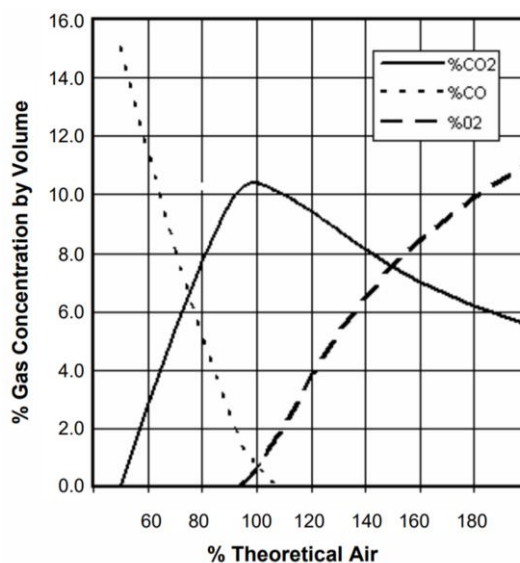


Figure 2.5. The relationship between %theoretical air and  $O_2$ ,  $CO_2$  and  $CO$  [14].

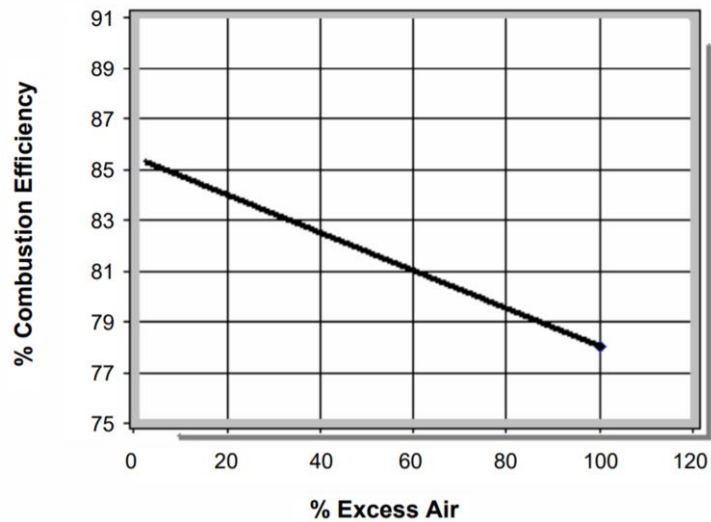


Figure 2.6. The effect of increasing excess air on combustion efficiency (fuel oil) [14].

### 2.3. PID controller

A proportional-integral-derivative controller (PID controller) is a control loop feedback mechanism (controller) widely used in industrial control systems. A PID controller calculates an error value as the difference between a measured process variable and a desired set point. The controller attempts to minimize the error by adjusting the process through use of a manipulated variable [15].

The PID controller algorithm involves three separate constant parameters called three-term control: the proportional, the integral and derivative values, denoted P, I, and D. P depends on the present error, I on the accumulation of past errors, and D is a prediction of future errors, based on current rate of change.

#### 2.3.1. Proportional Term

The proportional response can be adjusted by multiplying the error by a constant  $K_p$ , called the proportional gain constant. The proportional term is given in equation (2.3) [15].

$$P_{out} = K_p e(t) \quad (2.3)$$

A high proportional gain results in a large change in the output for a given change in the error. If the proportional gain is too high, the system can become unstable. In contrast, a small gain results in a small output response to a large input error, and a less responsive or less sensitive controller. Figure 2.7 [15] shows the effect of proportional gain ( $K_p$ ) on output response.

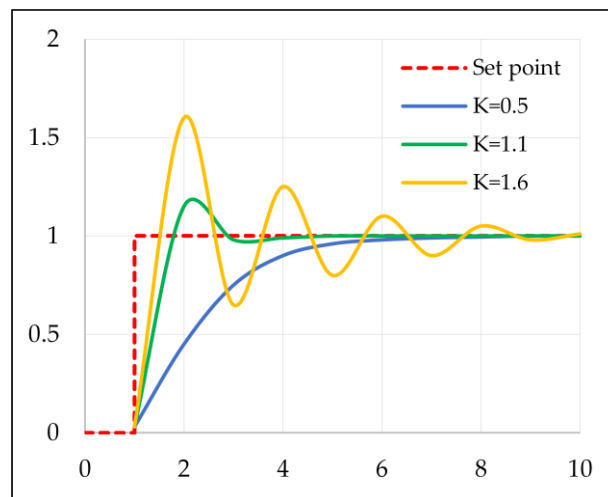


Figure 2.7. The effect of add  $K_p$  ( $K_i$ , and  $K_d$ ) held constant [15].

### 2.3.2. Integral Term

The integral in a PID controller is the sum of the instantaneous error over time and gives the accumulated offset that should have been corrected previously. The integral term is given in equation (2.4) [15].

$$I_{out} = K_i \int_0^t e(t) dt, \quad K_i = \frac{K_p}{T_i} \quad (2.4)$$

The integral term accelerates the movement of the process towards set-point and eliminates the residual steady-state error that occurs with a pure proportional controller. However, since the integral term responds to accumulated

errors from the past, it can cause the present value to overshoot the set-point value. Figure 2.8 [15] shows the effect of  $K_i$  on output response.

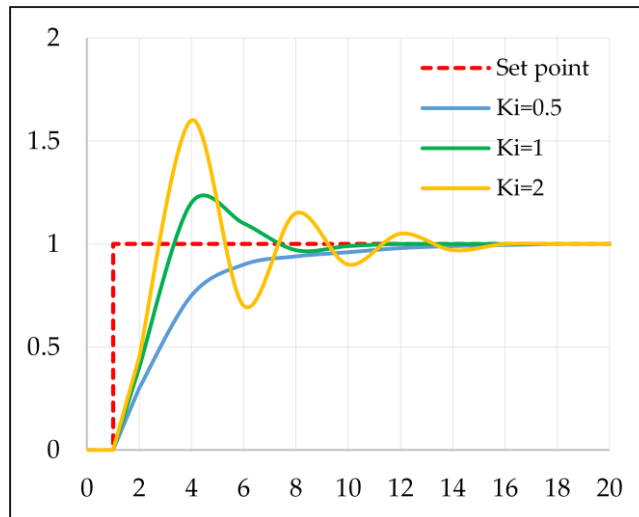


Figure 2.8. The effect of add  $K_i$  ( $K_p$ , and  $K_d$ ) held constant [15].

### 2.3.3. Derivative Term

The derivative of the process error is calculated by determining the slope of the error over time. The derivative term is given in equation (2.5) [15].

$$D_{out} = K_D \frac{d}{dt} e(t), K_D = K_p T_D \quad (2.5)$$

Derivative action predicts system behavior and thus improves settling time and stability of the system. An ideal derivative is not causal, so that implementations of PID controllers include an additional low pass filtering for the derivative term, to limit the high frequency gain and noise. Derivative action is seldom used in practice though - by one estimate in only 20% of deployed controllers- because of its variable impact on system stability in real-world applications. Figure 2.9 [15] shows the effect of  $K_d$  on output response. Table 2.1 [15] shows the effect of increasing  $K_p$ ,  $K_i$ , and  $K_d$  on Rise Time, Overshoot, Settling Time, Steady-State Error, and Stability.

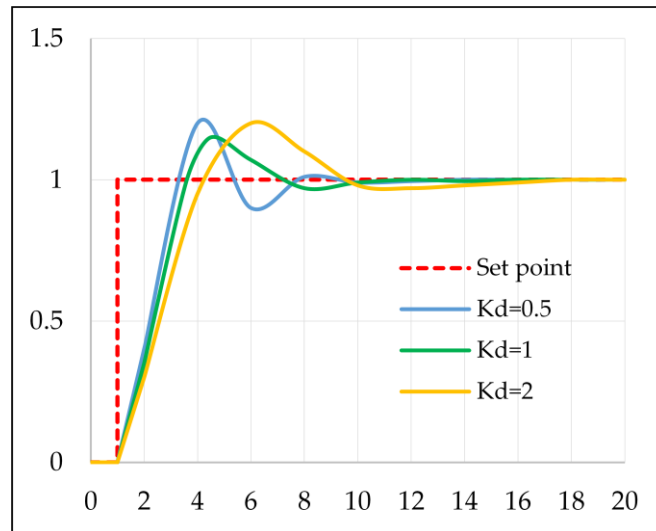


Figure 2.9. The effect of add  $K_d$  ( $K_p$ , and  $K_i$ ) held constant [15].

Table 2.1: Effect of increasing  $K_p$ ,  $K_i$ , and  $K_d$  independently [15].

Parameter	Rise Time	Overshoot	Settling Time	Steady-State Error	Stability
$K_p$	Decrease	Increase	Small Change	Decrease	Decrease
$K_i$	Decrease	Increase	Increase	Eliminate	Degrade
$K_d$	Minor Change	Decrease	Decrease	No Effect	Improve if $K_d$ small

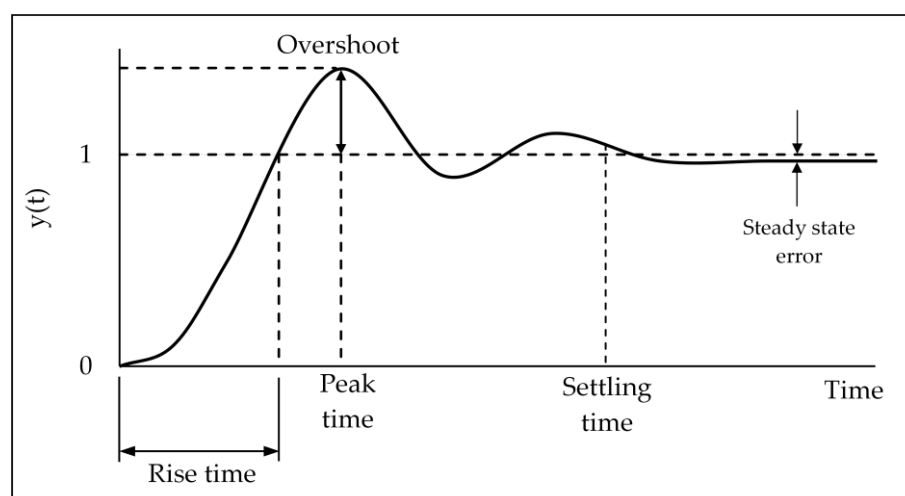


Figure 2.10. Responding of Underdamped system.

### 2.3.4. Tuning Method

There are many means for tuning a PID controller. The most effective methods normally involve the development of some portion of the process model, then selecting P, I, and D based on the dynamic model parameters.

The choosing of the method will depend on whether or not the control loop can be taken "offline" mode for tuning, and depend on the response time of the process. If the process can be taken offline, the best tuning method often involves subjecting the system to a step change in input. Then, measuring the output as a function of time, and using the output response to define the control parameters. Table 2.2 [15] shows the advantages and disadvantages of 3 different tuning methods.

Table 2.2. Choosing a Tuning Method [15].

Method	Advantages	Disadvantages
Manual Tuning	No math required , Online	Requires experienced personnel
Ziegler-Nichols	Proven Method, Online	Process upset, some trial-and error, very aggressive tuning
Cohen-Coon	Good process models	Some math; offline; only good for first-order processes

#### 2.3.4.1. Open Loop Method

In this method, the PID controller is tuned in open loop, the system is isolated from the process plant. First a step change of input is applied to the plant and the system response curve is obtained. Using the system response curve with one of the First Order Plus Dead Time (FOPDT) estimation methods an approximation of the process is calculated. Knowing  $K_m$ ,  $\tau$  and  $t_d$  the PID parameters can be evaluated



from the correlations according to the method used. First Order Plus Dead Time (FOPDT) is given in equation (2.6) [15].

$$G(s) = \frac{K_m}{\tau_m s + 1} e^{-t_d s} \quad (2.6)$$

- **Ziegler-Nichols Open Loop Method**

The Ziegler-Nichols open-loop method is also referred to as S-shaped curve method, because it tests the open-loop response of the process to a change in the control variable output as shown in figure 2.11. This method requires that the response of the system be recorded, especially by using the software on the computer. Once process response values are found, they can be put into the equation of Ziegler-Nichols with specific multiplier constants for the gains of a P, PI, or PID controller.

- **Tuning Procedure**

1. Performing an open loop input step test.
2. From the system reaction curve as shown in figure 2.11 [15] determine the dead time ( $t_d$ ), the time constant ( $\tau$ ), and the ultimate value that the response reaches at steady-state ( $K_m$ ) for an input step change of  $X_0$ .
3. Defining the loop tuning constants. Plug the values of  $t_d$ ,  $\tau$ ,  $K_m$ , and  $X_0$  to the Ziegler-Nichols open-loop tuning equations for the suitable controller (P, PI, or PID) to calculate the tuning parameters by using the table 2.3 [15].

The PID controller tuned by this method gives in equation (2.7) [15].

$$G_c(s) = K_p \left[ 1 + \frac{1}{T_i s} + T_d s \right] \quad (2.7)$$

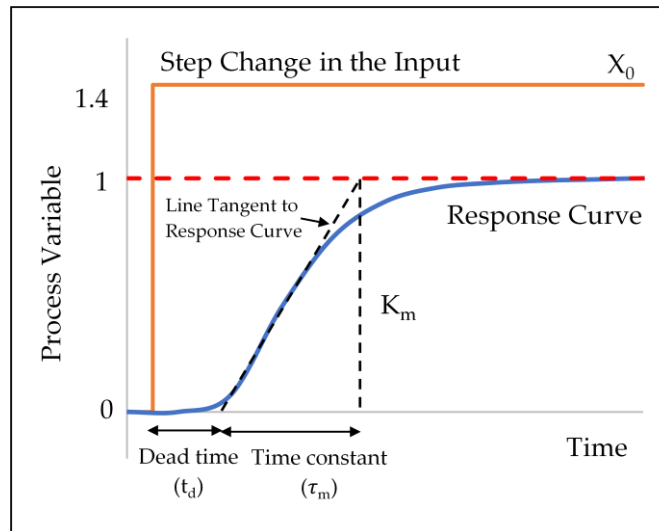


Figure 2.11. Open Loop of First order system plus dead Time (s-shaped curve) [15].

Table 2.3. Open-loop Calculation of ( $K_p$ ,  $T_i$ ,  $T_d$ ) [15].

Controller	$K_p$	$T_i$	$T_d$
P-Controller	$\frac{X_0 \tau_m}{K_m t_d}$	$\infty$	0
PI-Controller	$0.9 \frac{X_0 \tau_m}{K_m t_d}$	$3.3 t_d$	0
PID-Controller	$1.2 \frac{X_0 \tau_m}{K_m t_d}$	$2 t_d$	$0.5 t_d$

## 2.4. Air preheater

### 2.4.1. Introduction of an Air preheater

Air preheater is a heat recovery equipment, which designed to heat air by transferring heat from other sources such as flue gas. It is an essential accessory to improve the thermal efficiency of the boiler. It can reduce the consumption of fuel (wood chips is used in this work), which mean to save production costs.

The purpose of the air preheater in this work is to recover the heat from the boiler flue gas transferring to air before admitting to the burner. The target of air temperature in this work is above 70 °C.

#### **2.4.2. Design guidelines**

Thermal design of a shell and tube heat exchanger includes the consideration of heat transfer area, tube number, tube length and diameter, tube layout, tube pass, shell diameter and thickness, number of baffles, type of heat exchanger, pressure drop, etc. Heat exchanger configurations are defined by the standard of the Tubular Exchanger Manufacturers Association or TEMA.

##### **2.4.2.1. Tube diameter**

The common outside diameter sizes of tube are 3/4" and 1" [16]. The most efficient condition for heat transfer is to have the maximum number of tubes in the shell to increase turbulence motion. The tube thickness is depending on the internal pressure and the corrosion allowance. The wall thickness is defined by the Birmingham wire gage or BWG.

##### **2.4.2.2. Tube number and length**

More tube number causes less tube inside pressure drop. Choosing the appropriate tube number to give optimal tube side velocity of 10-30 m/s for the gas case at nearby atmospheric pressure in order to avoid or reduce the fouling problem when velocity is too low and avoid the tube vibration when velocity is too high [17]. If the velocity cannot be achieved in a single pass consider increasing the number of tube passes. Tube length is defined by considering the required heat transfer and pressure drop constraints. The longer tube is mean higher pressure drop.

### 2.4.2.3. Tube Layout, Pitch, and Clearance

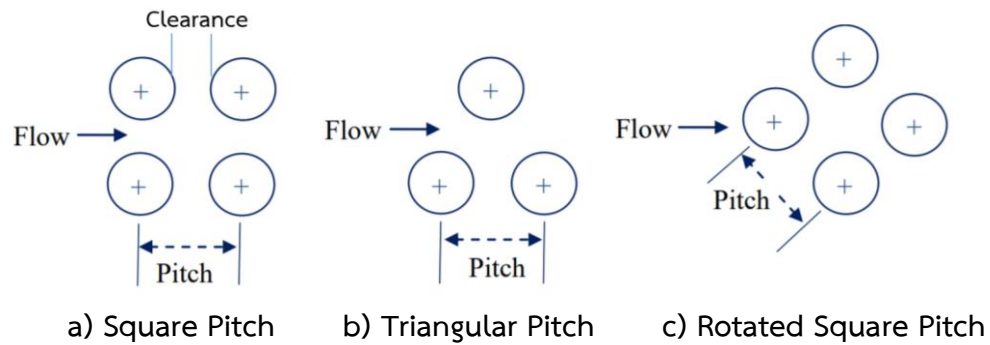


Figure 2.12. Heat exchanger tube layouts. [18].

Figure 2.12 [18] shows the type of tube layouts. Tube pitch is defined by using equation (2.8) [16]. The triangular pattern provides a more strong tube sheet construction. Square pattern simplifies cleaning and has a lower shell side pressure drop. Normally, the tube pitch is 1.25 – 1.33 times of tube outside diameter [16].

$$\text{Tube Pitch} = \text{Tube outside diameter} + \text{Clearance} \quad (2.8)$$

### 2.4.2.4. Tube passes

The number of tube passes is chosen to get the required tube side fluid velocity in order to obtain an appropriate heat transfer coefficient and in order to reduce scale formation. The tube passes vary from 1 to 16. The tube passes of 1, 2 and 4 are commonly used [18].

The simplest shell-and-tube heat exchanger, called 1-1, which means that there is a single shell pass and a single tube pass as shown in figure 2.13 [19]. The most of shell and tube heat exchangers have multiple passes to enhance the heat transfer. Figure 2.14 [19] is an example of a 1-2 heat exchanger (1 shell pass and 2 tube passes).



condition. The pressure drop is higher with closer baffle spacing. The types of baffles are shown in figure 2.15 [18]. In case of the cut-segmental baffle, a segment is removed to form the baffle expressed as a percentage of the baffle diameter. Baffle cuts from 15 to 45% are commonly used. A baffle cut of 20 to 25% provides a good heat transfer with an appropriate pressure drop [18]. The percent cut for segmental baffle refers to the cutaway height from its diameter.

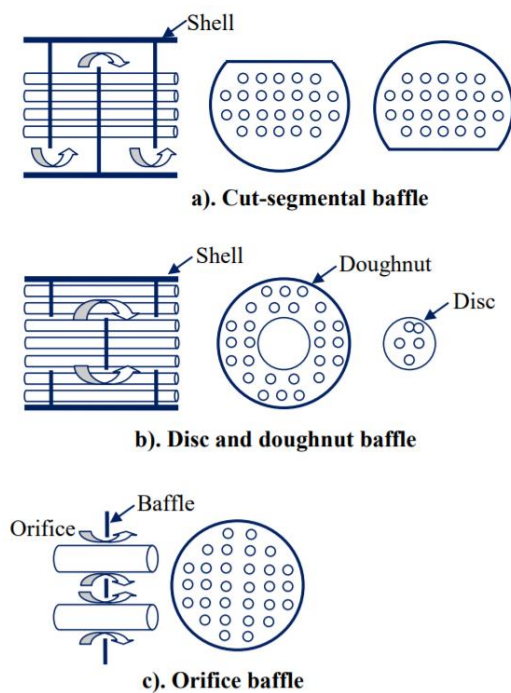


Figure 2.15. Different type of heat exchanger baffles [18].

#### 2.4.2.7. Fouling Considerations

The deposited material reduces the effective heat transfer rate due to relatively low thermal conductivity. So, the total amount of heat transfer with clean surface should be higher to expiate for the performance reduction during operation. Fouling of exchanger increases the cost of additional energy due to the bad performance of exchanger, construction due to oversizing, and cleaning for removing deposited materials [18]. The effect of fouling is considered in the design of heat

exchanger by including the tube side and shell side fouling resistances. Normal values for the fouling coefficients and resistances are shown in Table B1 [18] in Appendix B.

#### 2.4.2.8. Selection of fluids for tube and the shell side

Fluid designation of the shell side and tube side has massive effects on the design of heat exchanger. The guidelines for positioning the fluids are given in table 2.4 [18].

**Table 2.4. Guidelines for positioning the fluids [18].**

Tube-side fluid	Shell-side fluid
Corrosive fluid	Condensing vapor (unless corrosive)
Cooling water	Fluid with large temperature difference (>40°C)
Fouling fluid	High flow rate
High-pressure steam Hotter fluid	Pressure drop constraint
Less viscous fluid	No suspension

#### 2.4.3 Detailed design of Air preheater

Air preheater type in this work is a shell and tube heat exchanger which is the flue gas is inside the tube and the air is inside the shell. The design method based on the theoretical design refers to Sukmanee (2015) [17] as shown in Appendix C.

## 2.5 Requirement tools

### 2.5.1 Aspen Plus

ASPEN is an abbreviation of Advanced System for Process ENgineering. It is based on the flowsheet simulation. The flowsheet simulation is computer software which is used to simulate quantitatively model a chemical process, which, in addition to the main reactor unit, also includes pre and post-treatment processes. Aspen Plus provides us to predict the behavior of the process using fundamental engineering relationships such as mass, mole, and energy balance equations of thermodynamics, thermodynamic relationships for reaction and non-reaction process, rate correlations for heat, momentum, and mass transfer, and data of reaction stoichiometry and kinetic [20].

Aspen Plus gives reliable data of thermodynamic, reasonable operating conditions, and rigorous equipment models, Aspen Plus can simulate real plant behavior. With Aspen Plus process simulator, we can design better processes and increase the profit [20].

### 2.5.2 Aspen Dynamics

Aspen Dynamics takes steady-state process simulation to the unsteady-state process, providing you to create dynamic simulation processes for better analysis of plant safety and behavior. Aspen Dynamics can completely process control design, safety studies, and failure analysis. Develop paths for start-up, shutdown and other transition conditions. Aspen Dynamics relies on a database with 127 property packages, 37,000 components, and 5+ million data points and interaction parameters. Use the reliable state of the activity coefficient models and equations of state [21].



## 2.6. Literature review

### 2.6.1. Simulation of combustion process and gasification process using Aspen Plus

Lan et al. (2018) [9] performed the simulation of wood flour gasification-gas turbine combustion by using Aspen plus. The objective were to develop the model and to predict the performance of gasifier process and power generation. There have 3 simulation models consist of gasification model, gas cleaning model and gas turbine combustion model. For the gasification model, the RYIELDS reactor was used for decomposition of the biomass to conventional elements and the RGIBBS reactor was used as the fluidized gasifier. The RKS-BM physical properties method was used for gasification model. For the combustion model, the RGIBBS reactor was also used for representing the burner. The result of the simulation is consistent with the experimental result. At higher temperature of fluidized bed, the amount of CO increased significantly while the amount of CO<sub>2</sub> decreased. The simulated data of the amount of CO and CO<sub>2</sub> are lower than the experimental results. At higher equivalent ratio (ER), the amount of CO increased while the amount of CO<sub>2</sub> decreased.

Gaglianoa et al. (2017) [10] performed the simulation of equilibrium based model of biomass gasification by using Aspen Plus. The RYIELDS and RGIBBS reactors were also used for representing the gasification reactor.

Pei et al. (2013) [11] performed the simulation of oxy-coal combustion for a 300 MW pulverized coal-fired power plant by using Aspen Plus. The RYIELDS block was used for simulating the coal decomposition process. The RGIBBS block was used to model the combustion reaction that comes to chemical equilibrium and phase equilibrium. They founded that the increasing in excess oxygen ratio in combustion process led to decrease in the amount of CO while the amount of CO<sub>2</sub> increased. The increasing in furnace temperature led to decrease in the amount of CO<sub>2</sub> while the

amount of CO, NO<sub>x</sub>, and SO<sub>2</sub> increased. The amount of CO increased hugely when the flame temperature more than 1,200 °C.

Doherty et al. (2013) [12] performed the simulation of biomass Circulating fluidized bed gasifier by using Aspen plus. They founded that the increasing of air feed temperature led to an increase in the amount of CO while the amount of CO<sub>2</sub> decreased. In addition, the increase of biomass moisture content led to a decrease in the CO emission.

### **2.6.2. Dynamic simulation of combustion process and gasification process using Aspen Dynamics**

Robinson and Luyben (2008) [7] performed the simulation of steady state coal gasification in Aspen plus and the approximate dynamic model of coal gasification in Aspen dynamics. They used the high molecular weight hydrocarbon (C<sub>18</sub>H<sub>20</sub>), which have the same hydrogen to carbon ratio founding in coal, representing the coal in exporting to Aspen Dynamics. They used the RCSTR model representing the partial oxidation zone. The heat duty in RCSTR was dissociation heat of psuedofuel (C<sub>18</sub>H<sub>20</sub>) which was constant heat duty. The kinetic reactions which defined in RCSTR were the partial oxidation of the hydrocarbon, the water gas shift reaction, methanation reaction, oxidation of carbon monoxide reaction, and hydrogen sulfide production reaction. The steady state model in Aspen Plus was exported to the dynamic model in Aspen Dynamics as a pressure driven simulation. There have 8 PI control structure loops were the flow rate control of fuel feed, the ratio control of water to fuel ratio, the ratio control of oxygen to fuel, combustion temperature cascade control in the RCSTR by adjusting oxygen to fuel ratio, RCSTR pressure control and temperature of gas leaving control. The Tyreus-Luyben tuning method was used. The robustness tests were performed by 10% step changing of fuel flow rate and water flow rate. The result shows that the controller can control well at a certain level and the dynamics are quite fast.

Jin et al. (2014) [8] performed the dynamic modeling of oxy combustion of coal by using Aspen Dynamics. The pseudo coal was used to represent the real coal due to limitation of Aspen Dynamics. The objective of control design is that the amount of O<sub>2</sub> in flue gas within the range from 2 to 7 % mole by manipulating the flow rates of oxygen from cryogenic air separation unit. The robustness test of controller was done under the disturbances step changes of load change and, oxygen purity (from cryogenic air separation unit).

### 2.6.3 Air preheater design

Basheer et al. (2018) [22] performed the design of air preheater to improve boiler efficiency. The objective was to minimize the use of furnace oil which is the liquid fuel for the combustion process. The air preheater was designed by using theoretical design method. The air preheater is a regenerative type. The assumptions in design were negligible heat loss, constant properties, and negligible tube wall thermal resistance and fouling factors. The using of value of overall heat transfer coefficient is 65 W/m<sup>2</sup>-°C. The data collected for design were 260°C of flue gas inlet temperature with 1.3 KJ/kg-K of specific heat capacity, 4 ton/hr of steam production, 2,820 kg/min of flue gas flow rate, and 900 kg/min of air flow rate. The requirement of air outlet temperature is at 75 °C. From the design calculation, the area of heat transfer is 32.6 m<sup>2</sup>, tube length is 10.7 m, tube outside diameter is 20 mm, number of tube is 50, number of tube passes is 2, and shell diameter is 270 m. The air preheater can reduce the use of fuel by about 60 kg/hr and can increase boiler efficiency by about 12%.

## CHAPTER 3

## METHODOLOGY, RESULT AND DISCUSSION

## 3.1. Original parawood chips combustion boiler process of wood manufacturing company

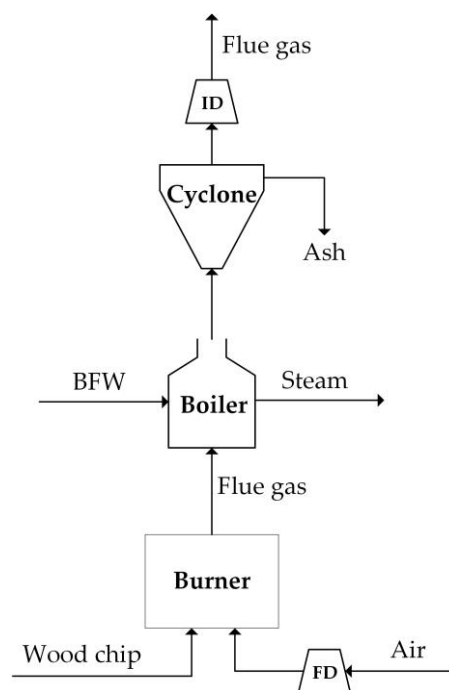


Figure 3.1. Block flow diagram of the original boiler process of wood manufacturing company in the south of Thailand.

The boiler is an equipment used to generate steam by applying heat energy to boiler feed water (BFW). Heat energy is produced from a combustion of fuel in burner. The generated heat energy is transferred to BFW providing clean steam. Figure 3.1 shows block flow diagram (BFD) of the original parawood chips combustion boiler process of wood manufacturing company in the south of Thailand. Here, parawood chips is used as a combustion raw material, and its composition analysis is shown in table 3.1 Combustion air is fed to the burner via forced draft (FD) fan. Process

steam capacity in this case is 4-7 ton/hr at steam pressure of 5.5 bar. Flue gas from boiler is passed through a cyclone in order to separate ash before discharging through stack.

Main disadvantage of the original process is the combustion process operates without A/F ratio control providing inefficient combustion, significant heat loss, and undesired emission production especially CO, NO<sub>x</sub>, and SO<sub>x</sub> [4]. The emissions are focused by controlling A/F ratio at its designed value. Moreover, flue gas recirculation technique was applied to reduce NO<sub>x</sub> emissions. Another disadvantage is the flue gas at stack still have high energy content which can be recovered to the process. Air preheater is an interesting option to improve thermal efficiency of the boiler process by transferring the heat energy from flue gas to the combustion air.

**Table 3.1. Composition analysis of parawood chips (as received basis).**

Parameter	Unit	Result
<b>Proximate analysis</b>		
Moisture content	wt %	40.48
Volatile matter	wt %	48.55
Fixed carbon	wt %	10.17
Ash content	wt %	0.80
H.H.V.	kcal/kg	2,895
L.H.V.	kcal/kg	2,251
<b>Ultimate analysis</b>		
Carbon	wt %	29.67
Hydrogen	wt %	8.15
Nitrogen	wt %	0.097
Sulphur	wt %	0.067
Oxygen	wt %	62.02

### 3.2. Simulation of parawood chips combustion boiler process

In this study, the simulation of parawood chips combustion boiler process was achieved under the normal condition as operating at the wood manufacturing company by Aspen Plus v.9 (as shown in figure 3.2). The reference condition was given as shown in table 3.2. In the Aspen Plus software, parawood chips were defined as non-conventional solid then its proximate analysis, ultimate analysis and heat of combustion (Table 3.1) were required as input. The value of combustion heat used is high heating value (HHV) in dry basis, HCOALGEN and DCOALIGT were used for calculation of its enthalpy and density [23]. R-YIELD and R-GIBBS was considered here to represent a combustion reaction. The R-YIELD block simulates the decomposition of parawood chips by converting the non-conventional solid to (1) conventional gas consisting of  $H_2O$ ,  $H_2$ ,  $N_2$ ,  $O_2$  and S, (2) conventional solid such a C (3) and non-conventional elements such an ash. The R-YIELD also calculates the enthalpy change of the decomposition process (Q-DECOMP) which is transferred to the R-GIBBS block. In this work, FORTRAN code was developed in the R-YIELD block (calculation sheet) for calculating product yield distribution. The R-GIBBS block simulates the equilibrium reactor, it calculates phase and chemical equilibriums by minimizing Gibbs free energy. All possible products of the combustion in the R-GIBBS, consisting of  $H_2O$ ,  $H_2$ ,  $O_2$ , CO,  $CO_2$ ,  $N_2$ ,  $NO_2$ , NO, S,  $SO_2$ ,  $SO_3$ ,  $Cl_2$ , and ash, are in the gas phases except for ash which is in solid phase. Since product components must be initially specified in the R-YIELD block, atomic balance of the defined products was then achieved at first in this study via solver in EXCEL in sense of minimizing sum of absolute difference of defined products and ultimate analysis results. The optimum results are shown in table 3.3.

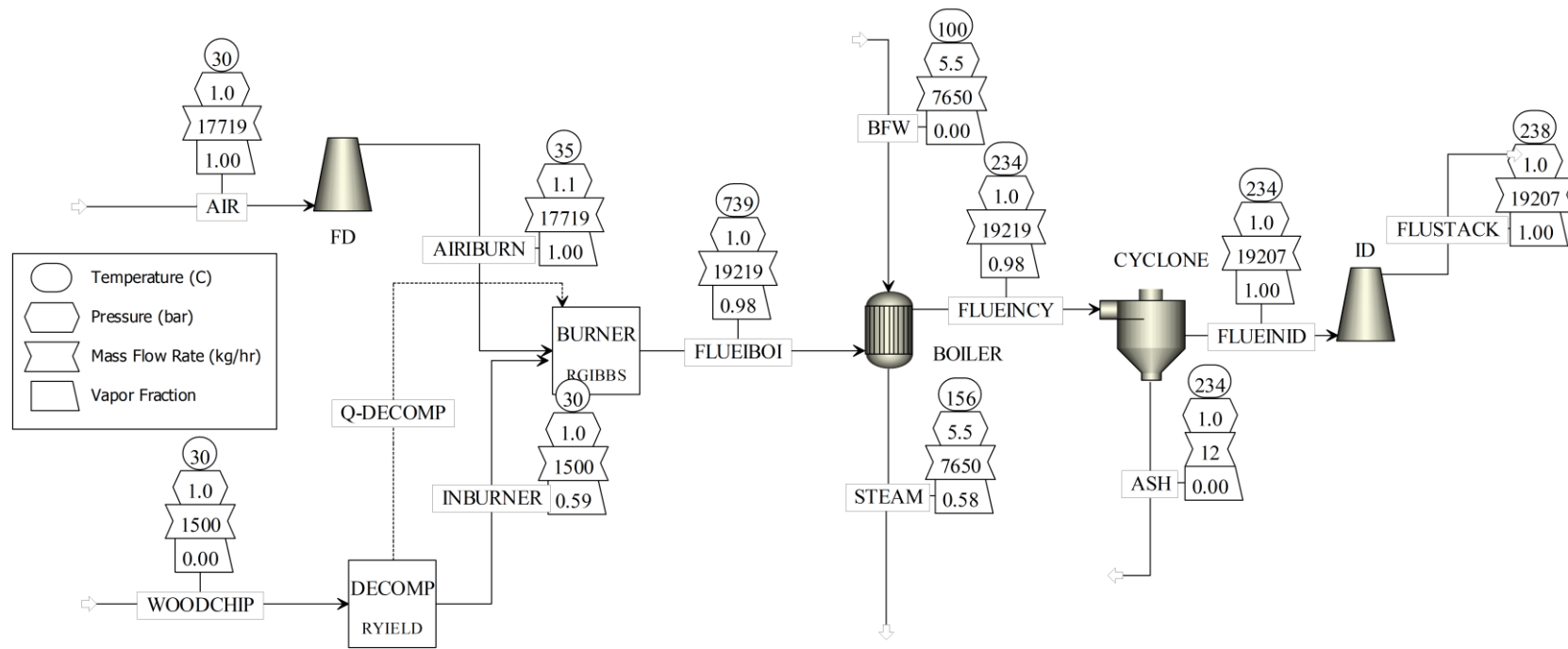


Figure 3.2. Process flow diagram of the parawood chips combustion boiler process under normal operating conditions.

Table 3.2. Normal operating data of parawood manufacturing company.

Stream name / Block name	Description	Value	Unit
AIR	Flow rate	17,700 (9,060)	kg/hr (ft <sup>3</sup> /min)
	Temperature	30	°C
	Pressure	1.01325	bar
	%RH	50	%
WOODCHIP	Flow rate	1,500	kg/hr
	Temperature	30	°C
	Pressure	1.01325 <sup>o</sup>	bar
	Moisture content	40.48	%by wt
BFW	Flow rate	7,650	kg/hr
	Temperature	100	°C
	Pressure	5.5	bar
FD fan	Forced	16	in-water
	Maximum flow rate	9,060	ft <sup>3</sup> /min
ID fan	Induced	8	in-water
	Maximum flow rate	30,000	ft <sup>3</sup> /min

To validate the process simulation, optimum heat transfer area of the boiler was determined by a graphical method. The boiler heat exchanger area was varied to find the optimal value which give the minimum Mean Absolute Error (MAE) of stack temperature (FLUSTACK stream in figure 3.2) deviation between measured and simulated data. In this case, the assumption used for determining the optimum boiler heat transfer area is as following,

1. Inlet data of wood chips flow rate, flow rate and pressure of BFW has been collected from parawood manufacturing company in the south of Thailand. The



operating data has been collected during April – June, 2018 (27 scenarios of data as shown in table A. in Appendix A).

2. Air flow rate is constant at 17,700 kg/hr.
3. Heat transfer coefficient of boiler is assumed as  $850 \text{ W/m}^2 \text{ }^\circ\text{C}$ . (default setting by Aspen)

Figure 3.3 shows that the optimum boiler heat exchanger area is 13.4 sqm with MAE of 12.5. The comparison results between the measured and simulated stack temperature are shown in figure 3.4. It is found that the simulation error is less than 5% (considering with 27 scenarios of the collected data). The error is caused from inconstant, uncontrolled and unmeasured value of the moisture content in the parawood chips since of the rainy season in Thailand.

Table 3.3. Optimum distribution of decomposed product yield (R-YIELD).

**Basis: 100 g total weight of wet basis**

Decomposed elements from atom balance	Calculating in mole atom	Mole atom from ultimate analysis
2.47 mol C	2.47 mol C	2.47 mol C
1.90 mol H <sub>2</sub>	3.80 mol H	8.15 mol H
2.27 mol H <sub>2</sub> O	4.54 mol H	
	2.27 mol O	3.88 mol O
0.710 mol O <sub>2</sub>	1.42 mol O	
0.002 mol S	0.002 mol S	0.002 mol S
0.0035 mol N <sub>2</sub>	0.007 mol N	0.007 mol N
<b>SAE = 0.38</b>		

\* SAE = Sum Absolute Error

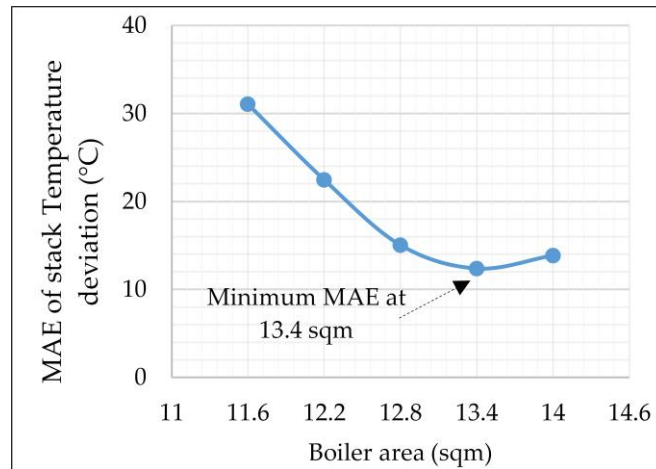


Figure 3.3. Optimum boiler heat exchanger area by graphical method.

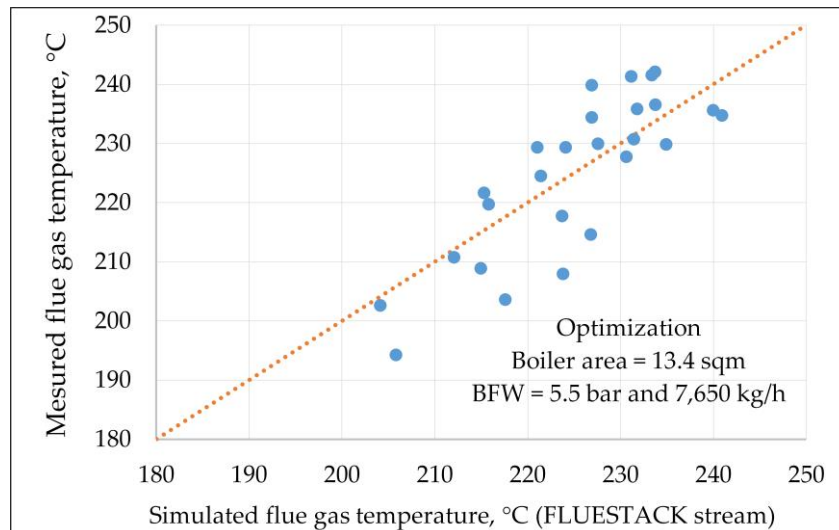


Figure 3.4. The comparison between simulated and measured flue gas temperature.

### 3.2.1. Effect of excess air on the pollution emissions, heat loss, and steam production.

Effect of excess air on flue gas quality (FLUSTACK), was investigated by varying air flow rate (AIR). In this case, mass flow rate of wood chips (WOODCHIP) was

fixed at a normal operating value which is 1,500 kg/hr. The equation for calculating excess air is shown in equation (3.1) referred to [14].

$$\% \text{ Excess air} = \frac{\%O_2 - \frac{\%CO}{2}}{20.9 - \left(\%O_2 - \frac{\%CO}{2}\right)} \times 100 \quad (3.1)$$

Where,  $\%O_2$  is the percent by volume of oxygen containing in flue gas

$\%CO$  is the percent by volume of carbon monoxide containing in flue gas

Sensitivity analysis was performed by varying %excess air. The aim of the sensitivity analysis is to find the optimal range of %excess air, which provides the best condition in terms of maximum steam production, and the CO, NO<sub>x</sub>, and SO<sub>x</sub> emission accords with emission standard regulated by Industrial Estate Authority of Thailand or IEAT. Another aim is to find the optimal condition which is used as a set point in the controller design section.

### 3.2.1.1. CO, CO<sub>2</sub>, NO<sub>x</sub>, and SO<sub>x</sub> VS excess air

Normally, CO emissions was reported in unit of parts per million (ppm). However, there are two types of concentration units; one is "as-measured ppm" and the other is "air-free ppm" [25]. In this work, air-free CO amount (ppm) is focused according to the emission standard. CO air-free ppm can be calculated by converting CO in unit of mg/m<sup>3</sup> to CO in unit of ppm as shown in equation (3.2) referred to [26], and CO in unit of ppm is then further converted to CO in unit of air-free ppm as shown in equation (3.3) referred to [25].

$$CO_{ppm} = \left( \frac{24.45}{MW_{CO}} \right) \times CO_{mg/m^3} \quad (3.2)$$

$$CO_{AFppm} = \left( \frac{20.9}{20.9 - O_2} \right) \times CO_{ppm} \quad (3.3)$$

where;  $CO_{AFppm}$  is air-free carbon monoxide amount, air-free ppm

$CO_{ppm}$  is as-measured carbon monoxide amount, as-measured ppm

$CO_{mg/m^3}$  is carbon monoxide concentration,  $mg/m^3$

$O_2$  is mole percentage of oxygen in flue gas

$MW_{CO}$  is molecular weight of carbon monoxide, 28 g/mol

The emission report in unit ppm under the standard conditions regulated by Industrial Estate Authority of Thailand (IEAT) is at 25 °C, 1 atm, dry basis, and 7 vol%  $O_2$  containing in flue gas [24]. The equation for corrected standard ppm was shown in equation (3.4) [27]. The standard legal of  $CO$ ,  $NO_x$ , and  $SO_x$  emissions for biomass boiler process were 690, 200, and 60 ppm respectively [24].

$$ppm_{std.} = ppm_{measured} \times \left( \frac{20.9\% - 7\%}{20.9\% - \text{actual } O_2\%} \right) \times \left( \frac{1}{1 - \frac{\text{moisture \%}}{100}} \right) \times \left( \frac{273 + 25}{273 + \text{Temp}_{flue}} \right) \quad (3.4)$$

where;  $ppm_{std.}$  is standard ppm at 25 °C, 1 atm, dry basis, and 7 vol%  $O_2$  containing in flue gas, ppm

$ppm_{measured}$  is measured ppm from flue gas, ppm

actual  $O_2$  % is concentration of  $O_2$  containing in flue gas, volume %

moisture % is concentration of moisture containing in flue gas, volume %

$\text{Temp}_{flue}$  is flue gas temperature, °C

Sensitivity analysis was achieved in Aspen Plus. CO, CO<sub>2</sub>, NO<sub>x</sub>, and SO<sub>x</sub> trajectories were monitored in cases of increasing excess air percentage. From the results in figure 3.5, CO amount decreases considerably with increasing %excess air while CO<sub>2</sub> amount increases proportionally with %excess air. Both of CO and CO<sub>2</sub> emissions are moving on their trends until at 0%excess air (complete combustion), both graphs are then flat or constant. Insufficient air flow rate provides incomplete combustion and then CO will be released hugely. On the other hand, too much excess air causes heat loss and decreases combustion efficiency which will make more cost of fuels. Hence, the effects of excess air on heat loss is also important which discussed in the next section.

Figure 3.6, 3.7, and table 3.4 show the values of CO, NO<sub>x</sub>, and SO<sub>x</sub> ppm which changed according to the increase in excess air. For NO<sub>x</sub> emissions, the concentration of NO<sub>x</sub> reaches a maximum value at around 10-15% excess air and then continuously decrease when increasing %excess air. The major formation of NO<sub>x</sub> is thermal NO<sub>x</sub> which caused by the excess O<sub>2</sub>, remaining from the combustion reaction, combines with the N<sub>2</sub> coming from combustion air and reacts at a high combustion temperature.

For SO<sub>x</sub> emissions, the formation of SO<sub>x</sub> comes from the sulfur (S) contained in fuel reacts with the O<sub>2</sub> contained in combustion air. SO<sub>x</sub> formation directly depends on the combustion temperature. It is noted that the optimal range of %excess air is chosen here by considering the amount of CO, NO<sub>x</sub>, and SO<sub>x</sub> ppm which is  $\geq$  73.5% excess air since this provides the emissions less than their limitations (CO < 690 ppm, NO<sub>x</sub> < 200 ppm, and SO<sub>x</sub> < 60 ppm) [24].

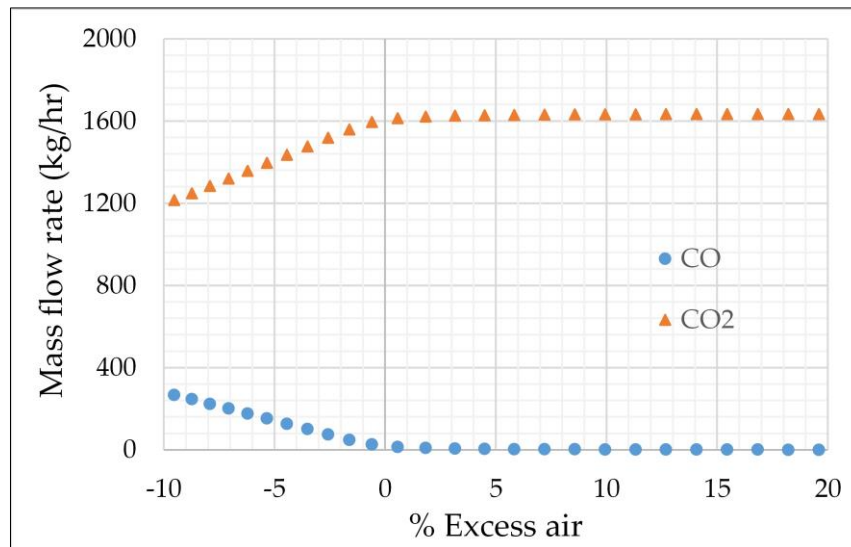


Figure 3.5. Effect of excess air on CO and CO<sub>2</sub> mass flow rate.

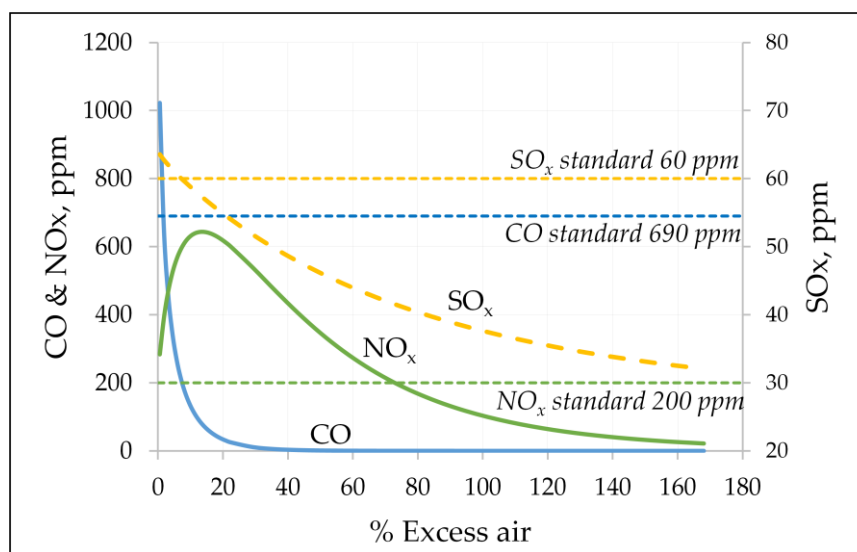


Figure 3.6. Effect of excess air on CO, NO<sub>x</sub>, and SO<sub>x</sub> ppm.

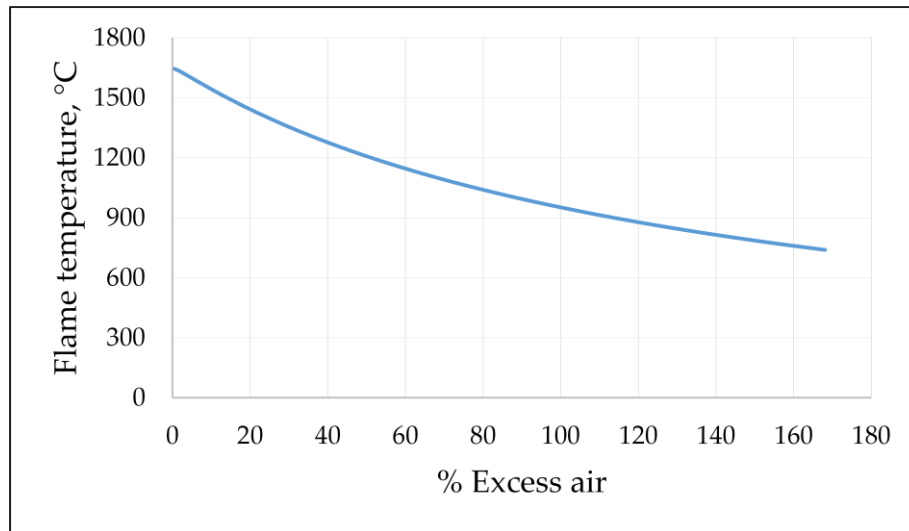


Figure 3.7. Effect of excess air on flame temperature.

Table 3.4. The effect of excess air on the amount of CO, NO<sub>x</sub>, and SO<sub>x</sub> ppm (at 1500 kg/hr wood chips flow rate and 40.48% moisture content).

Air flow rate (kg/hr)	Flue gas at stack					
	%O <sub>2</sub> by mole	%CO by mole	% Excess air	CO, air-free ppm	NO <sub>x</sub> , ppm	SO <sub>x</sub> , ppm
5,400	0.217	2.02E-01	0.56	1023	284	64
5,800	1.177	4.92E-02	5.83	264	566	61
6,100	1.900	2.38E-02	9.93	134	630	59
6,500	2.801	1.03E-02	15.44	61	641	57
6,900	3.627	4.73E-03	20.98	30	611	55
7,500	4.736	1.60E-03	29.30	11	538	52
8,500	6.300	2.99E-04	43.15	2	405	48
9,000	6.972	1.35E-04	50.06	1	346	46
10,000	8.144	2.92E-05	63.84	0.27	249	43
10,500	8.657	1.40E-05	70.71	0.14	211	42
10,700	8.850	1.05E-05	73.45	0.10	197	41
17,719	13.103	1.39E-09	168.06	<0.10	22	32

### 3.2.1.2. Stack temperature, heat loss, and steam production VS excess air

In this section, the effects of excess air on stack temperature, stack heat loss, and steam production were discussed because the appropriate excess air can increase the thermal efficiency of the process and also increase steam production. Heat loss at stack (FLUSTACK) can be calculated by using equation (3.5).

$$Q_{\text{loss}} = \frac{m_{\text{flue}} C_{p\text{flue}}}{10^6} (T_{\text{flue}} - T_{\text{ref}}) \quad (3.5)$$

where;  $Q_{\text{loss}}$  is heat loss of flue gas at stack, MJ/hr

$m_{\text{flue}}$  is flue gas mass flow rate, kg/hr

$C_{p\text{flue}}$  is heat capacity at constant pressure of flue gas, J/kg-K

$T_{\text{flue}}$  is temperature of flue gas at stack, °C

$T_{\text{ref}}$  is reference temperature, 25 °C

From the heat loss equation, the amount of heat loss depends on the temperature and flow rate of flue gas at stack. The results from figure 3.8 and table 3.5 show that increasing excess air increases the stack temperature because excess air is also heated up by a portion of heat from combustion leading to lower flame temperature [28]. Moreover, the increased excess air also increases overall flue gas flow rate. These lead to lower enthalpy and lower heat transfer efficiency of boiler resulting in increasing the temperature of flue gas at stack. From equation (3.5), the terms of  $m_{\text{flue}}$  and  $T_{\text{flue}}$  increase which mean increased heat loss at stack. Hence, the amount of excess air is a key factor which has an influence on heat loss.

For the case of steam production, less heat from flue gas applies to generate steam when increasing excess air since the heat loss at stack increases. As a result, steam production also decreases when increasing excess air (figure 3.9.)



The optimal range of excess air should be operated at possible lowest excess air in order to avoid heat loss. From the discussion in section 3.3.1 and 3.3.2, the optimal excess air is at about 73.5% excess air (10,700 kg/hr air) since it provides emissions lower than their limitations and lowest possible heat loss (2,288 MJ/hr).

73.5% excess air is still too much although it is an optimal excess air for the current process. However, there has a technique called “flue gas recirculation (FGR)”. Flue gas recirculation is an effective technique for reducing  $\text{NO}_x$  and CO emissions from burners. Flue gas recirculation technique is discussed in the next section.

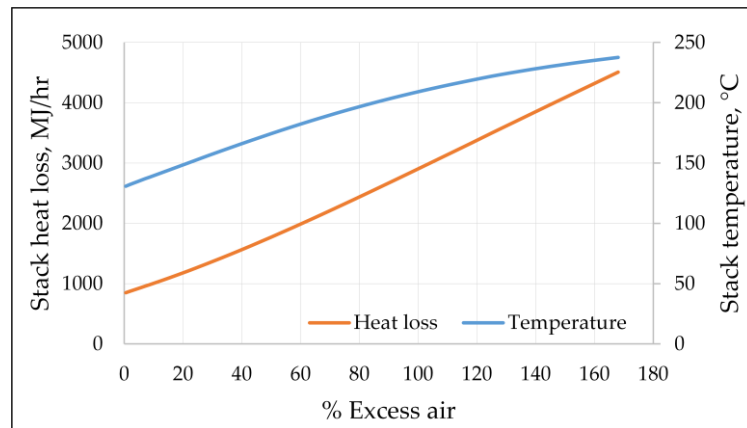


Figure 3.8. Effects of excess air on stack temperature and stack heat loss.

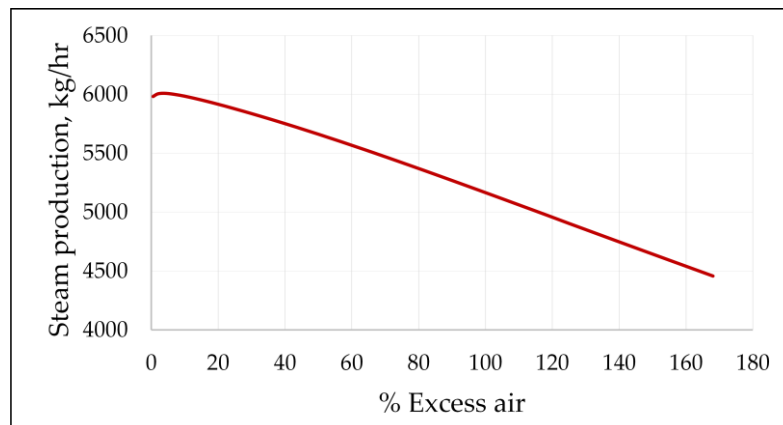


Figure 3.9. Effects of excess air on steam production.

Table 3.5. The effect of excess air on the flue gas heat loss at stack and steam production (no flue gas recirculation).

% Excess air	Flue gas mass flow rate (kg/hr)	$C_p$ (J/kg-K)	Flue gas temperature (°C)	Heat loss at stack (MJ/hr)	Steam production (Kg/hr)
0.56	6,888	1,166	131	850	5,982
5.83	7,288	1,160	136	936	6,004
9.93	7,588	1,156	139	1,004	5,985
15.44	7,988	1,151	144	1,097	5,949
20.98	8,388	1,147	149	1,196	5,909
29.30	8,988	1,141	157	1,352	5,842
43.15	9,988	1,134	169	1,628	5,724
50.06	10,488	1,131	174	1,772	5,661
63.84	11,488	1,126	185	2,072	5,530
70.71	11,988	1,123	190	2,226	5,463
73.45	12,188	1,123	192	2,288	5,436
104.80	14,488	1,115	212	3,016	5,115
151.85	17,988	1,106	233	4,130	4,624
168.06	19,207	1,104	238	4,508	4,457

### 3.3. Simulation of parawood chips combustion boiler process with flue gas recirculation (FGR)

Flue gas recirculation is an effective technique for reducing  $NO_x$  emission from burner. There are two ways to reduce  $NO_x$ . First, the recirculated flue gases absorb heat from the burner and lower peak flame temperatures resulting in lower the formation of thermal  $NO_x$ . Second, the recirculated flue gases lower the  $O_2$  concentration in burner coming from combustion air, as a result the forming of  $NO_x$  reaction is starved.

There are two types of flue gas recirculation, Internal and External recirculation. In the internal recirculation (IFGR) as shown in figure 3.10 (a), flue gas is recirculated inside the furnace back to the burner and applied into the flame. In external recirculation (EFGR) as shown in figure 3.10 (b), flue gas is recirculated outside of the furnace and blend it with fresh air before applied into the burner [5].

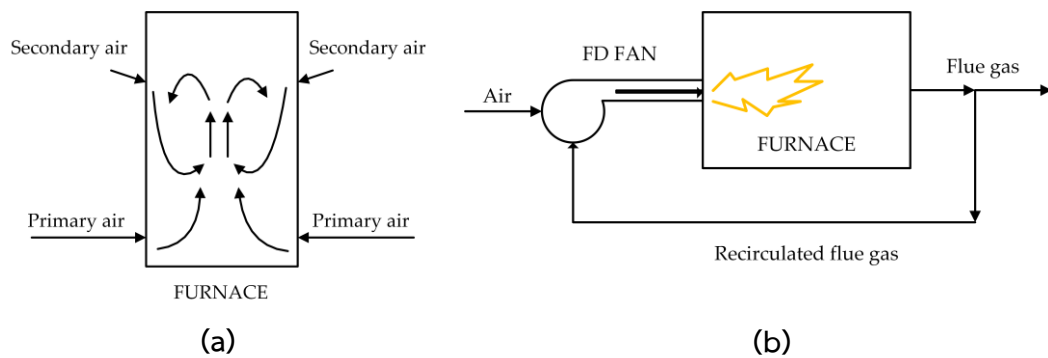


Figure 3.10. (a) Internal flue gas recirculation, (b) External flue gas recirculation.

In this work the external flue gas recirculation (EFGR) technique was used as shown in figure 3.11. The concept is that flue gas is separated from a location downstream of the main boiler bank and is then mixed with the combustion air before fed to the burner. In a coke oven heating system referred to [13], the 20% recirculated flue gas resulted in 50% of the  $\text{NO}_x$  reduction. In the oxy-fuel natural gas combustion referred to [5], the 40% recirculated flue gas resulted in 85% of the  $\text{NO}_x$  reduction. In this section, the optimal flue gas recirculation ratio and the new optimal %excess air were performed in sense of low emissions and low stack heat loss

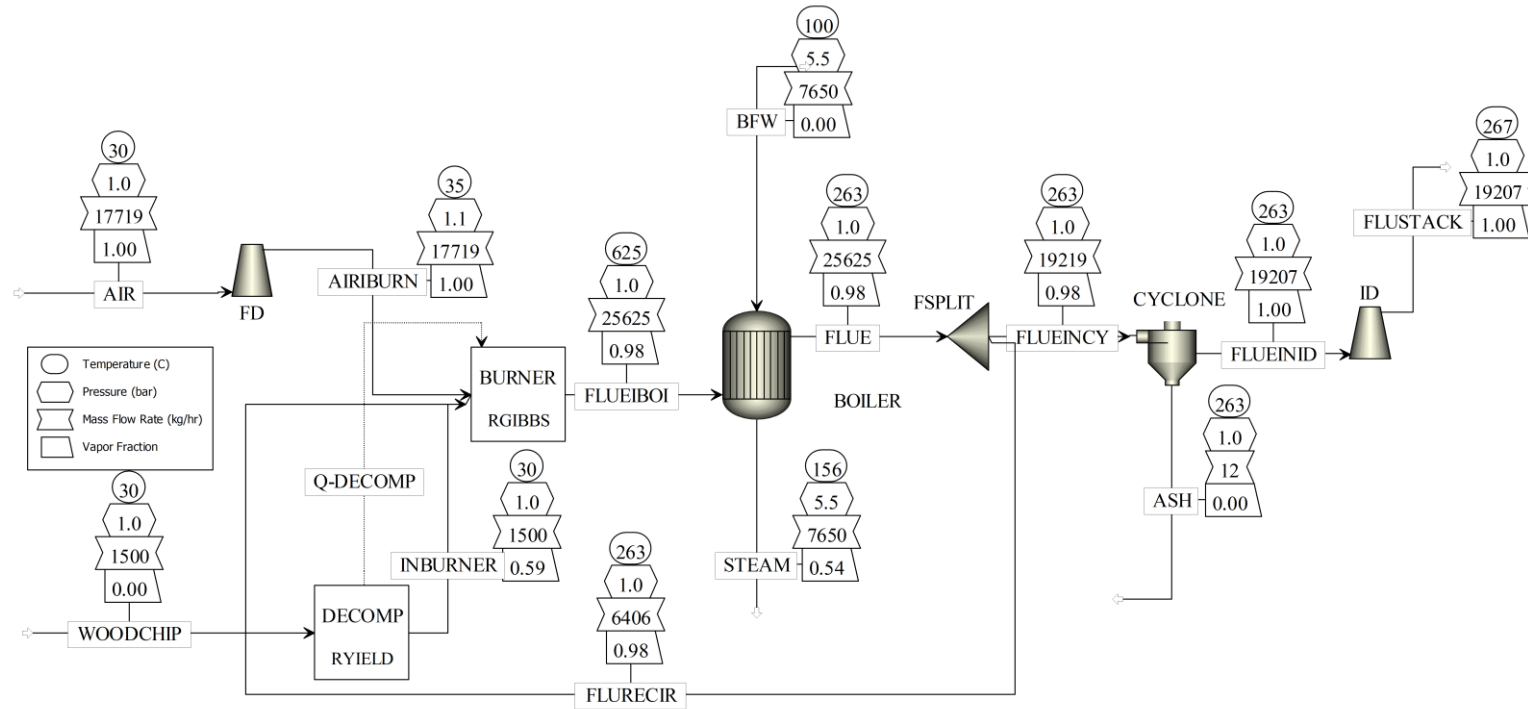


Figure 3.11. Process flow diagram of the parawood chips combustion boiler process with external flue gas recirculation technique

### 3.3.1. Effect of flue gas recirculation and excess air on the pollution emissions, heat loss, and steam production.

The objective of this section is to find the optimal %excess air at the optimal % flue gas recirculation in the sense of low CO, NO<sub>x</sub>, and SO<sub>x</sub> emissions, low heat loss, and high steam production. Sensitivity analysis was investigated by varying air flow rate (AIR) and the percentage of flue gas recirculation (FLURECIR) while mass flow rate of wood chips (WOODCHIP) was fixed at a normal operating value which is 1,500 kg/hr at 40.48 moisture wt %.

#### 3.3.1.1 CO, NO<sub>x</sub>, and SO<sub>x</sub> emissions.

%Excess air and %flue gas recirculation were varied in the range from 0-50% excess air and 0-30% flue gas recirculation. From figure 3.12 (d) shows that increasing of %flue gas recirculation provides a decrease in flame temperature. This is because the recirculated flue gases increase the total gas volume and absorb heat from the burner. The cooling effect obtains from the moisture and CO<sub>2</sub> contained in the flue gas. As a result the NO<sub>x</sub> formation is significantly decrease as shown in figure 3.12 (b). At 25% flue gas recirculation provides the NO<sub>x</sub> emissions under its limitation in every excess air operating and provides the reduction of NO<sub>x</sub> around 70%.

For CO emissions, the CO emissions is significantly decrease while increase %flue gas recirculation. To ensure the result from simulation is reliable, the research (propane as a fuel) referred to [29] concludes that the increasing of flue gas recirculation provides a decrease in CO emissions for the flue gas recirculation < 30%. Another research referred to [30] concludes that the CO emissions are stable while increase flue gas recirculation ratio in the range of 0-30 and significantly increase while

flue gas recirculation ratio more than 30% due to dilution effect and low flame temperature.

For  $\text{SO}_x$  emissions (figure 3.12 (c)), Calpenn Associates, Inc. [31] claimed that the flue gas recirculation for stoker boilers can reduce  $\text{SO}_x$  emissions. It is because of the lower flame temperature provides the lower reaction rate. However, the sulfur content in wood chips is not too high to make the  $\text{SO}_x$  higher than its limitation.

In this section, the criteria for choosing the optimal %flue gas recirculation and %excess air is that it can provide the pollution emissions under their limitations. It is noted that at 25% flue gas recirculation provides the  $\text{NO}_x$  emissions under its limitation in every excess air operating and provides the reduction of  $\text{NO}_x$  around 70%. The optimal flue gas recirculation is chosen at 25%. %Excess air should be selected at a low value because it provides a low heat loss. However, at 0% excess air should not be selected although the emissions are lower than limitations. Because in the real combustion more air must be supplied to burn all fuel completely. Hence, 5% excess air is chosen as optimal excess air.

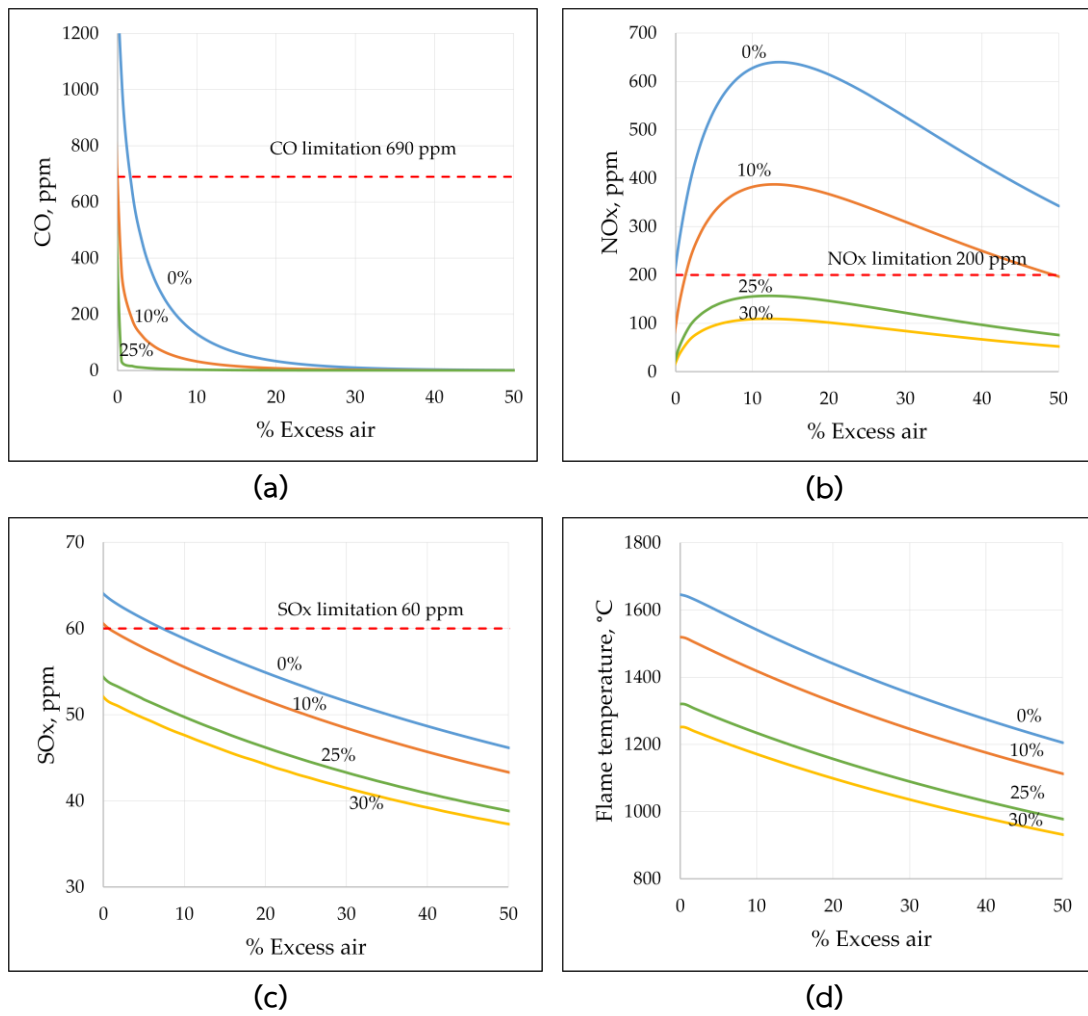


Figure 3.12. Effect of excess air and flue gas recirculation on (a) CO, (b) NO<sub>x</sub>, (c) SO<sub>x</sub>, (d) Flame temperature.

Table 3.6. The effect of % excess air and % flue gas recirculation on the amount of CO, NO<sub>x</sub>, SO<sub>x</sub> ppm, and flame temperature (at 1500 kg/hr wood chip flow rate).

Air flow rate (kg/hr)	Flue gas at stack				Flame temperature, C
	% Excess air	CO, air-free ppm	NO <sub>x</sub> , ppm	SO <sub>x</sub> , ppm	
	0 % flue gas recirculation				
5,400	0.56	1,011	281	64	1,643
6,100	9.93	131	627	59	1,542
6,900	20.98	29	607	55	1,431
7,600	30.69	9	520	51	1,346
8,300	40.38	3	426	49	1,272
9,000	50.06	1	342	46	1,205
	10 % flue gas recirculation				
5,400	0.50	349	145	60	1,518
6,100	10.04	32	382	56	1,418
6,900	21.13	6.62	362	51	1,317
7,600	30.83	1.97	305	48	1,240
8,300	40.53	0.64	247	46	1,172
9,000	50.19	0.22	196	43	1,112
	25 % flue gas recirculation				
5,400	0.48	36	52	54	1,320
5,730 (optimal)	5.02	6	136	52	1,277
6,100	10.16	2.46	156	50	1,233
6,900	21.27	0.47	144	46	1,148
7,600	30.97	0.13	119	43	1,083
8,300	40.66	0.04	95	41	1,027
9,000	50.31	0.01	75	39	976
	30 % flue gas recirculation				
5,400	0.48	13	36	52	1,251
6,100	10.18	0.88	109	48	1,170
6,900	21.30	0.17	100	44	1,090
7,600	31.00	0.05	82	41	1,030
8,300	40.68	0.01	66	39	977
9,000	50.33	<0.01	52	37	930



### 3.3.1.2. Stack heat loss and Steam production

Figure 3.13 (a) and table 3.7 show that stack heat loss increases with the increase in %flue gas recirculation. Figure 3.13 (b) and table 3.7 show that steam production decreases with the increase in %flue gas recirculation because less heat applied into the boiler.

It is noted that both of the optimal %flue gas recirculation and %excess air should be selected at the low value in order not to lose the heat through flue gas. From the discussion in 3.3.1.1 and 3.3.1.2, the optimal %flue gas recirculation is 25% and the optimal %excess air is 5%. They provide 6 CO ppm, 136 NO<sub>x</sub> ppm, 52 SO<sub>x</sub> ppm, and 5,901 kg/hr of steam production.

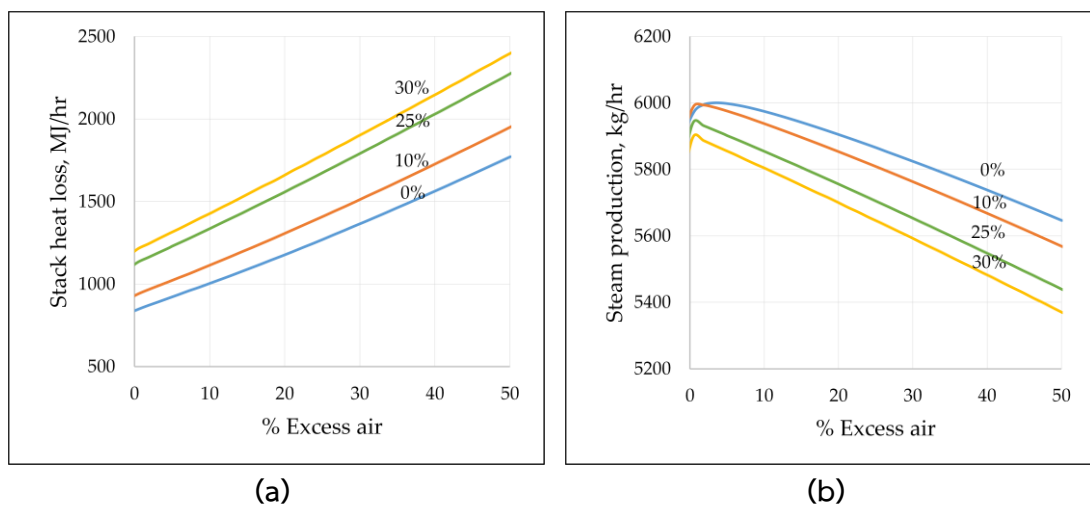


Figure 3.13. Effects of excess air and flue gas recirculation on (a) stack heat loss, and (b) steam production.

Table 3.7. The effect of % excess air and % flue gas recirculation on the flue gas heat loss at stack and steam production.

% Excess air	Flue gas mass flow rate (kg/hr)	$C_p$	Flue gas temperature (°C)	Heat loss at stack (MJ/hr)	Steam production (Kg/hr)
		(J/kg-K)			
<b>0 % flue gas recirculation</b>					
0.56	6,888	1,166	131	850	5,982
9.93	7,588	1,156	139	1,004	5,985
20.98	8,388	1,147	149	1,196	5,909
30.69	9,088	1,140	158	1,378	5,819
40.38	9,788	1,135	166	1,571	5,735
50.06	10,488	1,131	174	1,772	5,661
<b>10 % flue gas recirculation</b>					
0.50	6,888	1,169	142	941	5,999
10.04	7,588	1,159	152	1,115	5,947
21.13	8,388	1,151	163	1,329	5,855
30.83	9,088	1,144	172	1,529	5,768
40.53	9,788	1,139	181	1,737	5,677
50.19	10,488	1,135	189	1,954	5,581
<b>25 % flue gas recirculation</b>					
0.48	6,888	1,176	165	1,134	5,943
5.02 (optimal)	7,218	1,172	170	1,230	5,901
10.16	7,588	1,167	176	1,339	5,853
21.27	8,388	1,158	188	1,588	5,743
30.97	9,088	1,152	198	1,814	5,643
40.66	9,788	1,147	207	2,045	5,541
50.31	10,488	1,142	215	2,282	5,436
<b>30 % flue gas recirculation</b>					
0.48	6,888	1,179	175	1,216	5,908
10.18	7,588	1,170	186	1,433	5,811
21.30	8,388	1,161	199	1,691	5,697
31.00	9,088	1,155	209	1,926	5,593
40.68	9,788	1,150	217	2,165	5,488
50.33	10,488	1,145	225	2,406	5,381

### 3.4. The Optimum operating condition

As the above discussion on section 3.3.1.1 and 3.3.1.2, the optimal excess air and optimal flue gas recirculation is 5% and 25% respectively (or air flow rate of 5,730) at parawood chips flow rate 1,500 kg/hr. They provide 6 CO ppm, 136 NO<sub>x</sub> ppm, 52 SO<sub>x</sub> ppm, and 5,901 kg/hr of steam production which the pollution emissions are under their limitations. The optimal condition was further used as the set point condition in the control structure design to maintain the optimal process operating condition. Inlet feeds at optimal condition are shown in table 3.8. Figure 3.14 shows the process flow diagram of the simulation under the optimal condition.

Comparison between optimal conditions of process with and without flue gas recirculation as shown in table 3.9. It can be seen that the process with flue gas recirculation can operate with lower excess air which provides higher thermal efficiency due to lower heat loss. It can produce steam higher than original process condition about 32.4% and higher than optimal process condition without flue gas recirculation about 8.6%.

Although the optimal excess air and flue gas recirculation can provide higher efficiency of the process. However, another method to improve more efficiency of the process is the heat recovery from remaining heat of flue gas which discussed in the next section.

Table 3.8. Optimal mass flow rates of air, wood chips, and flue gas recirculation.

Stream name	Description	Value	Unit
AIR	Flow rate of supplied air	5,730 (5% excess air)	kg/hr
WOODCHIP	Flow rate of wood chips	1,500	kg/hr
FLURECIR	Flow rate of flue gas recirculation	2,410 (25% recirculation)	Kg/hr

Table 3.9. Result comparison of the original process and optimal process with and without flue gas recirculation.

Process	Supplied air	Flue gas recirculation	CO, air-free ppm	NO <sub>x</sub> , ppm	SO <sub>x</sub> , ppm	Steam production kg/hr
Original process condition	17,719 kg/hr (168 % excess air)	-	<0.01	22	32	4,457
Optimal process condition	10,700 kg/hr (73.5% excess air)	-	0.1	197	41	5,436
	5,730 kg/hr (5% excess air)	25%	7	136	52	5,901

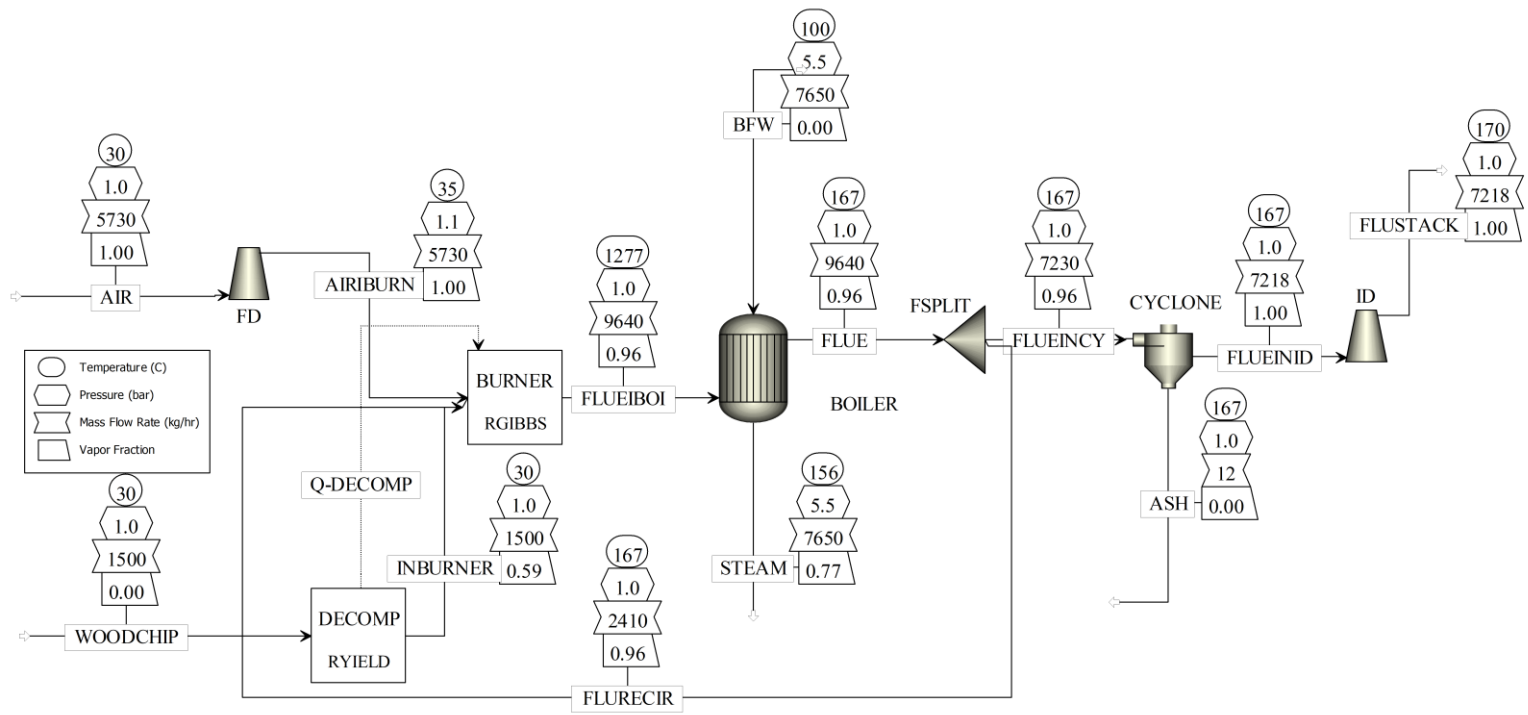


Figure 3.14. Process flow diagram of the parawood chips combustion boiler process under optimal conditions.

### **3.5. Simulation of the parawood chips combustion boiler process with air preheater**

The objective of this section is to improve the efficiency of the process by using the heat recovery method. The remaining heat of flue gas is transferred through fresh air by shell and tube heat exchanger (Air preheater).

#### **3.5.1. Theoretical design of air preheater**

The aim of air preheater is to increase boiler efficiency by transferring heat from flue gas to combustion air before the combustion process. In this work, the requirement of air temperature is higher than 70 °C. The design method based on the theoretical design refers to Sukmanee (2015) [17]. Air preheater is a shell and tube heat exchanger, which flue gas flows inside the tubes and air flows outside. One tube pass was used to prevent fouling of flue gas. The design assumptions are no heat loss, as well as properties of flue gas and air are constant. Operating and properties data for design is shown in table 3.10. The detailed calculation is shown in appendix C. Designed air preheater specification is shown in table 3.11.

Table 3.10. Operating and properties data for air preheater design.

Boiler					
Capacity	7.65	ton/hr, max	Pressure of steam and BFW	5.5	Bar
	4-7	ton/hr	BFW temperature	100	°C
Parawood chips					
Mass flow rate	1,500	kg/hr	Components and calorific value are shown in table 3.1		
Cold side (shell side)			Hot side (tube side)		
Properties	Air		Properties	Flue gas	
$MW_s$	29	kg/kmol	$MW_t$	28	kg/kmol
Mass flow rate ( $W_s$ )	6,876	kg/h	Mass flow rate ( $W_t$ )	8,662	kg/h
Density ( $\rho_s$ )	1.16	kg/m <sup>3</sup>	Density ( $\rho_t$ )	1	kg/m <sup>3</sup>
$Cp_s$	1.02	kJ/kg K	$Cp_t$	1.05	kJ/kg K
Absolute viscosity ( $\mu_s$ )	0.02	mPa.s	Absolute viscosity ( $\mu_t$ )	0.022	mPa.s
Conduction coefficient ( $k_s$ )	0.026	W/m.°C	Conduction coefficient ( $k_t$ )	0.05	W/m.°C
Operating			Operating		
Temperature inlet ( $T_1$ )	30	°C	Temperature inlet ( $t_1$ )	170	°C
			(from simulation)		
Temperature outlet ( $T_2$ ) (defined)	70	°C	Temperature outlet ( $t_2$ ) (calculated)	139	°C
Pressure inlet ( $P_{s1}$ )	105	kPa	Pressure inlet ( $P_{t1}$ )	103	kPa

Table 3.11. Designed air preheater specification.

Detail	Shell side	Tube side
Fluid	Air	Flue gas
Mass flow (kg/h)	6,876	8,662
Inlet Temperature (°C)	30	170
Outlet Temperature (°C)	70	139
Heat duty (kW)	78.08	
No. pass	1	1
Tube Arrangement		Triangular stainless 304
Tube outside diameter (mm)		88.90
Tube pitch (mm)		118.20
Number of Tube		41
Inside diameter (mm)	1,200	82.09
Thickness (mm)	6	3.404
Baffle		
Type	Segmental	
% cut	25 [18]	
Spacing (mm)	1,500.00	
Heat transfer coefficient (W/m <sup>2</sup> .°C)	17.55	
Required heating area (m <sup>2</sup> )	43.42	
Existing heating area (m <sup>2</sup> )	51.53	



### 3.5.2. Process simulation combined with air preheater by Aspen Plus

Figure 3.15 shows the proposed process flow diagram combined with air preheater. The air preheater was used to heat the AIR stream by using the energy from the FLUEINEX stream. At the optimal operating condition (1,500 kg/hr of parawood chips, 5,730 kg/hr or 5% excess air, and 25% flue gas recirculation), air temperature was heated up to 82 °C. The heat recovery was considered at boiler. The results were shown in table 3.12.

It is noted that the effect of preheated air provides more supplied heat which can produce a higher amount of steam. However, the emissions also increase but not more than the limitations. For results of steam production, the optimal process condition with air preheater provides steam production more than the original process about 35.4 % and provides steam production more than the optimal process condition without air preheater about 2.2%. For result of boiler heat duty, the optimal process condition with air preheater provides heat recovery compared with the original process about 29% and provides heat recovery compared with the optimal process condition without air preheater about 1.9%.

It can be seen that the effect of preheated air from 30 °C to 82 °C slightly increases the thermal efficiency and steam productivity. It is suggested that the temperature of preheated air should be more but must consider the increase in heat exchanger price and also pollution emissions.

Table 3.12. Result comparison of the original process and optimal process with and without air preheater.

Process	Supplied air	Flue gas recirculation	CO, air-free ppm	NO <sub>x</sub> , ppm	SO <sub>x</sub> , ppm	Steam production, kg/hr	Boiler heat duty, MJ/hr
Original process	17,719 kg/hr (168 % excess air)	-	<0.01	22	32	4,457	11,398
Optimal process condition	5,730 kg/hr (5% excess air)	25%	7	136	52	5,901	14,422
Optimal process condition combined with air preheater	5,730 kg/hr (5% excess air)	25%	10	172	60	6,033	14,699

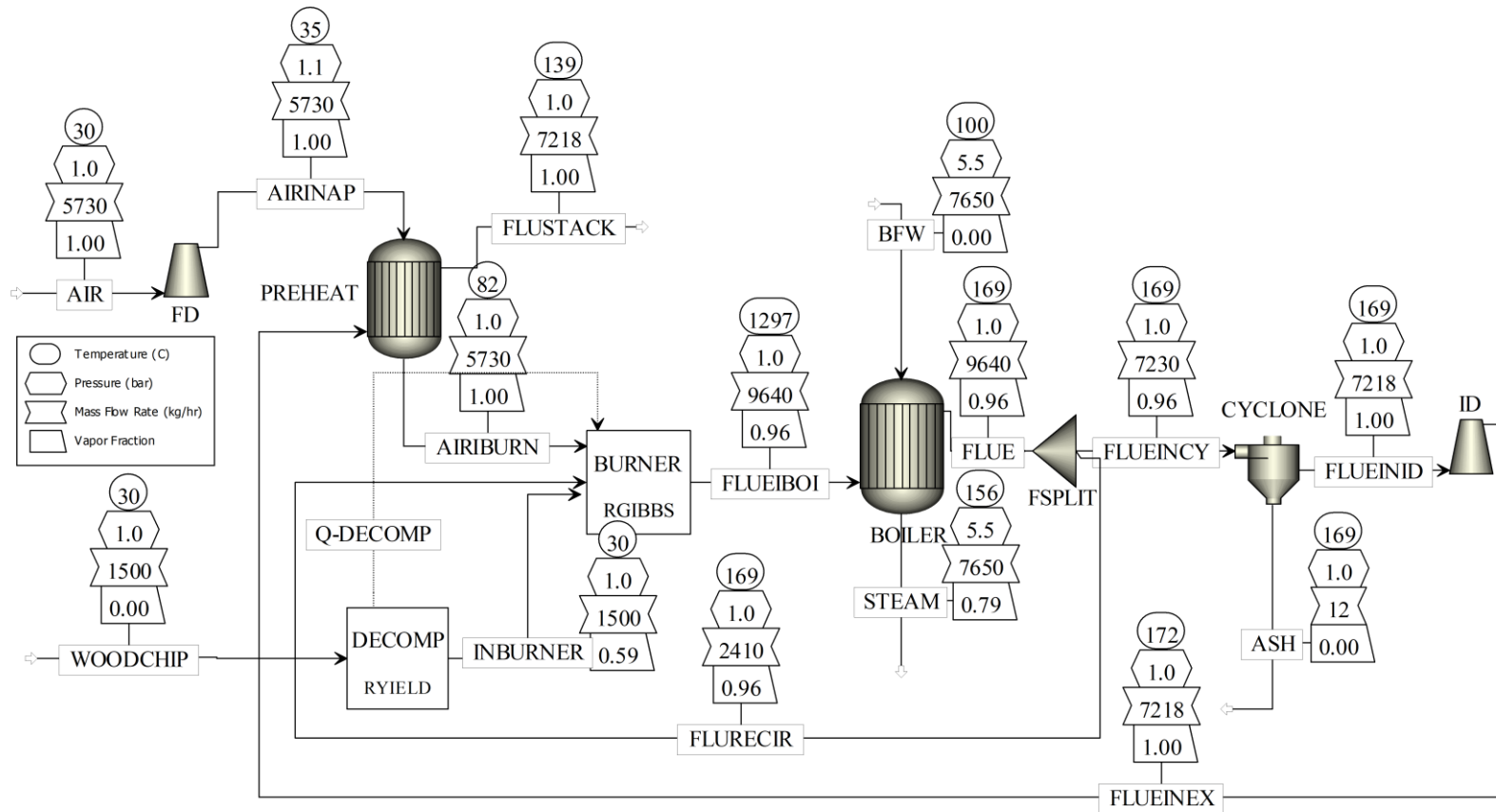


Figure 3.15. Proposed process flow diagram combined with air preheater.

### 3.5.3. Cost estimating of air preheater and controller and payback period calculation

The equation (3.6) and (3.7) [32] are the method for preliminary estimating equipment cost (with controller) which proposed in Chemical engineering design textbook by Towler and Sinnott (2013) [32].

$$C_e \approx (a+bS^n) \approx (32000+70 \times 51.53^{1.2}) \approx 39,935 \text{ USD} \quad (3.6)$$

$$C_{e,\text{total}} \approx C_e \times f_i \times f_m \times \frac{\text{CEPCI}_{2018}}{\text{CEPCI}_{2010}} \times f_L \quad (3.7)$$

$$C_{e,\text{total}} \approx 39,935 \times 3.5 \times 1.3 \times \frac{591.3}{532.9} \times 1.12$$

$$C_{e,\text{total}} \approx 225,812 \text{ USD} \approx 7,113,000 \text{ THB}$$

Where;

- $C_e$  is purchased equipment cost (Carbon steel material) on a U.S. Gulf Coast basis, Jan. 2010 (CEPCI = 532.9, NF refinery inflation index = 2281.6).
- $C_{e,\text{total}}$  is total equipment cost including purchased cost, installation cost, material cost, and location cost.
- $a, b$  are cost constants which equal to 32,000 and 1.2 respectively for floating head shell and tube heat exchanger.
- $S$  is size parameter, area  $\text{m}^2$
- $n$  is exponent depending on the type of equipment which equals to 1.2 for floating head shell and tube heat exchanger.
- $f_i$  is installation factor including controller cost which equals to 3.5 for heat exchanger.
- $f_m$  is material factor which equals to 1.3 for stainless steel 304.
- $f_L$  is location factor which equals to 1.12 for Southeast Asia.

- $CEPCI_{2010}$  is Chemical Engineering Plant Cost Index, Jan. 2010 = 532.9
- $CEPCI_{2018}$  is Chemical Engineering Plant Cost Index, Jan. 2018 = 591.3 [33]

The original process condition (1,500 kg/hr of wood chips and 17,719 kg/hr of air) can produce 4,457 kg/hr of steam. For the optimal process condition combined with air preheater, 1,145 kg/hr of wood chips are used for producing steam at the same flow rate at 4,457 kg/hr. It can be seen that the using of wood chips are reduced =  $1500 - 1145 = 355$  kg/hr of wood chips which can save cost of wood chips around 2.84 million baht per year. The payback period calculation is shown in table 3.13.

**Table 3.13. Simple payback period calculation.**

Variables	Unit	Values
Reducing wood chips consumption	kg/hr	355
Price of wood chips	THB/kg	1 [34]
Operation time	hr/year	8,000
Save cost of wood chips	THB/year	2,840,000
Cost of air preheater and controller	THB	7,113,000
Maintenance cost (assume 4% of total cost [35])	THB	284,520
Total cost	THB	7,400,000
<b>Payback period</b>	<b>year</b>	<b>2.61</b>

### 3.6. Conventional controller design by Aspen Dynamics

The aim of this section is to design PID controller for regulating the optimal condition by adjusting air to fuel ratio. The pollution emissions consist of CO, NO<sub>x</sub>, and SO<sub>x</sub> including steam production are monitored. Moreover, the pressure and level of boiler are controlled for safety purpose.

#### 3.6.1. Switch the steady state model in Aspen Plus to dynamic model in Aspen Dynamics

The steady state model in Aspen Plus was switched to the dynamic model in Aspen Dynamics using flow driven mode. Since solid component (C in INBURNER) and non-conventional components (WOODCHIP and ASH) were not allowed in the Aspen Dynamics, then RYIELD module has to be removed. The approximate model to handle these problems were proposed and described as follows:

1. Ash was assumed to be separated completely from flue gas, then it was not considered in this case. As a result, the cyclone unit was removed.
2. All of the components of parawood chips (C, H, O, S, and N) were totally decomposed into gas phase products (INBURNER). Then, C and H elements were replaced by organic compound or hydrocarbon (C<sub>n</sub>H<sub>n</sub>) [7] Two criteria considered here is as following: (1) major content of wood chips is cellulose, which has the molecular formula as (C<sub>6</sub>H<sub>10</sub>O<sub>5</sub>)<sub>n</sub> and decomposition temperature about 200 °C [36], and (2) atomic ratio of C:H in ash free basis is 8.37:1 by mass. From both criteria above, C<sub>12</sub>H<sub>18</sub> was then chosen, since it has 203 °C decomposed temperature and the mass ratio of C:H is 8:1. Figure 3.16 shows the approximate model of parawood chips decomposition.

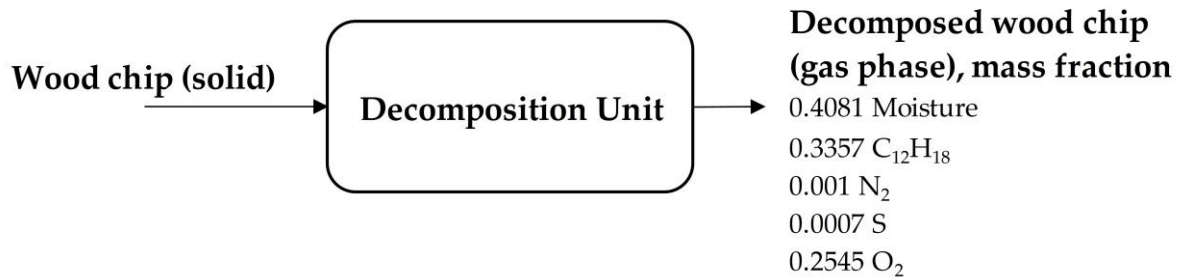


Figure 3.16. Approximate model of wood chips decomposition.

3. The heating energy value of “Q-DECOMP” stream represents the enthalpy change in the decomposition process of parawood chips into its constituent elements [23]. This energy has to be transferred from BURNER (R-GIBBS) to DECOMP (R-YIELDS), however DECOMP was removed due to a limitation of Aspen Dynamics. Then a prediction equation of the Q-DECOMP was developed in this work as a function of wood chips flow rate (1300 - 2200 kg/hr) and wood chips moisture content (30 - 50%). In this case, the relationship between the enthalpy of wood chips decomposition (Q-DECOMP) and wood chips flow rate at different moisture content was a linear function as shown in figure 3.17(a). It can also be seen that the specific enthalpy (or slope of the plot between QDECOMP and wood chips flow rate at specific moisture content) and moisture content of wood chips has a linear relationship as shown in figure 3.17(b). Thus, the linear equation obtained from Figure 3.17(b) was used for predicting the slope value. Then, the predicted slope value was used for calculating QDECOMP which Y-intercept was negligible. The approximate model equation for QDECOMP was shown in equation (3.8). The comparison between Q-DECOMP value from simulation and from approximate model in equation (3.8) was shown in table 3.14.

$$\text{QDECOMP} = \text{Wood chip flow rate} \times [(569.13 \times \text{mass frac moisture content}) - 1246.2] \quad (3.8)$$

4. In order to control the level and pressure of boiler, boiler need to be changed from “HEATX” to “FLASH2” as shown in figure 3.18. The vessel type was also changed from “Instantaneous” to “Vertical” with 4 meters of length and 1 meter of diameter. The unit name “HEATX” was added for carrying the heat from flue gas to boiler which the value of heat duty (stream “QTOBOIL”) need to manually specified in dynamic model by using the value from steady state model.

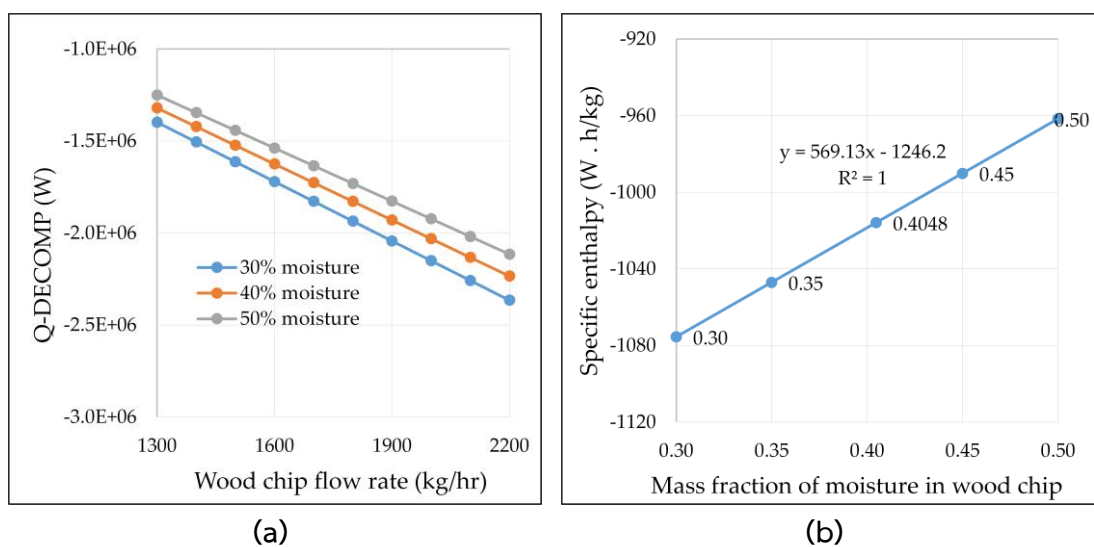


Figure 3.17. Relationship between (a) heating value Q-DECOMP and wood chips flow rate at different moisture content; (b) specific enthalpy and mass fraction of moisture in wood chips.



Table 3.14. Comparison between Q-DECOMP value from simulation and from approximate model.

Wood chips flow rate, kg/hr	Wood chips moisture content, Mass fraction	Q-DECOMP, Watt	
		From simulation	From approximate model equation
1,300	0.3	-1.398E+06	-1.398E+06
	0.35	-1.361E+06	-1.361E+06
	0.4048	-1.321E+06	-1.321E+06
	0.45	-1.287E+06	-1.287E+06
	0.5	-1.250E+06	-1.250E+06
1,500	0.3	-1.613E+06	-1.613E+06
	0.35	-1.570E+06	-1.571E+06
	0.4048	-1.524E+06	-1.524E+06
	0.45	-1.485E+06	-1.485E+06
	0.5	-1.443E+06	-1.442E+06
1,700	0.3	-1.828E+06	-1.828E+06
	0.35	-1.780E+06	-1.780E+06
	0.4048	-1.727E+06	-1.727E+06
	0.45	-1.683E+06	-1.683E+06
	0.5	-1.635E+06	-1.635E+06
1,900	0.3	-2.043E+06	-2.043E+06
	0.35	-1.989E+06	-1.989E+06
	0.4048	-1.930E+06	-1.930E+06
	0.45	-1.881E+06	-1.881E+06
	0.5	-1.827E+06	-1.827E+06
2,100	0.3	-2.258E+06	-2.258E+06
	0.35	-2.199E+06	-2.199E+06
	0.4048	-2.133E+06	-2.133E+06
	0.45	-2.079E+06	-2.079E+06
	0.5	-2.020E+06	-2.019E+06

### 3.6.2. Result comparison of the approximated model and original model

Figure 3.18 shows process flow diagram of the approximated model by Aspen plus. Since the solid components were not allowed in Aspen Dynamics. The carbon element was replaced by the pseudo fuel as  $C_{12}H_{18}$ . And, the amount of ash was neglected. Since the amount of ash contained in wood chips are 0.08 wt. %, the amount of burned fuel is 99.92 wt. % of the fed fuel. Hence, the fed fuel in the approximated model must be removed the amount of ash. For example, the actual wood chips flow rates are 1,500 kg/hr. So, the wood chips flow rates in the approximated model are 1,488 kg/hr (another 12 kg/hr is ash). The results from simulation are shown in table 3.15 which compared with the original model (figure 3.15).

Table 3.15. Result comparison of the approximated model and original model.

Air flow rate, kg/hr	Original model (Approximated model)				
	% Excess air	CO, ppm	NOX, ppm	SOX, ppm	Steam production, kg/hr
5,400	0.48 (0.38)	52 (62)	65 (59)	62 (59)	6,059 (6,059)
5,730	5.01 (4.90)	10 (11)	170 (169)	59 (57)	6,028 (6,028)
6,100	10.15 (10.03)	3.83 (4.24)	197 (197)	57 (55)	5,990 (5,990)
6,500	15.70 (15.57)	1.67 (1.86)	198 (199)	55 (53)	5,948 (5,948)
6,900	21.25 (21.12)	0.79 (0.89)	187 (188)	53 (51)	5,904 (5,904)
7,200	25.41 (25.27)	0.47 (0.53)	176 (178)	51 (50)	5,871 (5,871)
7,600	30.96 (30.81)	0.24 (0.28)	159 (161)	50 (48)	5,826 (5,826)
7,900	35.11 (34.96)	0.15 (0.17)	147 (149)	49 (47)	5,792 (5,792)
8,600	44.78 (44.61)	0.05 (0.06)	119 (121)	46 (45)	5,710 (5,710)
9,000	50.29 (50.12)	0.03 (0.03)	106 (109)	45 (44)	5,663 (5,663)
<b>MAE (%)</b>	<b>2.73±6.19</b>	<b>12.95±3.04</b>	<b>2.10±2.74</b>	<b>3.81±0.29</b>	<b>0</b>

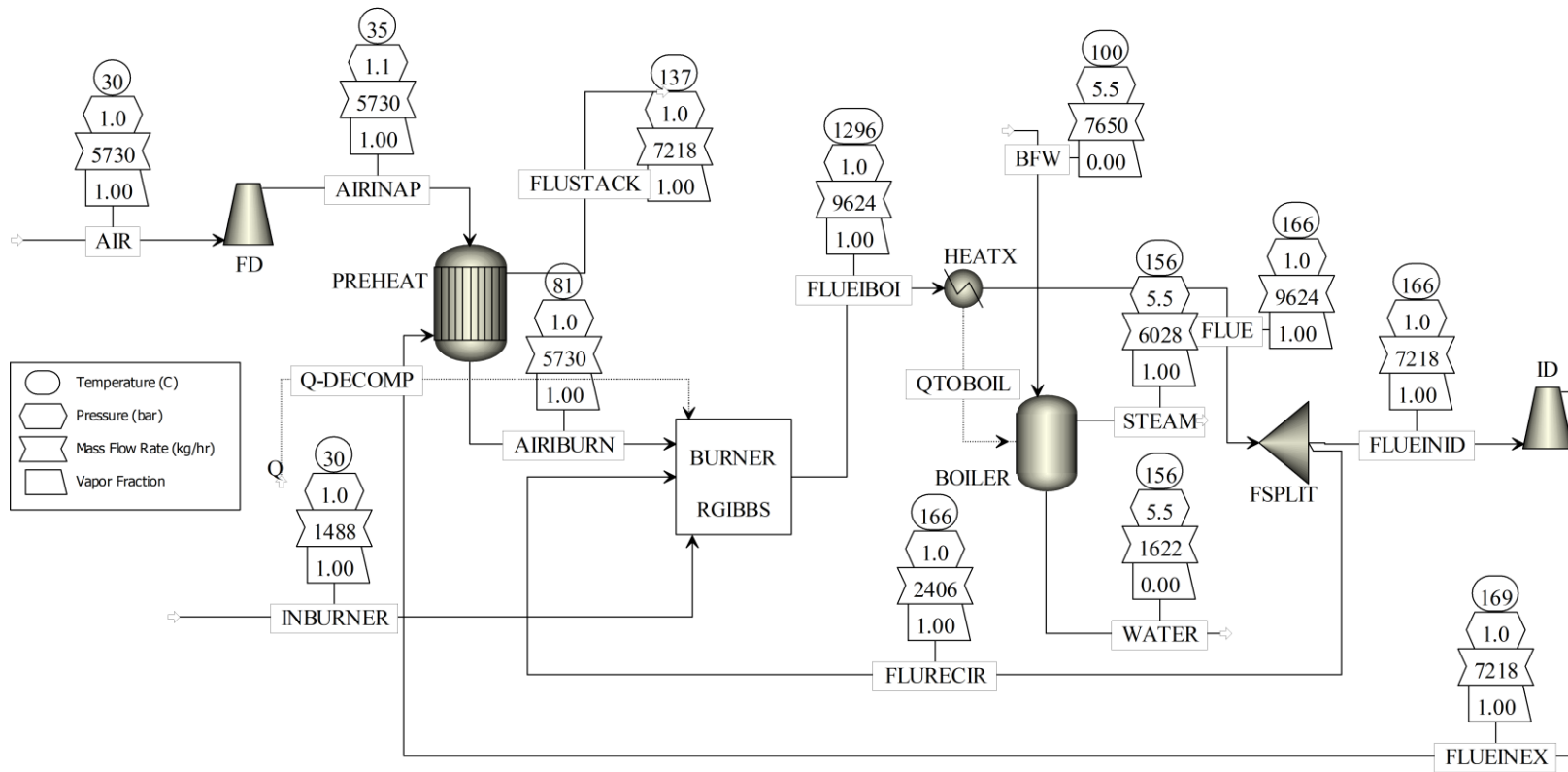


Figure 3.18. Process flow diagram of approximated model.

### 3.6.3. Control loop description

Figure 3.19 shows process simulation with developed by Aspen Dynamics. There are a total of 11 loops consist of 4 loops of controllers (loops number 5-8), 4 loops of indicators (loop number 3, 9-11), 2 loops of heat calculators (loops number 2, 4), and a loop of automatic air flow rate manipulator (loop number 1).

1. First, the loop number 1 is an automatic air flow rate manipulator. It calculates the optimal set point of air to fuel ratio. The air to fuel ratio (A/F) depends on the moisture content of wood chips as shown in figure 3.20. It can be seen that it is the 4<sup>th</sup> order polynomial relationship between A/F and moisture content at 30-50 %wt (equation 3.9). The result of optimal A/F at 30-50 wt% moisture content was shown in table 3.16. From result, the wood chips with lower moisture content is mean a higher amount of combustible elements which need a higher air flow rate in the combustion. And, they provide a higher amount of CO and NO<sub>x</sub> ppm and steam production. In the block “AF\_calc” as shown in figure 3.20 is used for calculating the A/F ratio by using equation 3.9 and then converting to air flow rate. The structure of block “AF\_calc” was shown in figure 3.21.

$$A/F = -2838.5 \times \text{moist}^4 + 4534.9 \times \text{moist}^3 - 2664.1 \times \text{moist}^2 + 678.71 \times \text{moist} - 58.963, \quad (3.9)$$

Where; **moist** is moisture content of wood chips, mass fraction

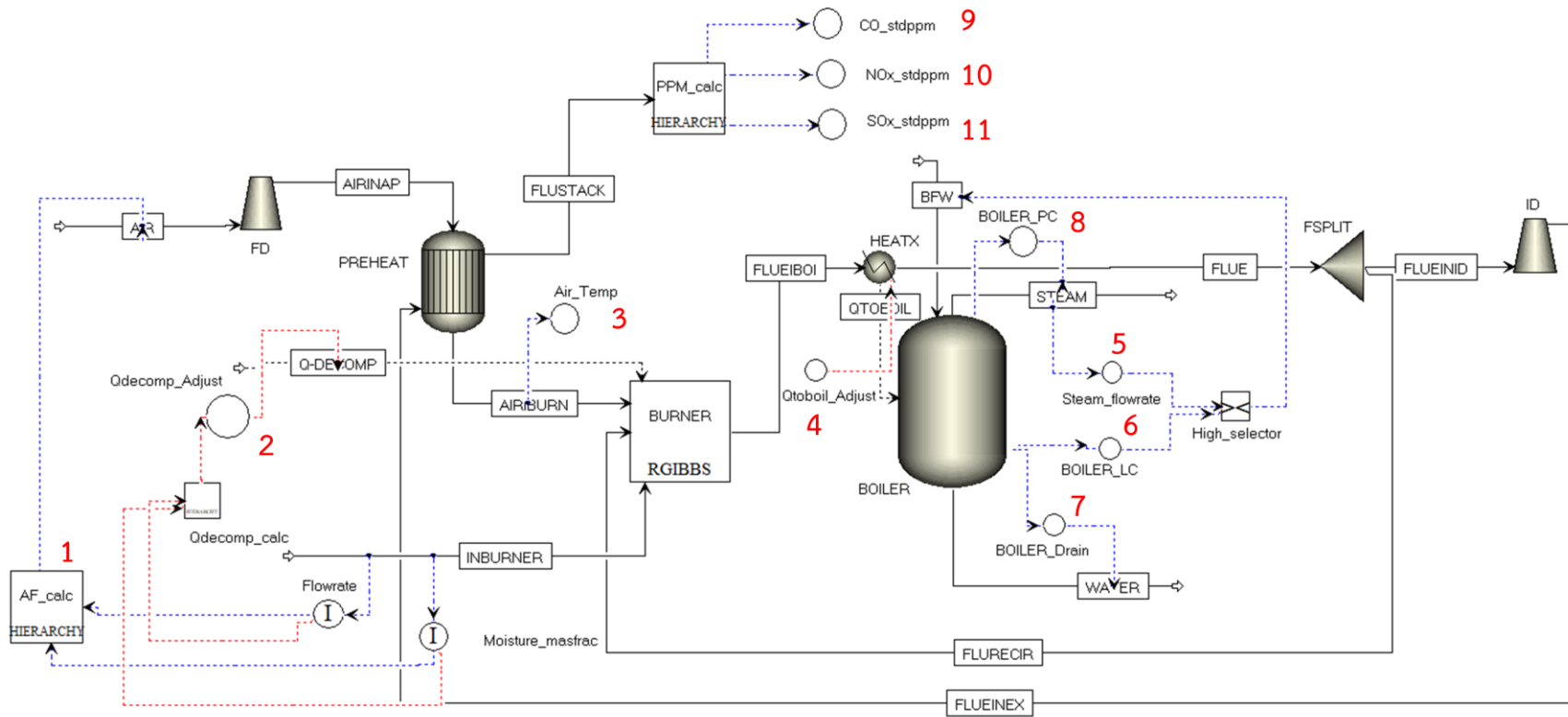


Figure 3.19. Process simulation with controllers by Aspen Dynamics.

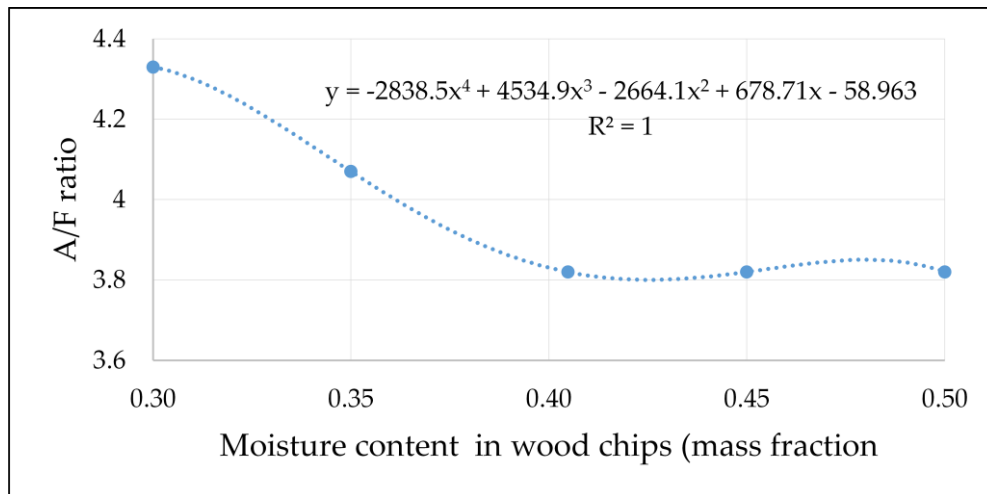


Figure 3.20. Relationship between A/F ratio and moisture content of wood chips.

Table 3.16. The result of optimal A/F ratio at different moisture content of wood chips.

Wood chips moisture content, mass fraction	Air flow rate, kg/hr	%Excess air	A/F	CO, ppm	NO <sub>x</sub> , ppm	SO <sub>x</sub> , ppm	Steam production, kg/hr
0.30	6,500	2.30	4.33	71	177	54	7,502
0.35	6,100	3.10	4.07	32	174	57	6,808
0.4048	5,730	5.00	3.82	10	170	59	6,028
0.45	5,730	11.30	3.82	1.5	163	59	5,350
0.50	5,730	19.00	3.82	0.16	117	59	4,600

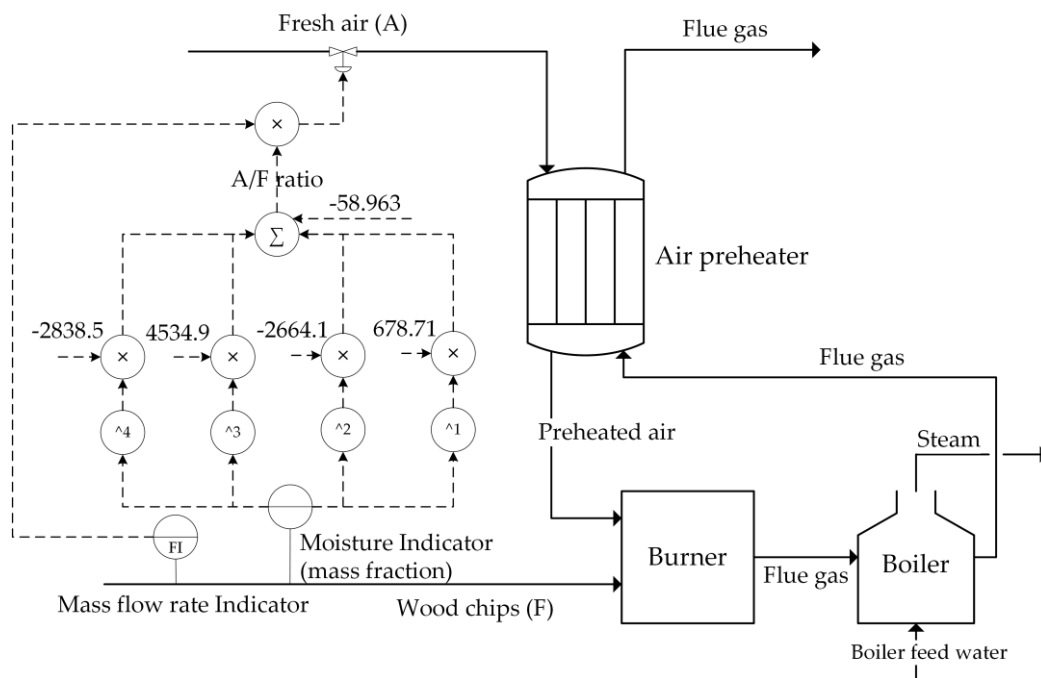


Figure 3.21. Structure of “AF\_calc” block.

2. “QDECOMP” loop is used for calculation of decomposition heating value of wood chips by using equation (3.8).
3. “Air\_Temp” is a preheated air temperature indicator.
4. “QTOBOIL” is used for manual specifying of the heat duty of boiler which gets from steady state model in Aspen plus.
5. “Steam\_Flowrate” and “BOILER\_LC” are an override control. The controlled variables of both controllers are different. For “Steam\_Flowrate” controller, the controlled variable is flow rate of steam production and another “BOILER\_LC” controller is a level control of boiler. While the manipulated variable of both controllers is the same which is boiler feed water flow rate. Only one signal of controller output is selected by the selector which is the high selector in this case. Consider the situation, if the steam flow rate goes below its set point, the output signal will higher and now it is higher than output signal of level controller. The

selector is then choosing the output signal from steam flow rate controller and will send the signal to adjust boiler feed water flow rate.

6. “BOILER\_Drain” is used for an emergency case when the water level of boiler is too high.
7. “BOILER\_PC” is the boiler pressure controller with the manipulated variable is the steam flow rate.
8. “CO\_stdppm”, “NO<sub>x</sub>\_stdppm”, and “SO<sub>x</sub>\_stdppm” are the CO, NO<sub>x</sub>, and SO<sub>x</sub>, ppm indicators respectively.

#### 3.6.4. Controller tuning parameters

In this work, 2 methods for tuning are Ziegler-Nichols open loop method (section 3.) and manual tuning method (section 3.). Ziegler-Nichols open loop method was used for boiler pressure control and steam production control. And, manual tuning method was used for boiler level control.

Since, the dynamic process model with flow driven mode provides the very fast responding system. So, the dead time was assumed at 2 min for Ziegler-Nichols open loop method.

For boiler level control, manual tuning method is more acceptable than the results achieved from an auto tuning tool in Aspen Dynamics due to the fast responding system. The manual tuning procedures are as follow [38].

1. Set the Integral time (Ti) to 10<sup>6</sup> min and derivative time (Td) to 0 min.
2. Increase proportional gain (Kp) until the loop oscillates at a constant amplitude. Now, the ultimate gain (Ku) is achieved.
3. Set the Kp of the controller to half of the Ku.



4. Adjust  $T_i$  until the offset is corrected in sufficient time for the process. However, too less  $T_i$  provides instability of the process.
5. Add  $T_d$  term if required.  $T_d$  can decrease the overshoot of the response. However, too much  $T_d$  provides an aggressive response.
6. Check the response by step changes in set point and disturbance.

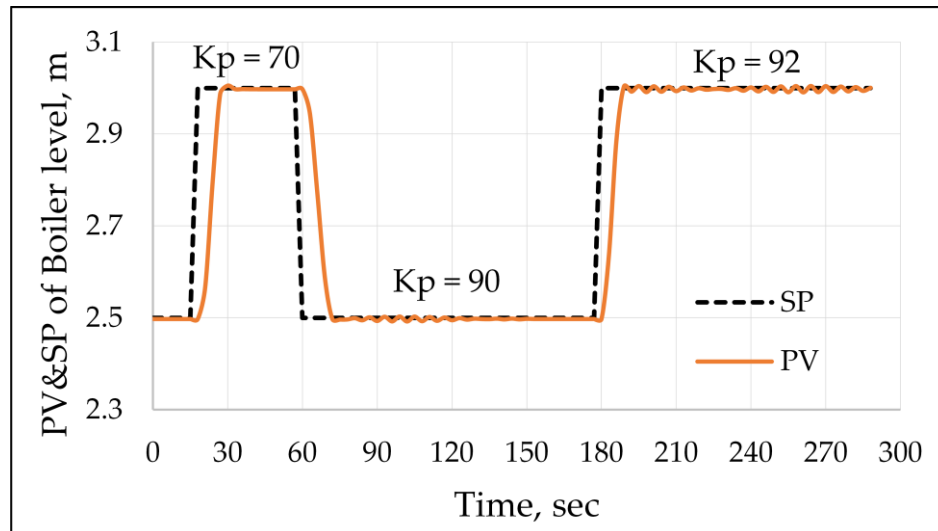
#### 3.6.4.1 Boiler level control

Height of the boiler is 4 meters and diameter is 1 meter. The level of boiler is controlled at 2.5 – 3.5 meters. The objective of the drum level controller is to maintain the level at constant steam production. A decrease in boiler level will uncover boiler tubes which cause them to become overheated and damaged. 2 controllers were used for level control.

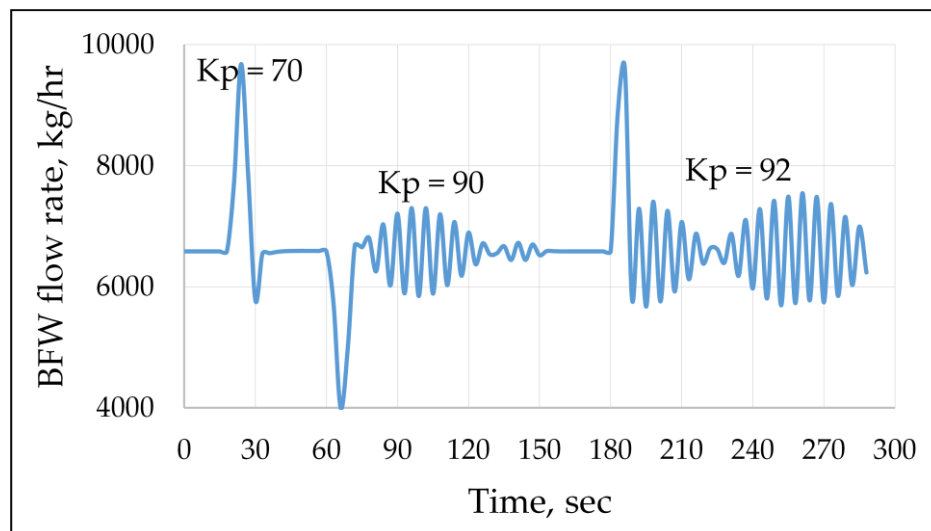
First controller is “BOILER\_LC”. The objective is to regulate the level at 2.5 – 3.5 meters by manipulating boiler feed water flow rate. The set point was set at 2.5 meters and dead band was set at 1 meter above its set point. The parameters tuning method was done by following the steps in section 3.6.4. The ultimate gain ( $K_u$ ) was 92 which the controller gain ( $K_p$ ) was set at 46 as shown in figure 3.22. The integral time ( $T_i$ ) was varied to find the appropriate value as shown in figure 3.23. It can be seen that at the low value of  $T_i$  decreases the rise time. However, too less of  $T_i$  provides the overshoot which is undesirable and provides too fast of a response. In this case, the derivative time is not required due to no overshoot of the signal. So, the “BOILER\_LC” is a PI controller with the reverse action which has the 46 of  $K_p$  and 5 min of  $T_i$ .

Second controller is “BOILER\_Drain”. The objective is to maintain the level at 3.5 meters by releasing the excess water. Only P controller was used due to

the response of the process is fast and the offset can be accepted in the case of level control.  $K_p$  was set at 15.

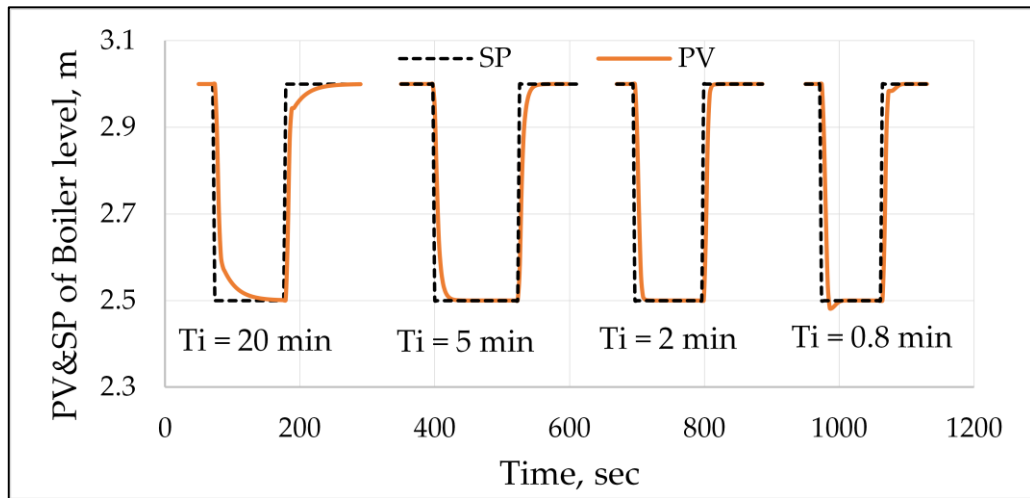


(a)

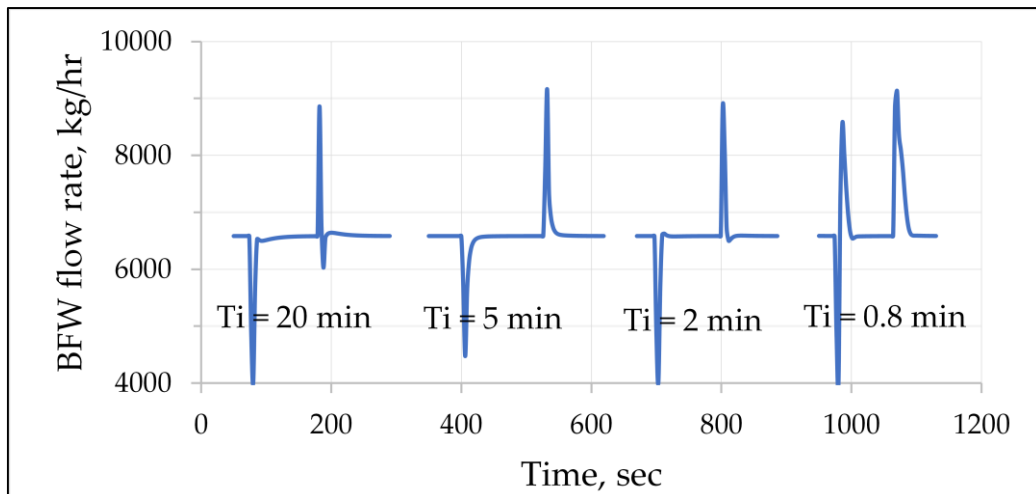


(b)

Figure 3.22. The effect of proportional gain of “BOILER\_LC” controller on (a) Process variable (boiler level), and (b) Controller output (BFW flow rate) at  $T_i = 10^6$  min and  $T_d = 0$  min.



(a)



(b)

Figure 3.23. The effect of integral time of “BOILER\_LC” controller on (a) Process variable (boiler level), and (b) Controller output (BFW flow rate) at  $K_p = 46$  and  $T_d = 0$  min.

### 3.6.4.2 Boiler pressure and Steam production control

Both of the boiler pressure controller (“BOILER\_PC”) and steam production controller (“Steam\_flowrate”) have the steam flow rate parameter which has interaction together. For boiler pressure control, the steam flow rate is a manipulated variable. For steam production control, the steam flow rate is a controlled variable. So, controller tuning is more complicated.

In this case, the Ziegler-Nichols open loop method was used. Controller parameters of “BOILER\_PC” were tuned first while the “Steam\_flowrate” was in the manual mode. Then, controller parameters of the “Steam\_flowrate” were then tuned while the “BOILER\_PC” was in the auto mode.

For “BOILER\_PC” controller, the controlled variable is boiler pressure with the PV range of 1 to 10 bar. The manipulated variable is steam flow rate with the output range of 4,000 to 7,000 kg/hr. The steam flow rate was step up by 2% of output range from 6,550 to 6,610 kg/hr. The PV response was shown in figure 3.24. The dead time ( $t_d$ ) was assumed at 2 mins. From figure, the delta PV equals to  $4.32 - 5.5 = -1.18$  bar or equals to -13.14 % and delta MV equals to 60 kg/hr or equals to 2% which provide open loop gain ( $K_{op}$ ) equals to -6.57 %PV/%MV. The time constant ( $\tau$ ) equals to 46 mins. Then, Calculating controller parameters for Controller Gain ( $K_p$ ), Integral Time ( $T_i$ ), and Derivative Time ( $T_d$ ) using the Ziegler-Nichols tuning rules. For PID controller,  $K_p = -4.2$ ,  $T_i = 4$  mins, and  $T_d = 1$  min.

For “Steam\_flowrate” controller, the controlled variable is steam flow rate with the PV range of 4,000 to 7,000 kg/hr. The manipulated variable is boiler feed water flow rate with the output range of 4,000 to 10,000 kg/hr. The boiler feed water was step up by 10% of output range from 6,848 to 7,446 kg/hr. The PV response was shown in figure 3.25. The dead time ( $t_d$ ) was also assumed at 2 mins. The delta PV equals to -2.57% and delta MV equals to 10% which provide open loop gain ( $K_{op}$ )

equals to  $-0.257\% \text{PV}/\% \text{MV}$ . The time constant ( $\tau$ ) equals to 2 mins. Then, Calculating PI controller parameters for Controller Gain ( $K_p$ ) and Integral Time ( $T_i$ ) using the Ziegler-Nichols tuning rules. For PI controller,  $K_p = -3.5$  and  $T_i = 6.6$  mins,

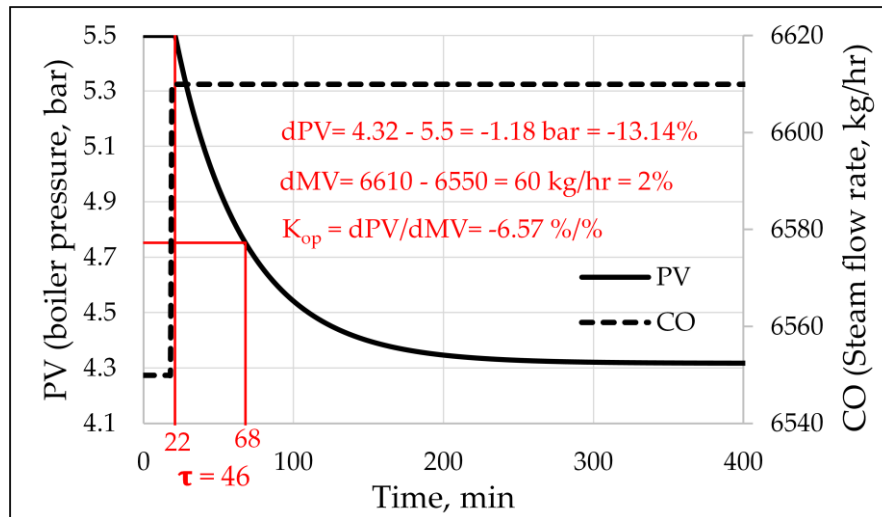


Figure 3.24. Open loop step test for "BOILER\_PC" controller.

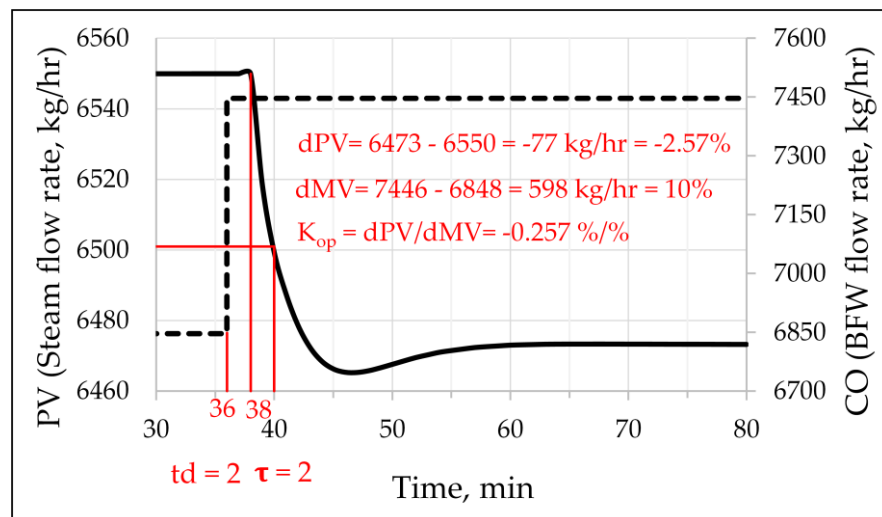


Figure 3.25. Open loop step test for "Steam\_flowrate" controller.

### 3.6.5. Robustness test

Robustness of controller was investigated in this section by slightly changing disturbance variables from their design conditions [38]. In this case, the disturbances consist of wood chips flow rate, wood chips moisture content and inlet temperature of boiler feed water (BFW).

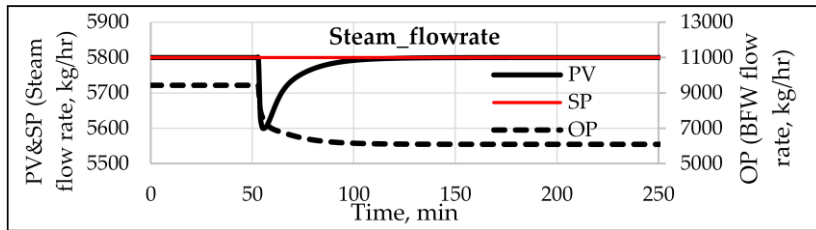
Figure 3.26 shows controller responses in case of the wood chips flow rate step-change. The wood chips flow rate was stepped down from 1,500 to 1,400 kg/hr at time 53 min. The air flow rate was adjusted along the air to fuel ratio which is 3.82 from 5,730 kg/hr to 5,348 kg/hr. It can be seen that the dynamics are quite fast. The steam flow rate instant decreased when the wood chips flow rate was decreased because the heat of combustion from fuel was decreased. After that, the BFW flow rate was continuous decreased in order to increase the steam production to its set point. As a result, the boiler level was decreased from 3.50 meter to 3.31 meter. For the emissions, all of CO, NO<sub>x</sub>, and SO<sub>x</sub> ppm increased due to the denominator of ppm which is total volume flow decreased.

Figure 3.27 shows controller responses in case of the wood chips moisture content step-change. The moisture content was stepped up from 40.5% to 45% at time around 25 min. The steam flow rate instant decreased when the moisture content was increased. It can be seen that the steam flow rate cannot reach the set point of 5,800 kg/hr of steam because when the BFW flow rate continuous decreased, the boiler level also continuous decreased until the minimum allowance at 2.5 meters the controller was switched from “Steam\_flowrate” to “BOILER\_LC” to maintain the boiler level higher than 2.5 meters. Then, the BFW flow rate was forced to increase by “BOILER\_LC” controller. It is noted that the heat of combustion from wood chips at 1500 kg/hr and 45% moisture content was not enough for producing steam at 5,800

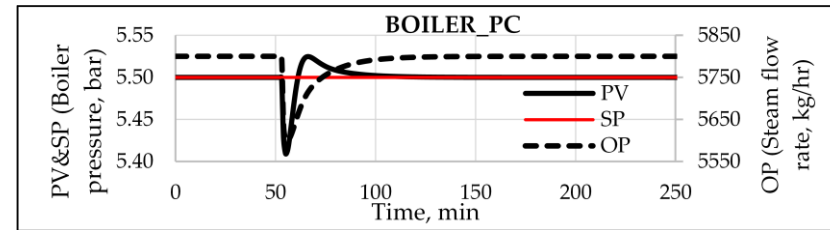
kg/hr. It should be supplied more fuel or should be supplied fuel with lower moisture content.

Figure 3.28 shows controller responses in case of the BFW inlet temperature step-change. The BFW inlet temperature was stepped down from 100°C to 80°C at time around 28 min. The controllers can perfectly maintain their set points.

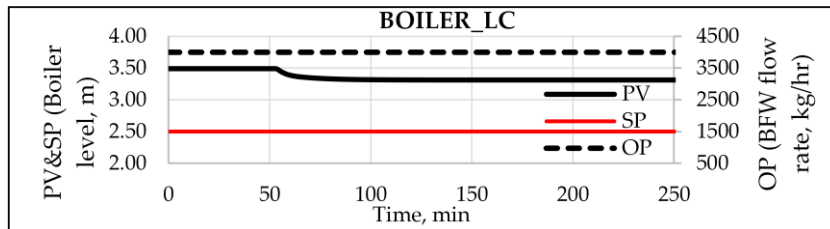
These results show that the dynamic model can be self-balanced although disturbance occurred. However, the caution is that the defined set point of steam production must be related together with wood chips flow rate and wood chips moisture content.



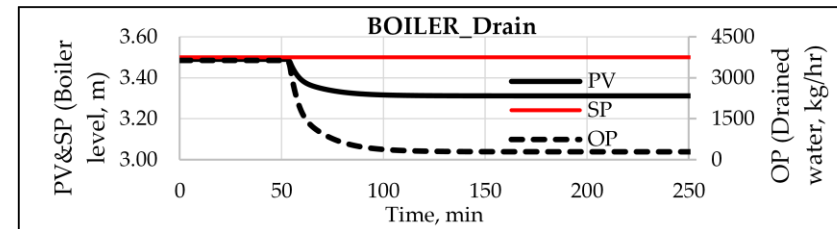
(a)



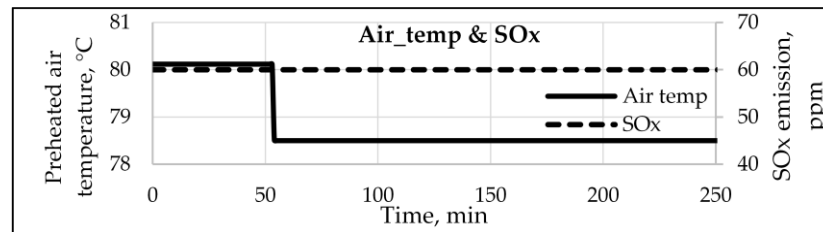
(b)



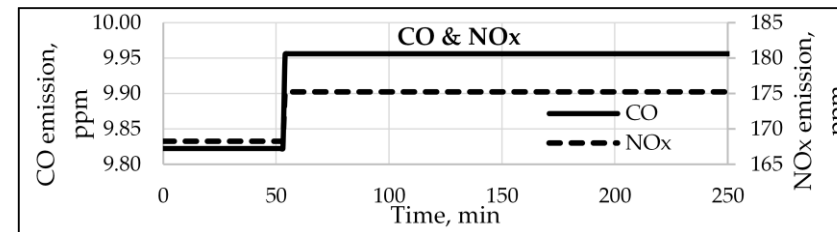
(c)



(d)



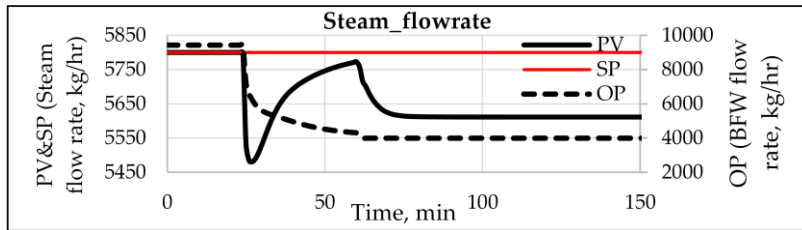
(e)



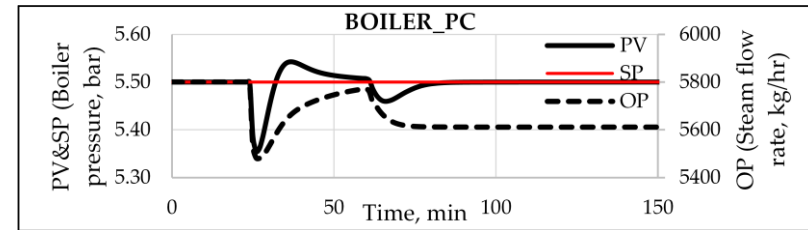
(f)

Figure 3.26. Robustness test in case of wood chips flow rate change (from 1,500 kg/hr to 1,400 kg/hr).

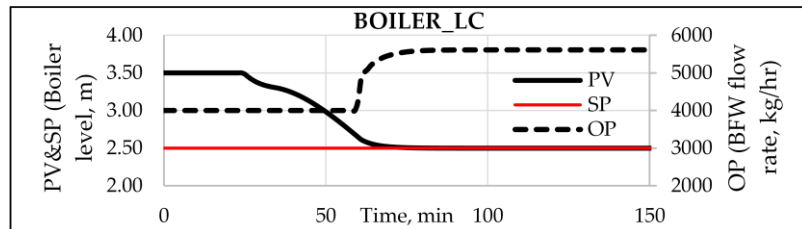




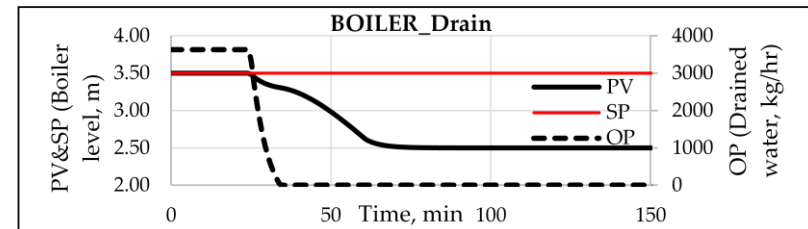
(a)



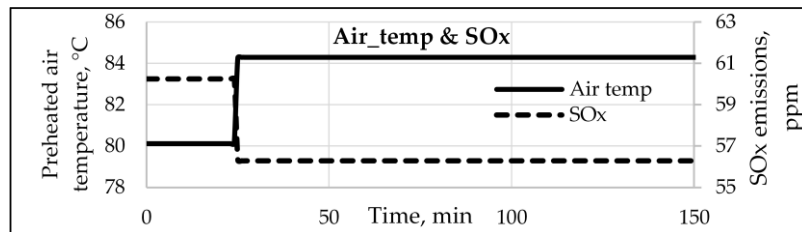
(b)



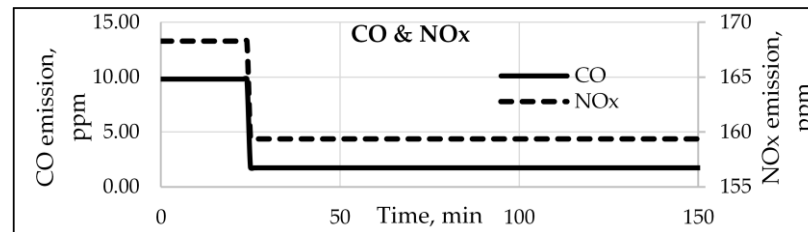
(c)



(d)

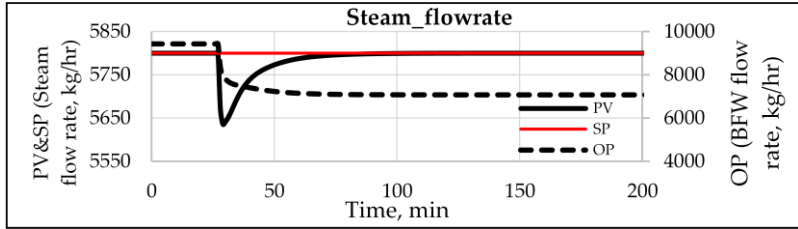


(e)

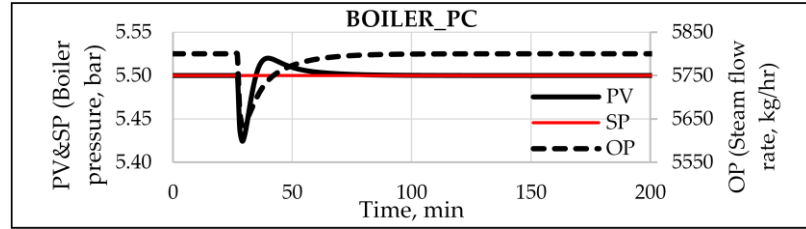


(f)

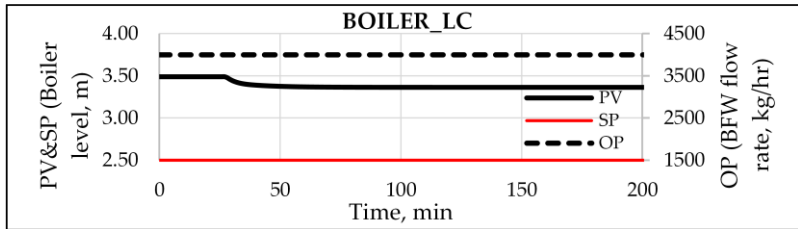
Figure 3.27. Robustness test in case of wood chips moisture content change (from 40.5% to 45%).



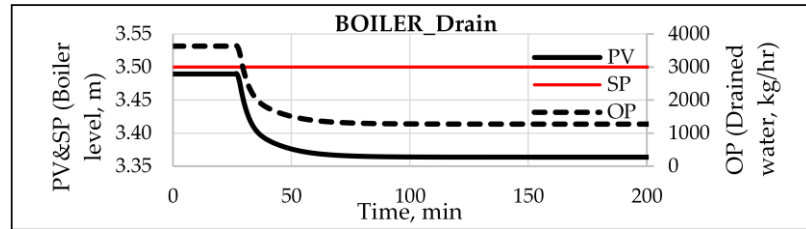
(a)



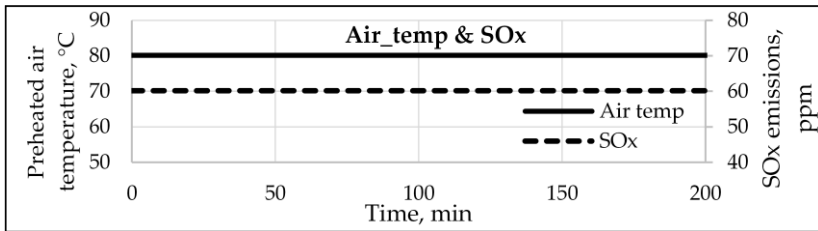
(b)



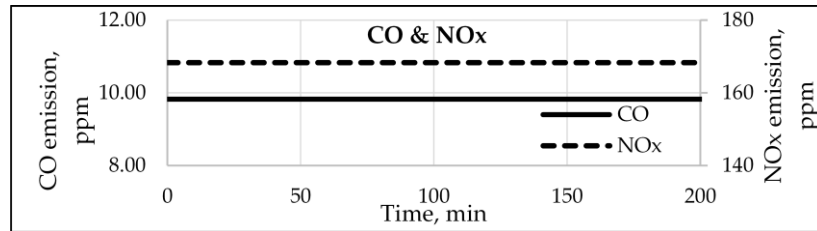
(c)



(d)



(e)



(f)

Figure 3.28. Robustness test in case of BFW inlet temperature change (from 100 to 80 °C).

## CHAPTER 4

### CONCLUSION

This work was divided into 2 main sections. First, a steady-state simulation of wood chips combustion boiler process was achieved by using Aspen Plus v.9. The optimal condition of air to fuel ratio combined with the flue gas recirculation technique was determined in the sense of using energy to be cost effective and in the meanwhile, the emissions consist of CO, NO<sub>x</sub>, and SO<sub>x</sub> are in their limitations. Furthermore, air preheater was designed and combined for energy recovery purpose.

In this case, manufacturing and pollution requirements are steam productivity of 4,000 to 7,000 kg/hr, the CO, NO<sub>x</sub>, and SO<sub>x</sub> emissions are less than 690, 200, and 60 ppm respectively and preheated air temperature more than 70 °C. The simulation model was further used for description of excess air and flue gas recirculation effect on the various factors consist of CO, NO<sub>x</sub>, SO<sub>x</sub> emission, flame temperature, stack temperature, stack heat loss, and steam production.

Second, a dynamic simulation scheme of wood chips combustion boiler process was proposed using Aspen Dynamics v.9. There have 4 controllers consist of air to fuel ratio controller which is ratio controller type, override control between boiler level and steam flow rate control which are both PI controller, boiler pressure control which is PID controller, and boiler drained water control which is P controller. For the boiler level controller, the tuning parameters was perform using manual tuning method. For the boiler pressure and steam flow rate controllers, the Ziegler-Nichols open loop method was used. Robustness tests were performed to prove the performance of the controller by stepping change the disturbance variables consist of

wood chips flow rate, wood chips moisture content, and BFW temperature. The simulation results can be summarized as follows.

1. Model validation is achieved by comparing with the sets of measured data collected by wood manufacturing company in the south of Thailand. Prediction error of flue gas temperature at stack is less than 5% (considering with 26 scenarios of the collected data).
2. CO amount decreases considerably with increasing %excess air while CO<sub>2</sub> amount increases proportionally with %excess air. Both of CO and CO<sub>2</sub> emissions are moving on their trends until at 0%excess air (complete combustion),
3. NO<sub>x</sub> reaches a maximum value at around 10-15% excess air and then continuously decrease when increasing %excess air.
4. SO<sub>x</sub> comes from the sulfur (S) contained in fuel reacts with the O<sub>2</sub> contained in combustion air. SO<sub>x</sub> formation directly depends on the combustion temperature.
5. Increase of excess air leads to increase of the stack temperature and stack heat loss.
6. For the case of steam production, less heat from flue gas applies to generate steam when increasing excess air since the heat loss at stack increases. As a result, steam production also decreases when increasing excess air
7. Flue gas recirculation technique was applied for reducing NO<sub>x</sub> emissions. 25% flue gas recirculation provides the reduction of NO<sub>x</sub> around 70%.
8. Optimal operating condition of the process is 5% excess air (5,730 kg/hr air flow rate) and 25% flue gas recirculation with 40.5%wt. moisture content of wood chips and 1,500 kg/hr of wood chips flow rate. It can produce steam higher than original process condition (168% excess air and no flue gas recirculation) about 32.4%.
9. Designed air preheater type is shell and tube heat exchanger. Flue gas is inside tubes and air is outside. The exchanger consists of 41 tubes with 88.90 mm OD,

3.405 mm thickness and 1,212 mm OD of shell with 6 mm thickness (1 tube pass and 1 shell pass). The preheated air was heated up from 30 °C to 82 °C. The effect of preheated air provides more supplied heat which can produce a higher amount of steam. It provides steam production more than the optimal process condition without air preheater about 2.2%.

10. For the dynamic model, Robustness tests were performed to prove the performance of the controller by stepping change the disturbance variables consist of wood chips flow rate, wood chips moisture content, and BFW temperature. The results show that the dynamic model can be self-balanced although disturbance occurred. However, the caution is that the defined set point of steam production must be related together with wood chips flow rate and wood chips moisture content.

## REFERENCES

- [1] Forbes Marshall Ltd. The Process of Combustion. Available online: [https://www.forbesmarshall.com/fm\\_micro/news\\_room.aspx?Id=Boilers&nid=179](https://www.forbesmarshall.com/fm_micro/news_room.aspx?Id=Boilers&nid=179) (accessed on 24 March 2019).
- [2] Mallikarjuna, V.; Jashuva, N.; Rama Bhupal Reddy, B. Improving Boiler Efficiency by Using Air Preheater. *Int. J. Adv. Res. Eng. Appl. Sci.* **2014**, *3*, 11–24.
- [3] Boilers Guide. Working principle of boiler. Available online: <http://www.boilers.guide/working-principle> (accessed on 25 March 2019).
- [4] Piteľ, J.; Mižáková, J.; Hošovský, A. Biomass combustion control and stabilization using low-cost sensors. *Adv. Mech. Eng.* **2013**, *5*.
- [5] Shi, B.; Hu, J.; Peng, H.; and Ishizuka, S. Effects of internal flue gas recirculation rate on the NO<sub>x</sub> emission in a methane / air premixed flame. *Combust. Flame.* **2018**, *188*, 199–211.
- [6] Prabowo, B.; Hantoko, D.; Yan, M.; Li, X.; Susanto, H.; Chen, C. Chapter 13 - Aspen Plus Modeling Approach in Solid Waste Gasification. In *Current Developments in Biotechnology and Bioengineering*; Kumar, S., Kumar, R., Pandey, A., Eds.; Elsevier B.V.: Amsterdam, Netherlands, 2019; pp. 259-281.
- [7] Luyben, W. L.; Robinson, P. J. A simple gasifier model that runs in aspen dynamics. *Ind. Eng. Chem. Res.* **2008**, *47*, 7784–7792.
- [8] Jin, B.; Zhao, H.; Zheng, C. Dynamic modeling and control for pulverized-coal-fired oxy-combustion boiler island. *Int. J. Greenh. Gas. Con.* **2014**, *30*, 97–117.
- [9] Lan, W.; Chen, G.; Zhu, X.; Wang, X.; Liu, C.; Xu, B. Biomass gasification-gas turbine combustion for power generation system model based on ASPEN PLUS. *Sci. Total Environ.* **2018**, *628–629*, 1278–1286.

- [10] Gagliano, A.; Nocera, F.; Bruno, M.; Cardillo, G. Development of an Equilibrium-based Model of Gasification of Biomass by Aspen Plus. *Energy Procedia*. **2017**, *111*, 1010–1019.
- [11] Pei, X.; He, B.; Yan, L.; Wang, C.; Song, W.; Song J. Process simulation of oxy-fuel combustion for a 300 MW pulverized coal-fired power plant using Aspen Plus. *ENERGY Convers. Manag.* **2013**, *76*, 581–587.
- [12] Doherty, W.; Reynolds, A.; Kennedy, D. The effect of air preheating in a biomass CFB gasifier using ASPEN Plus simulation. *Biomass and Bioenergy*. **2009**, *33*, 1158–1167.
- [13] Gamrat, S.; Poraj, J.; Bodys, J.; Smolka, J.; Adamczyk, W. Influence of external flue gas recirculation on gas combustion in a coke oven heating system. *FPT*. **2016**, *152*, 430–437.
- [14] TSI Inc. Combustion Analysis Basics. Available online: <https://inspectapedia.com/heat/Combustion-Analysis-Basics-tsi.pdf> (accessed on 31 October 2018).
- [15] Dmour, M. PID Controller. Available online: <http://engineering.ju.edu.jo/Laboratories/07-PID%20Controller.pdf> (accessed on 6 September 2018).
- [16] Edwards, J. Design and Rating Shell and Tube Heat Exchangers. Available online: [https://www.chemstations.com/content/documents/Technical\\_Articles\\_/shell.pdf](https://www.chemstations.com/content/documents/Technical_Articles_/shell.pdf) (accessed on 20 July 2018).
- [17] Sukmanee, S. Determining the details of the shell and tube heat exchanger. In *Chemical engineering equipment design*, 9th ed.; Audio Visual Center Department of Engineering Prince of Songkla University: Hatyai, Thailand, 2015; pp. 9-1 – 9-19.
- [18] National Programme on Technology Enhanced Learning. Process design of heat exchanger. Available online: <https://nptel.ac.in/courses/103103027/pdf/mod1.pdf> (accessed on 15 July 2018).

- [19] Subramanian, R. Shell-and-Tube Heat Exchangers. Available online: <https://web2.clarkson.edu/projects/subramanian/ch330/notes/Shell%20and%20Tube%20Heat%20Exchangers.pdf> (accessed on 20 July 2018).
- [20] Al-Malah, K. INTRODUCING ASPEN PLUS. In *Aspen Plus®: Chemical Engineering Applications*; John Wiley & Sons, Inc., Hoboken, New Jersey, Canada, 2017; pp. 1-3.
- [21] Aspen Technology, Inc. Aspen Plus Dynamics. Available online: <https://www.aspentech.com/en/products/engineering/Aspen-Plus-Dynamics> (accessed on 10 May 2019).
- [22] Bashee.P.V, S.; Assaf.C, M.; Mahin, S., Kumaran, A.B. Design of Air Pre-Heater to Improve the Efficiency of Boiler in TCC Plant. *IRJET*. **2018**, *5*, 2157-2163.
- [23] Aspen Technology, Inc. Getting Started Modelling Processes with Solids. Available online: [http://profsite.um.ac.ir/~fanaei/\\_private/Solids%208\\_4.pdf](http://profsite.um.ac.ir/~fanaei/_private/Solids%208_4.pdf) (accessed on 17 May 2018).
- [24] Ministry of Industry of Thailand. Determining the amount of impurities in the air that is discharged from the factory, 2006. Available online: <http://www.diw.go.th/hawk/law/air/A11.pdf> (accessed on 4 March 2018).
- [25] R.J. Karg Associates. Air-Free Measurement of Carbon Monoxide Emissions from Gas Ranges. Available online: [http://www.karg.com/pdf/coairfree\\_article.pdf](http://www.karg.com/pdf/coairfree_article.pdf) (accessed on 15 December 2018).
- [26] Project Environment Department of EGAT. Environmental quality standards. Available online: [https://www.egat.co.th/index.php?option=com\\_content&view=article%20&id=336&Itemid=127&catid=37](https://www.egat.co.th/index.php?option=com_content&view=article%20&id=336&Itemid=127&catid=37). (accessed on 15 December 2018).
- [27] Pollution Control Department. Calculation of emissions from measurement data, 1st ed.; Wirana Press Co.,Ltd: Bangkok, Thailand, 2012 pp. 5-21



- [28] FireBridge Inc. Understanding the Impact of Excess Air. Available online: <https://www.firebridgeinc.com/understanding-the-impact-of-excess-air/> (accessed on 26 January 2019).
- [29] Costa, M.; RuÃo, M.; Carvalho, M.G. On the influence of flue-gas recirculation on pollutant emissions from a small-scale laboratory furnace. *ARCOM*. 1996, 16, 77-86.
- [30] Abdelaal, M.; El-Riedy, M.; El-Nahas, A. Effect of flue gas recirculation on burner performance and emissions. *AUEJ*, 2016, 11, 1275-1284.
- [31] Maloney, K. Flue gas recirculation for stoker boilers. Available online: [http://www.combustionexperts.com/pdf/fgr\\_brochure.pdf](http://www.combustionexperts.com/pdf/fgr_brochure.pdf) (accessed on 01 June 2019).
- [32] Towler, G.; Sinnott, R. Capital Cost Estimating. In *Chemical Engineering Design: Principles, Practice and Economics of Plant and Process Design*, 2nd ed.; Butterworth-Heinemann, USA, 2013; pp. 321-339.
- [33] Jenkins, S. CEPCI UPDATES: JANUARY 2018 (PRELIM.) AND DECEMBER 2017 (FINAL). Available online: <https://www.chemengonline.com/cepci-updates-january-2018-prelim-and-december-2017-final/?printmode=1> (accessed on 15 September 2018).
- [34] Energy for Environment Foundation. Price of parawood chips 2018. Available online: <http://www.efe.or.th/efe-book.php?task=25> (accessed on 01 June 2019).
- [35] IISWBM. Detailed project report on air pre heater HOWRAH CLUSTER. Available online: [http://www.sameeksha.org/pdf/Howrah\\_galvanising/DPR\\_on\\_Air\\_Pre\\_Heater\\_for\\_galvanizing\\_and\\_annealing\\_furnace.pdf](http://www.sameeksha.org/pdf/Howrah_galvanising/DPR_on_Air_Pre_Heater_for_galvanizing_and_annealing_furnace.pdf) (accessed on 20 June 2019).
- [36] MartÃnez, I. Fuel properties. Available online: <http://webserver.dmt.upm.es/~isidoro/bk3/c15/Fuel%20properties.pdf> (accessed on 26 January 2019).

- [37] Faculty of Chemical Engineering and Technology University of Zagreb. Controller tuning control loop optimization. Available online: [https://www.fkit.unizg.hr/\\_download/repository/PMC\\_06\\_Controller\\_tuning\\_\\_loop\\_optimization.pdf](https://www.fkit.unizg.hr/_download/repository/PMC_06_Controller_tuning__loop_optimization.pdf) (accessed on 20 June 2019).
- [38] Wikipedia. Control theory. Available online: [https://en.wikipedia.org/wiki/Control\\_theory](https://en.wikipedia.org/wiki/Control_theory) (accessed on 27 March 2019).

## APPENDIX

## APPENDIX A

## OPERATING DATA OF WOOD FACTORY

Table A. Operating data of wood factory.

No.	Wood chips flow rate (kg/h)	Steam production (kg/h)	Boiler pressure (Bar)	Temperature of Flue gas (°C)
April				
1	1,367	8,300	4.5	229.3
2	1,309	7,844	5.0	219.7
3	1,400	8,544	5.0	229.3
4	1,581	9,846	5.5	234.7
5	888	3,979	7.0	208.3
6	1,429	8,600	6.5	239.8
7	1,491	9,648	6.0	234.4
8	1,483	9,738	5.0	235.8
9	1,517	9,475	5.0	229.8
10	1,438	9,885	5.5	229.9
11	1,475	9,600	5.5	241.3
May				
12	1,504	10,000	5.0	242.1
13	1,500	9,208	6.0	241.5
14	1,542	9,600	5.5	251.1
15	1,429	8,046	5.0	214.6
16	1,329	6,204	4.5	203.6
17	1,571	9,133	6.5	235.6
18	1,479	8,371	6.0	230.7
19	1,371	7,588	6.0	224.5
20	1,300	5,700	5.5	208.9

No.	Wood chips flow rate (kg/h)	Steam production (kg/h)	Boiler pressure (Bar)	Temperature of Flue gas (°C)
June				
21	1,450	6,433	5.0	210.7
22	1,396	5,383	5.0	207.9
23	1,200	4,010	5.5	194.3
24	1,181	4,217	5.0	202.6
25	1,304	4,183	5.5	221.6
26	1,396	5,692	4.5	217.7
27	1,471	6,833	6.0	227.7

## APPENDIX B

## COEFFICIENT VALUE FOR AIR PREHEATER DESIGN

Table B1. Typical values of fouling coefficients and resistances [18].

Fluid	Coefficient ( $W \cdot m^{-2} \cdot ^\circ C^{-1}$ )	Resistance ( $m^2 \cdot ^\circ C \cdot W^{-1}$ )
River water	3,000 - 12,000	0.0003-0.0001
Sea water	1,000 - 3,000	0.001-0.0003
Cooling water (towers)	3,000 - 6,000	0.0003-0.00017
Towns water (soft)	3,000 - 5,000	0.0003-0.0002
Towns water (hard)	1,000 - 2,000	0.001-0.0005
Steam condensate	1,500 - 5,000	0.00067-0.0002
Steam (oil free)	4,000 - 10,000	0.0025-0.0001
Steam (oil traces)	2,000 - 5,000	0.0005-0.0002
Refrigerated brine	3,000 - 5,000	0.0003-0.0002
Air and industrial gases	5,000 - 10,000	0.0002-0.0001
Flue gases	2,000 - 5,000	0.0005-0.0002
Organic vapors	5,000	0.0002
Organic liquids	5,000	0.0002
Light hydrocarbons	5,000	0.0002
Heavy hydrocarbons	2,000	0.0005
Boiling organics	2,500	0.0004
Condensing organics	5,000	0.0002
Heat transfer fluids	5,000	0.0002
Aqueous salt solutions	3,000 - 5,000	0.0003-0.0002

Table B2. Safe working fiber stress (N/mm<sup>2</sup> or MPa) [17].

Piping materials	Tensile (MPa)	Yield (MPa)	Temperature C							
			Room	100	150	200	250	300	350	400
Carbon steel, ASTM A53	331	206.8		109.3	104.8	99.9	95.5	91.2	86.6	82.2
Stainless steel 304	517.1	206.8	129.3	126.1	113.4	103.2	94.9	87.6	81.7	76.6
Stainless steel 309	517.1	206.8		129.3	128.1	119.2	115.5	114.6	114	113.3
Stainless steel 310	517.1	206.8		129.3	129.1	127.5	125.7	122.7	119.6	116
Stainless steel 316	517.1	206.8		129.3	128.6	123.4	120.9	119	118.2	117.5
Aluminium ASTM B241, 6063-T6	206.8	172.4	51.7	50.5	45.7	30.6	15			
Copper, annealed ASTM B42	206.8	62.1	41.4	38.6	33.1	22.2	21.8			
Brass, Admiralty	310	105								
Brass, Aluminium	345	125								
Brass, red, ASTM B43	275.8	82.7	55.2	55.2	55.2	54.6	24			
Carbon steel, lab-welded				65.5	62.4	59.7	57	54.1	45.9	45.9
Wrought iron, lab-welded									33.1	33.1
Wrought iron, butt-welded									28.6	28.6
Stainless steel 304 welded annealed	517.1	206.8	109.6	103.3	97.2	95.3	93.3	93.1	91.6	91.6
Stainless steel 316, welded	517.1	206.8	110.3	110	107.5	105.7	105.5	101.5	94.4	94.4

Table B3. The value of  $U_{\text{service}}$  for shell and tube heat exchanger [17].

Shell and tube (Heating-Cooling)		
Tube side	Shell side	$U_{\text{service}}(\text{W}/\text{m}^2 \text{ } ^\circ\text{C})$
Gas	Gas	10-50
	Steam	30-300
Low-pressure gas (1bar)	Low-pressure gas (1bar)	5-55
High-pressure gas (20bar)	High-pressure gas (20bar)	300
	Low-pressure gas (1bar)	90
	Very heavy liquid	120-135
	Medium organic liquid	375-380
	Process water	425-500
Very high-pressure gas (250bar)	Very high-pressure gas (250bar)	145-285
Light hydrocarbon	Steam	70-170
Hydrocarbon vapor	Flue gas	30-100



Table B4. TEMA standard tube dimensional data [17].

Tube O.D.		B.W.G. Gage	Thickness		Tube O.D.		B.W.G. Gage	Thickness							
inches	mm		inches	mm	inches	mm		inches	mm						
1/4	6.35	22	0.028	0.711	1	25.40	8	0.165	4.191						
		24	0.022	0.559			10	0.134	3.404						
		26	0.018	0.457			11	0.120	3.048						
		27	0.016	0.406			12	0.109	2.769						
3/8	9.53	18	0.049	1.245			1-1/4	31.75	13	0.095	2.413				
		20	0.035	0.889					14	0.083	2.108				
		22	0.028	0.711					15	0.072	1.829				
1/2	12.70	16	0.065	1.651					1-1/2	38.10	16	0.065	1.651		
		18	0.049	1.245							18	0.049	1.245		
		20	0.035	0.889							20	0.035	0.889		
5/8	15.88	22	0.028	0.711							2	50.80	7	0.180	4.572
		12	0.109	2.769									8	0.165	4.191
		13	0.095	2.413	10	0.134							3.404		
		14	0.083	2.108	11	0.120							3.048		
		15	0.072	1.829	12	0.109							2.769		
		16	0.065	1.651	13	0.095							2.413		
		17	0.068	1.727	14	0.083	2.108								
		18	0.049	1.245	16	0.065	1.651								
19	0.042	1.067	18	0.049	1.245										
3/4	19.05	20	0.035	0.889	2-1/2	63.50	20	0.035	0.889						
		10	0.134	3.404			10	0.134	3.404						
		11	0.120	3.048			12	0.109	2.769						
		12	0.109	2.769			14	0.083	2.108						
		13	0.095	2.413			16	0.065	1.651						
		14	0.083	2.108			11	0.120	3.048						
		15	0.072	1.829			12	0.109	2.769						
		16	0.065	1.651			13	0.095	2.413						
17	0.058	1.473	14	0.083			2.108								
7/8	22.23	18	0.049	1.245			3	76.20	10	0.134	3.404				
		20	0.035	0.889					12	0.109	2.769				
		10	0.134	3.404					14	0.083	2.108				
		11	0.120	3.048	10	0.134			3.404						
		12	0.109	2.769	12	0.109			2.769						
		13	0.095	2.413	14	0.083			2.108						
		14	0.083	2.108	10	0.134			3.404						
		15	0.072	1.829	12	0.109			2.769						
16	0.065	1.651	14	0.083	2.108										
17	0.058	1.473													
18	0.049	1.245													
20	0.035	0.889													

## APPENDIX C

## DETAILED CALCULATION OF AIR PREHEATER DESIGN

## 1. Detailed design of Air preheater

Air preheater type in this work is a shell and tube heat exchanger which is the flue gas is inside the tube and the air is outside. The objective is to preheat the air temperature at 70 °C.

Table C1. Nomenclature.

Data	Unit	Tube side fluid (flue gas)	Shell side fluid (Air)
Mass flow rate	kg/h	$W_t$	$W_s$
Volume flow rate	$m^3/h$	$Q_t$	$Q_s$
Inlet temperature	°C	$t_1$	$T_1$
Outlet temperature	°C	$t_2$	$T_2$
Density	kg/m <sup>3</sup>	$\rho_t$	$\rho_s$
Absolute viscosity	mPa.s	$\mu_t$	$\mu_s$
Specific heat	kJ/kg-K	$C_{pt}$	$C_{ps}$
Conduction coefficient	W/m-°C	$k_t$	$k_s$

Data	Unit	Nomenclature
Shell side pressure drop	kPa	$\Delta P_s$
Tube side pressure drop	kPa	$\Delta P_t$
Mean temperature difference	-	$\Delta T_{mean}$

Heat transfer area available	$m^2$	$A_a$
Preliminary heat transfer area	$m^2$	$A_p$
Heat transfer area requirement	$m^2$	$A_r$
Corrosion allowance	Mm	$C$
Tube clearance	Mm	$C'$
Bundle clearance	Mm	$C_b$
Shell nominal diameter	Mm	$D$
Tube bundle diameter	Mm	$D_b$
Baffle diameter	Mm	$D_B$
Shell side equivalent diameter	Mm	$D_e$
Tube inside diameter	Mm	$d_i$
Shell inside diameter	Mm	$D_i$
Tube outside diameter	Mm	$d_o$
Modulus of elasticity	$kN/mm^2$ (Gpa)	$E$
Tube side correction factor	-	$F$
Shell side correction factor	-	$F'$
Temperature correction factor	-	$F_T$
Correction factor	-	$F_T$
Tube side mass velocity	$kg/(m^2 s)$	$G_t$
Baffle cut height	Mm	$h_{BC}$
Shell side heat transfer coefficient	$W/m^2-^{\circ}C$	$h_s$
Tube side heat transfer coefficient	$W/m^2-^{\circ}C$	$h_t$
Effective tube length	Mm	$L_{eff}$
Logarithmic Mean Temperature Difference	-	LMTD
Tube length	Mm	$L_T$
Number of roll of tube at baffle openings	-	$n_{BC}$
Maximum number of tubes	-	$n_{max}$
Number of shell pass	-	$n_{SP}$

Total number of tubes	-	$n_T$
Number of tube pass	-	$n_{TP}$
Number of tubes per pass	-	$n_{TPP}$
Baffle spacing	Mm	$P_B$
Percent baffle cut	%	$P_{BC}$
Design pressure	Mpa	$P_{des}$
Maximum pressure	Mpa	$P_{max}$
Normal operating pressure	Mpa	$P_n$
shell side Prandtl's number	-	$Pr_s$
Tube side Prandtl's number	-	$Pr_t$
Maximum pressure of fluid in shell side	Mpa	$P_{s,max}$
Safe working pressure	Mpa	$P_{safe}$
Tube pitch	Mm	$P_T$
Maximum pressure of fluid in tube side	MPa	$P_{t,max}$
Heat transfer rate	Watt	$Q$
Shell side Reynold's number	-	$Re_s$
Tube side Reynolds' number	-	$Re_t$
Shell side fouling resistance	$m^2\text{-}^\circ\text{C}/\text{W}$	$r_{fs}$
Tube side fouling resistance	$m^2\text{-}^\circ\text{C}/\text{W}$	$r_{ft}$
Safe working fiber stress	$\text{N}/\text{mm}^2$ or Mpa	$S_s$
Cross sectional area per each of tube pass	$m^2$	$S_t$
Minimum tube thickness	Mm	$t_m$
Minimum shell thickness	Mm	$t_{shell,m}$
Design heat transfer coefficient	$\text{W}/\text{m}^2\text{-}^\circ\text{C}$	$U_{design}$
Shell side fouling coefficient	$\text{W}/\text{m}^2\text{-}^\circ\text{C}$	$U_{fs}$
Tube side fouling coefficient	$\text{W}/\text{m}^2\text{-}^\circ\text{C}$	$U_{ft}$
Service heat transfer coefficient	$\text{W}/\text{m}^2\text{-}^\circ\text{C}$	$U_{service}$
Tube side velocity	m/s	$V_t$

Table C2. Operating and properties data for air preheater design.

Boiler					
Capacity	7.65	ton/hr, max	Pressure of steam and BFW	5.5	Bar
	4-7	ton/hr	BFW temperature	100	°C
Parawood chips					
Mass flow rate	1,500	kg/hr	Components and calorific value are shown in table 3.1		
Cold side (shell side)			Hot side (tube side)		
Properties	Air		Properties	Flue gas	
MW <sub>s</sub>	29	kg/kmol	MW <sub>t</sub>	28	kg/kmol
Mass flow rate (W <sub>s</sub> )	6,876	kg/h	Mass flow rate (W <sub>t</sub> )	8,662	kg/h
Density ( $\rho_s$ )	1.16	kg/m <sup>3</sup>	Density ( $\rho_t$ )	1	kg/m <sup>3</sup>
Cp <sub>s</sub>	1.02	kJ/kg K	Cp <sub>t</sub>	1.05	kJ/kg K
Absolute viscosity ( $\mu_s$ )	0.02	mPa.s	Absolute viscosity ( $\mu_t$ )	0.022	mPa.s
Conduction coefficient (k <sub>s</sub> )	0.026	W/m.°C	Conduction coefficient (k <sub>t</sub> )	0.05	W/m.°C
Operating			Operating		
Temperature inlet (T <sub>1</sub> )	30	°C	Temperature inlet (t <sub>1</sub> )	170	°C
			(from simulation)		
Temperature outlet (T <sub>2</sub> ) (defined)	70	°C	Temperature outlet (t <sub>2</sub> ) (calculated)	139	°C
Pressure inlet (P <sub>s1</sub> )	105	kPa	Pressure inlet (P <sub>t1</sub> )	103	kPa

**Step 1:** Calculation of heat transfer rate (Q) from air side.

$$Q = \left(\frac{1000}{3600}\right) W_s C_{ps} |T_1 - T_2| = 78,081 \text{ W} \quad (\text{C.1})$$

**Step 2:** Performing energy balance to find out the flue gas outlet temperature.

$$t_2 = t_1 - \frac{W_s C_{pts}}{W_t C_{pt}} (T_1 - T_2) = 139 \text{ } ^\circ\text{C} \quad (\text{C.2})$$

**Step 3:** Calculation of LMTD.

$$\text{LMTD} = \frac{(T_2 - t_1) - (T_1 - t_2)}{\ln \left( \frac{T_2 - t_1}{T_1 - t_2} \right)} = 104.5 \text{ } ^\circ\text{C} \quad (\text{C.3})$$

**Step 4:** Defining the tube diameter, tube layout and tube material. 88.90 mm (3-1/2'') outside diameter of stainless steel 304 tube was used. Tube layout was triangular pattern. The tube pitch was given by 1.33 tube pitch/tube diameter ratio [16] which equal to 118.20 mm.

**Step 5:** Calculation of the minimum tube thickness ( $t_m$ ). The  $t_m$  equation for seamless steel pipe was used.

$$t_m = \frac{d_o}{2.3} \left( \frac{P_{\text{safe}}}{S_s} + \frac{1}{30} \right) + C = 3.03 \text{ mm} \quad (\text{C.4})$$

Where;

- $P_{\text{safe}}$  is safe working pressure or design pressure which multiple by 1.25 from maximum fluid pressure = 105 kPa \* 1.25 = 131 kPa or 0.131 MPa
- $S_s$  is safe working stress. Using 113.4 MPa (See in table B2 [17] in Appendix B).
- C is corrosion allowance. For nominal tube diameter more than 25mm using 1.7 mm.

From TEMA standard tube thickness (Table B4 [17] in Appendix B), 3.404 mm wall thickness (B.W.G. Gage 10) was used.

**Step 6:** The number of shell pass ( $n_{sp}$ ) and number of tube pass ( $n_{TP}$ ) were defined. 1 shell pass was used. Tube pass should be selected at 1 pass due to prevent fouling problem from flue gas.

**Step 7:** Calculating the correction factor ( $F_T$ ) which is a function of the fluid temperatures and the number of tube and shell passes and. Moreover,  $F_T$  is correlated with a function of two dimensionless temperature ratios ( $R$  and  $S$ ).  $R$  is temperature difference ratio.  $S$  is the temperature efficiency of air preheater.

$$R = \frac{T_1 - T_2}{t_2 - t_1} = 1.29 \quad (C.5)$$

$$S = \frac{t_2 - t_1}{T_1 - t_1} = 0.211 \quad (C.6)$$

The correction factor ( $F_T$ ) can be determined from the Blackwell and Haydu equation as shown in equation (C.8) in cases of  $R \neq 1$ .

Where  $R \neq 1$

$$X = \frac{1 - \left(\frac{RS-1}{S-1}\right)^{1/n_{sp}}}{R - \left(\frac{RS-1}{S-1}\right)^{1/n_{sp}}} = 0.22 \quad (C.7)$$

$$F_T = \left(\frac{\sqrt{R^2+1}}{R-1}\right) \frac{\ln\left(\frac{1-X}{1-RX}\right)}{\ln\left(\frac{2/X - 1 - R + \sqrt{R^2+1}}{2/X - 1 - R - \sqrt{R^2+1}}\right)} = 0.98 \quad (C.8)$$

The determination criteria is in the case, the less number of shell pass which provide the value of  $F_T$  not less than 0.8.

**Step 8:** Calculating the temperature different.

$$\Delta T_{\text{mean}} = F_T \cdot \text{LMTD} = 102.48 \text{ } ^\circ\text{C} \quad (\text{C.9})$$

**Step 9:** Calculating the preliminary heat transfer area ( $A_p$ ).

$$A_p = \frac{Q}{U_{\text{service}} \Delta T_{\text{mean}}} = 50.80 \text{ m}^2 \quad (\text{C.10})$$

Where;  $U_{\text{service}}$  is the service heat transfer coefficient.  $15 \text{ W/m}^2 \text{ } ^\circ\text{C}$  was used (see table B3 [17] in Appendix B).

**Step 10:** Defining tube length ( $L_T$ ). 4,000 mm tube length is recommend for primary calculation and should be less than 6,000 mm due to the maximum tube length which can use with major standard heat exchanger. Adjustment of tube length should be increase or decrease 250 or 500 mm. In this work, **4,500 mm** tube length was used.

**Step 11:** Approximating the effective tube length ( $L_{\text{eff}}$ ) which is usable tube length for heat transfer.

$$L_{\text{eff}} = L_T - 75 \text{ mm} = 4,425 \text{ mm} \quad (\text{C.11})$$

**Step 12:** Calculating the total number of tubes ( $n_T$ ) by following procedure

- i. Approximating the primary total number of tubes.



$$n_T = \frac{318310A_p}{d_o L_{\text{eff}}} = 41 \quad (\text{C.12})$$

- ii. Calculating the number of tubes per pass ( $n_{\text{TPP}}$ ).

$$n_{\text{TPP}} = \frac{n_T}{n_{\text{TP}}} = 41 \quad (\text{C.13})$$

- iii. Adjusting the value to an integer (round up in all decimal cases).  
iv. Recalculating the total number of tubes.

$$n_T = n_{\text{TP}} \times n_{\text{TPP}} = 41 \quad (\text{C.14})$$

**Step 13:** Defining the shell nominal diameter ( $D$ ) which depends on number of tubes, tube layout, tube outside diameter and tube pitch by Coulson et al. (1999) method in [17].

- i. Approximating the tube bundle diameter ( $D_b$ ).

$$D_b = d_o \left( \frac{n_T}{K} \right)^{1/n} = 858.01 \text{ mm} \quad (\text{C.15})$$

For triangle tube pattern and 1 tube pass,  $K=0.319$  and  $N=2.142$ .

- ii. Approximating the bundle clearance ( $C_b$ ) which depends on feature of shell.

For fixed tube sheet;

$$C_b = 8 + 0.01D_b = 16.58 \text{ mm} \quad (\text{C.16})$$

- iii. Calculating the shell inside diameter ( $D_i$ ).

$$D_i = D_b + C_b = 874.59 \text{ mm} \quad (\text{C.17})$$

- iv. Adjusting the shell inside diameter ( $D_i$ ). **1200 mm** shell diameter was used to avoid pressure drop of air stream.

**Step 14:** Calculating the minimum shell thickness ( $t_{shell,m}$ ).

$$t_{shell,m} = \frac{P_{safe} D_i}{2S_s - 1.2P_{safe}} + C = 2.39 \text{ mm} \approx 3 \text{ mm} \quad (C.18)$$

Where; **C** is corrosion allowance which depends on corrosion strength of fluid. Using  $C=1.7$  mm for moderately corrosive of expensive material.

**Step 15:** Calculating the shell diameter ( $D$ ).

$$D = D_i + 2t_{shell,m} = 1206 \text{ mm} \quad (C.19)$$

**Step 16:** Defining the detail of baffles. Baffles are used to increase the fluid velocity by diverting the flow across the tube bundle to obtain higher transfer co-efficient. Basically, the segmental type was used. The percent baffle cut is the percentage of ratio of baffle cut height and baffle diameter. Baffle cuts from 15 to 45% are normally used. In this work using 2 baffles at 25% baffle cut and 1500 mm baffle spacing.

Once completed, steps 1 through 14 will provide a complete detail design of shell and tube heat exchanger. The next steps are detailed inspection of tube and shell and overall efficiency of heat exchanger.

## 2. The detailed design inspection of tube

**Step 1:** Calculating the tube side mass velocity ( $G_t$ )

$$G_t = \frac{353.68W_t}{n_{\text{TPP}}d_i^2} = 11.1 \text{ kg/m}^2\text{s} \quad (\text{C.20})$$

**Step 2:** Calculating and inspecting tube side velocity ( $V_t$ )

$$V_t = \frac{G_t}{\rho_t} = 11.09 \text{ m/s} \quad (\text{C.21})$$

For gas case at atmospheric pressure,  $V_t$  should be in range of 10 to 30 m/s in order to prevent the fouling, suspension deposit, erosion and vibration problem.

**Step 3:** Calculating the tube side Reynolds' number ( $Re_t$ ) and tube side Prandtl's number ( $Pr_t$ ). The  $Re_t$  should be more than 10,000.

$$Re_t = \frac{d_i G_t}{\mu_t} = 41,371 \quad (\text{C.22})$$

$$Pr_t = \frac{C_{pt}\mu_t}{k_t} = 0.46 \quad (\text{C.23})$$

**Step 4:** Approximating the tube side heat transfer coefficient ( $h_t$ ) from Hewitt equation (1944) in case of  $Re_t > 10,000$  in [17]

$$h_t = \left(\frac{27}{F}\right) \left(\frac{k_t}{d_i}\right) \left(1 + \frac{0.07d_i}{L_T}\right) Re_t^{0.8} Pr_t^{0.33} = 50.39 \text{ W/m}^2 \text{ }^\circ\text{C} \quad (\text{C.24})$$

Where; F is tube side correction factor. For gas case, F equal to 1.25.

**Step 5:** Approximating the tube side pressure drop ( $\Delta P_t$ ) from Frank's method in case of  $Re_t > 10,000$  ( $\pm 3\%$  tolerance) in [17]

$$\Delta P_t = 10^{-3} n_{TP} \left[ 0.1635 \left( \frac{L_T}{d_i} \right) Re_t^{-0.176} + 2.5 \right] \left( \frac{\rho_t v_t^2}{2} \right) = 0.24 \text{ kPa} \quad (\text{C.25})$$

Checking the pressure drop from calculation with an appropriate pressure drop. The pressure of flue gas outlet stream must be more than atmospheric pressure.

### 3. The detailed design inspection of shell

**Step 1:** Calculating the shell side mass velocity ( $G_s$ ).

$$G_s = \frac{277.8 W_s P_T}{D_i P_B C'} = 4.3 \text{ kg/m}^2 \text{ s} \quad (\text{C.26})$$

**Step 2:** Calculating the shell side equivalent diameter ( $D_e$ ) due to parallel flow inside shell which depends on tube layout, tube outside diameter and tube pitch.

For triangle pattern;

$$D_e = \frac{1.10}{d_o} (P_T^2 - 0.971 d_o^2) = 77.92 \text{ mm} \quad (\text{C.27})$$

**Step 3:** Calculating the shell side Reynold's number ( $Re_s$ ) and shell side Prandtl's number ( $Pr_s$ )

$$Re_s = \frac{D_e G_s}{\mu_s} = 16,678 \quad (\text{C.28})$$

$$\text{Pr}_s = \frac{C_{p,s} \mu_s}{k_s} = 0.79 \quad (\text{C.29})$$

**Step 4:** Approximating the shell side heat transfer coefficient ( $h_s$ ) from Correlation equation ( $\pm 5\%$  tolerance) in [17]

$$h_s = \left( \frac{1457}{F'} \right) \left( \frac{k_s}{D_e} \right) P_{BC}^{-0.325} \text{Re}_s^{0.509} \text{Pr}_s^{0.33} = 28.51 \text{ W/m}^2\text{°C} \quad (\text{C.30})$$

Where;  $F'$  is shell side correction factor which depends on number of roll of tube at baffle openings ( $n_{BC}$ ). The  $n_{BC}$  depends on the tube layout as shown in equation (C.31).

For triangular-pitch;

$$n_{BC} \approx \frac{1.155 P_{BC} D}{100 P_T} \approx 2.9 \quad (\text{C.31})$$

For  $n_{BC}$  in range of 4-6,  $F'$  was equal to 0.9.

**Step 5:** Approximating the shell side pressure drop ( $\Delta P_s$ ) from Correlation equation of Kern's method ( $\pm 7.5\%$  tolerance) in [17]

$$\Delta P_s = 0.0199 \left( \frac{D_i}{D_e} \right) \left( \frac{L_T}{P_B} \right) P_{BC}^{-0.659} \text{Re}_s^{-0.193} \left( \frac{\rho_s V_s^2}{2} \right) = 0.133 \text{ kPa} \quad (\text{C.32})$$

Checking the pressure drop from calculation with an appropriate pressure drop. The pressure of air outlet stream must be more than atmospheric pressure.

#### 4. Inspection of overall efficiency of heat exchanger

**Step 1:** Calculating the design heat transfer coefficient ( $U_{\text{design}}$ ).

$$\frac{1}{U_{\text{design}}} \approx \frac{1}{h_s} + \frac{1}{U_{fs}} + \left(\frac{d_o}{d_i}\right) \left(\frac{1}{h_t}\right) + \left(\frac{d_o}{d_i}\right) \frac{1}{U_{ft}} \approx 0.0570 \quad (\text{C.33})$$

$$U_{\text{design}} = 17.55 \text{ W/m}^2\text{°C}$$

Where;  $U_{ft}$  is tube side fouling coefficient.  $U_{fs}$  is shell side fouling coefficient.

For flue gas fouling coefficient and air fouling coefficient using 5,000  $\text{W/m}^2\text{°C}$  (see table B1 [18] in Appendix B).

**Step 2:** Comparing  $U_{\text{design}}$  and  $U_{\text{service}}$ . Both values should be equal or close.

**Step 3:** Approximating the heat transfer area requirement ( $A_r$ ) and calculated heat transfer area available ( $A_a$ ). The ratio of  $A_a$  and  $A_r$  should be in range of 1.1 to 1.2 [17].

$$A_r = \frac{Q}{U_{\text{design}} \Delta T_m} = 43.42 \text{ m}^2 \quad (\text{C.34})$$

$$A_a = n_T \left[ \pi \left( \frac{d_o}{1000} \right) \left( \frac{L_{\text{eff}}}{1000} \right) \right] = 50.67 \text{ m}^2 \quad (\text{C.35})$$

$$\frac{A_a}{A_r} = 1.17 \quad (\text{C.36})$$

**VITAE**

**Name** Mr. Jirateep Premsuksatian

**Student ID** 6110120062

**Education Attainment**

<b>Degree</b>	<b>Name of Institution</b>	<b>Year of Graduation</b>
Bachelor of Engineering (Chemical Engineering)	Prince of Songkla University	2018

**Scholarship Awards during Enrollment**

1. 5-Year Bachelor's-Master's Degree Program Scholarship 2018.